

POLITECNICO DI TORINO

**Master of Science
in Mechanical Engineering**

Master Thesis

**Topology Optimization and Design for
Additive Manufacturing: the case
study of a hydraulic module for
automotive application**



Supervisor

Prof. Luca Iuliano

Co-Advisor

Ing. Manuela Galati

Company Supervisors

Dipl. Wirt-Ing Martin Pagel

MSc Dushan Pamunuwa

Candidate

Alessia Toscano

Academic Year 2018-2019

CONTENTS

I. Summary (Italian version).....	5
I.I Obiettivi	5
I.II Risultati principali.....	6
I.III Conclusioni	7
II. Introduction	9
III. Abstract.....	15
IV. Introduction to Oerlikon Additive Manufacturing.....	16
1. Introduction to Additive Manufacturing	20
1.1. Additive Manufacturing technology	20
1.2. Powder Bed Fusion – Laser Powder Bed Fusion Process.....	21
2. Critical analysis of the original component.....	27
2.1. Component selection.....	27
2.2. Loads, constraints and boundary conditions	31
2.3. Design space identification	35
2.4. Finite element method structural analysis.....	41
3. Topology optimization	53
3.1. Mathematics in topology optimization.....	53
3.2. Topology optimization of the original component.....	57
4. Component redesign.....	69
4.1. Design for Additive Manufacturing.....	69
4.2. Redesign.....	72
5. Design verification – structural analysis	81
6. Manufacturing and post processing.....	87
6.1. Building orientation and support structure generation.....	87

6.2. Part production	95
6.3. Post processing	97
7. Comparison between original and optimized component	100
8. Conclusion	108
A. List of figures	112
B. List of equations	117
C. List of tables	118
D. Abbreviations	119
E. Bibliography	121
F. Acknowledgments	125

I. Summary (Italian version)

I.I Obiettivi

L'obiettivo di questo lavoro di tesi è quello seguire l'intero processo di produzione di un componente meccanico metallico mediante il processo di fabbricazione additiva chiamato Laser Powder Bed Fusion (L-PBF), utilizzando l'ottimizzazione topologica e le regole di Design for Additive Manufacturing (DFAM) per rendere il pezzo più conforme alla tecnologia.

Inizialmente è stato selezionato il pezzo protagonista di questa opera, scegliendo tra diversi componenti forniti dall'azienda Oerlikon Graziano Spa, in maniera tale che risultasse vantaggioso produrlo in AM. In seguito alla sua individuazione, sono stati applicati alla geometria i vincoli e i carichi forniti dall'azienda, in modo da ottenere lo stato di tensione e deformazione del componente originale mediante un'analisi FEM condotta con pari dimensione e tipo di elementi con diversi software: Inspire 2019 e NX/NX Nastran.

Successivamente la geometria della parte è stata divisa in due zone: il design space (ovvero la parte in cui il materiale può essere eliminato) e il non design space (ossia la zona su cui agiscono i carichi e i vincoli). In seguito, si è ampliata la zona di design space, eliminando inoltre filetti e raccordi, per semplificare la geometria e poter permettere una migliore distribuzione del materiale nello spazio. La forma dei canali interni è stata inoltre migliorata, in accordo con i requisiti dell'azienda cliente.

Si è passati alla ottimizzazione topologica del componente, effettuata con metodo Solid Isotropic Material with Penalization (SIMP), con entrambi i software. Con i risultati ottenuti è stato possibile ricostruire la geometria del componente mediante free forms. In aggiunta, sono state apportate ulteriori modifiche al design seguendo le regole di design for additive manufacturing prevalentemente presenti nelle normative ISO/TC 261/SC e ISO/DIS 52911-1:2017(E). Le regole di DFAM non

sono ancora state regolamentate del tutto da standard ASTM, in quanto precisi valori e dimensioni sono relativi a specifici materiali, macchine e spessori di layer, e più in generale dai parametri settati per le macchine. Una ulteriore analisi FEM è stata eseguita su questo nuovo componente per verificare che sostenesse i carichi applicati.

Come già accennato, per effettuare le analisi agli elementi finiti e l'ottimizzazione topologica sono stati utilizzati due diversi software messi a confronto: Altair Inspire 2019 e Siemens NX Nastran. Sono state analizzate le principali differenze nei risultati, in modo da poter valutare le performance di entrambi i programmi.

L'analisi FEM del componente iniziale e quella di quello ottimizzato sono state inoltre confrontate in modo da verificare la bontà dell'ottimizzazione. Soltanto in seguito a questa prova, un prototipo del componente, con sovrametallo aggiunto nelle zone da finire, è stato prodotto inserendo opportuni supporti e staffe sacrificali. Dopo diversi trattamenti post produttivi, come la rimozione dei supporti, è stato inviato all'azienda affinché lo testasse su un banco prova. Una volta conosciuti i risultati dei test, se il prodotto risulterà conveniente e soddisfacente per l'azienda cliente, verrà avviata la produzione in serie.

I.II Risultati principali

Tra i risultati principali ricavati da questo lavoro di tesi, c'è un'importante riduzione di peso del componente selezionato, per merito della ottimizzazione topologica, fino al 69 %.

Per di più, dato che l'additive manufacturing è una tecnologia ancora emergente, comparare i software utilizzati per l'analisi e la progettazione del componente può fornire interessanti spunti a chi è nel settore, in modo da poter decidere quale programma utilizzare per i propri scopi, ottimizzando i tempi. Il confronto tra Altair Inspire e Siemens NX e NX Nastran, sebbene siano software molto diversi, ha visto l'uno prevalere sull'altro per quanto riguarda diversi aspetti.

Il software più completo per la visualizzazione, la progettazione e le modifiche CAD è senza alcun dubbio Siemens NX, in quanto permette una più precisa ed efficiente manipolazione di superfici, punti e volumi. Ovviamente è necessario saper utilizzare il software per poterne trarre beneficio: per questo, per scrivere questa tesi è stato necessario partecipare a diverse giornate di formazione.

Inspire d'altro canto è un software molto potente benché presenti molti bug, anche nella nuova versione 2019. Essendo un programma semplificato e all-in-one del più complesso HyperWorks di Altair, è user friendly, far partire una ottimizzazione è semplice e veloce, ma non sempre funziona. Numerosi problemi sono stati riscontrati inoltre per quanto riguarda la conversione da step file a stmod file, dato che vengono create spesso delle superfici e non dei corpi solidi. Il comando *partition* inoltre non è riuscito a dividere la zona di design space creando offset per quanto riguarda le superfici più complicate, pertanto per definire il non design space dei canali interni è stato doveroso utilizzare un programma CAD più completo. Inoltre, la funzione Booleana di sottrazione si interrompe a causa di bug.

Cambiare programma in corso d'opera non è raccomandabile, in quanto si potrebbero perdere informazioni passando da un formato all'altro. Per questo è sempre preferibile utilizzare lo stesso software per eseguire tutti i passaggi. Questo è possibile soltanto con NX ma non con Inspire.

I.III Conclusioni

In conclusione, l'additive manufacturing non è la tecnologia più economicamente conveniente per la produzione in serie di questo componente, sebbene offra la possibilità di cambiare la forma dei canali interni, diminuendo le perdite fluidodinamiche, e di risparmiare circa il 70% del volume iniziale, in quanto risulta conveniente soltanto per un volume produttivo ridotto.

Da un punto di vista meramente economico, questi successi purtroppo non giustificano il costo più elevato delle parti, sebbene il prototipo in sé risulti molto più economico. D'altro canto, i vantaggi non quantificabili sono comunque

numerosi: il componente ottimizzato ha un risparmio di materiale che su un autoveicolo impatta sui consumi, provocando una leggera diminuzione di carburante e emissioni di CO2.

Dalla comparazione tra i due software utilizzati, Inspire e NX, è emerso che entrambi rappresentano una ottima soluzione per quanto riguarda l'ottimizzazione topologica del componente ma NX, essendo un software più completo, permette di apportare modifiche geometriche ben più complesse, senza la necessità di passare da un formato all'altro. Ovviamente però per utilizzare NX è necessario conoscere il software, altrimenti le opzioni sono molteplici e il rischio di sbagliare diventa alto.

Inspire d'altro canto, essendo un software semplice, rende più comoda e accessibile l'ottimizzazione topologica. Purtroppo, non essendo capace di effettuare grandi modifiche, il suo utilizzo rimane soltanto marginale.

II. Introduction

The objective of this master thesis is the study of a complete Additive Manufacturing (AM) engineering and production process of a metal component. Every step in the complete value chain will be followed to prove that this technology is not a hype anymore and that it can be a competitive solution to traditional manufacturing.

The reasons that made me decide on additive manufacturing are the unique advantages that this technology has: higher complexity of the shapes, shorter lead times and weight reduction possibilities [1]. However, this technology also has its own limitations: one way to overcome them is to adapt the component and the process for additive manufacturing, which is called design for additive manufacturing (DFAM) [2]. Following design for additive manufacturing guidelines, criteria that help with this adaptation, and topology optimization, it could be more convenient to produce this part with AM instead of traditional manufacturing.

DFAM is nowadays still a self-improving sector, because parameters and values are most of the times referred only to specific materials, machines and layer thicknesses, more in general to parameter development [3]. That is why it has been hard to find a proper guideline that can overcome all the needs in the industry. For this piece of work, mostly ISO general guidelines have been used, even if they have not yet been approved as standards by ASTM International.

Additive manufacturing is strongly linked with design. The main reason is the freedom of design that this technology can allow, but mostly because, varying the geometry of the component to produce, costs and production times can be decreased [4]. All the process must be considered when designing, especially because design can also help to overcome some building failures, avoiding for example the creation of sharp edges and points or also adding support structures on overhang angles to make the part manufacturable [3].

Design is mostly related to support structures and build orientation [5]. Orienting the component on the building platform can not only decrease the cost of the job (dependent on the height of the part), but also reduce support structures, which can help to make the part manufacturable, but are considered as a waste of material, since most of times the material is not reusable [5].

Topology optimization, a mathematical method invented some centuries ago, [6] found its way only in the latest 30 years, because, thanks to additive manufacturing, there was for the first time the possibility to really manufacture the complex resulting geometries, calculating it with the modern software [7]. The software available in the market nowadays are numerous. The first commercially available version of a topology optimization algorithm was Optistruct, belonging to Altair [7]. Altair's HyperWorks (including Optistruct, HyperMesh and HyperView) or Inspire (with Optistruct in the background) are among the most used programs for this kind of optimization. Some other software used are NX Frustum or NX Nastran from Siemens, MSC Nastran from MSC Software, Ansys Mechanical from Ansys, Abaqus-Tosca from Dassault Systèmes or Inventor from Autodesk.

The advantages of topology optimization and design changes are huge, especially for those fields that can save money in decreasing the weight of the component, like for instance aerospace or medical industry. In figure I.I there is a satellite antenna bracket, topology optimized with Altair's software [8]. The weight saving achieved with this optimization is over 40% of the original component, that leads to a significant cost reduction [8].

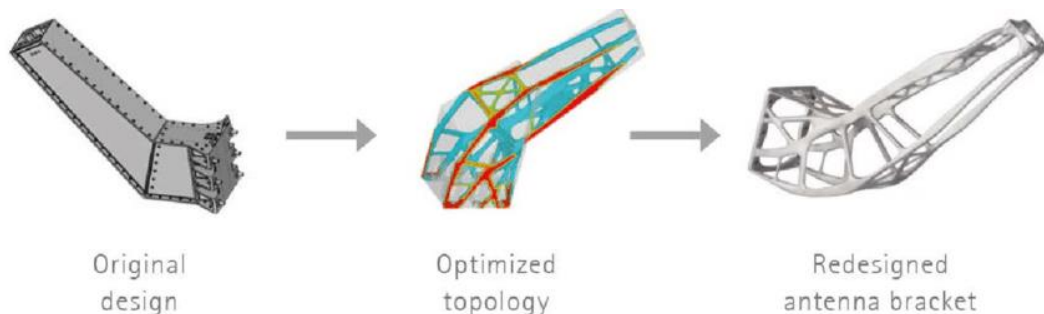


Figure I.I – Sentinel satellite antenna bracket: topology optimization example [8]

Another example to show the capabilities of topology optimization in additive manufacturing field, is the pedal in figure I.II. The original part, at left in the picture, has an initial weight of 2 kg [9]. The optimized part's weight is only 327 g, achieving 83.4% of weight saving [9].



Figure I.II – Pedal by © Prodways. Left original, right optimized [9]

Every chapter in this work is focused on the customization of the production process for this technology. The general methodology for transforming an original into an optimized component is presented in the chart below (figure I.III) and explained in detail as follows.

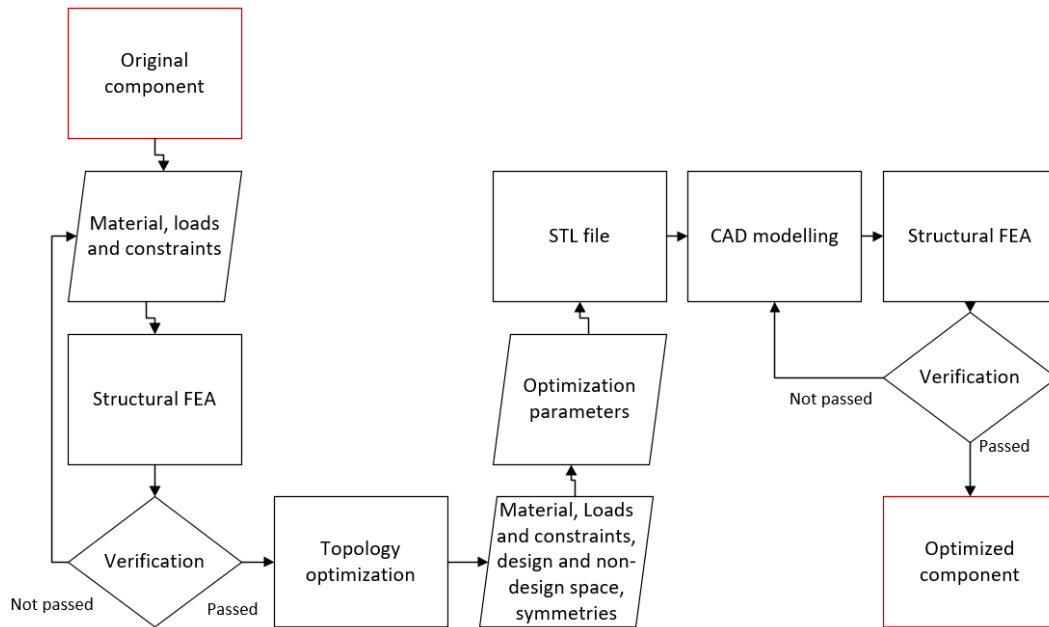


Figure I.III – Methodology for redesign and topology optimization [10]

After the application of loads and constraints on the original geometry and the application of the material's characteristics, a structural FEA is performed in order to check the behaviour of the original component on the performed stress. If the part fails, it will be necessary to change material, loads or constraints. When the verification is completed, the component is divided in design and non-design space and a topology optimization can be performed, applying the same loads and constraints, but with the possibility of changing the material and also to add some symmetric or building constraints. The result of the optimization, with the setup parameters, is a STL file that needs to be remodelled to make it a solid body again. Once the component is designed, a new structural FEA can be performed to verify that the optimized component can withstand all the loads applied, otherwise some CAD modification will be needed to accomplish the verification.

The aim of this thesis is to highlight the advantages of a process entirely focused on Additive Manufacturing, while comparing different software, Altair Inspire and Siemens NX and Siemens NX-Nastran, during all the steps in the chart just shown (figure I.II). The software used for the CAD modifications are Siemens NX 12 and Altair Inspire 2019. To perform FEA and topology optimization, Siemens NX

Nastran 12 and Altair Inspire 2019 have been used. For the creation of support structures and the decision of the orientation, Materialize Magics 21.11 has been run.

The body of this thesis is made up of eight chapters: chapter one provides a general introduction on the production technology called additive manufacturing and detailed information on the process called Laser Powder Bed Fusion (L-PBF) chosen to produce the selected component.

In the second chapter there is a critical analysis of the original component. This component has been selected following Additive Manufacturing criteria, making sure that it can take advantage of this technology. The customer provides all the technical information about the part (loads, constraints and boundary conditions and more) to perform a structural finite element analysis with both software and to detect the design space area, the regions in the component that will be optimized. The FEA is performed on the solid body with the same type and size of elements for both software.

The third chapter is focused on topology optimization: a brief explanation of what it is and a review of the results of the component are presented, using Solid Isotropic Material with Penalization (SIMP) method for both Inspire 2019 and NX-Nastran.

In the fourth chapter design for Additive Manufacturing (DFAM) rules are introduced. The regulations followed to design the part are mostly ISO/TC 261/SC and ISO/DIS 52911-1:2017(E). The component is redesigned with freeform and bionic structures and the shape of channels and other surfaces are changed to make it more suitable for AM.

In chapter five, once the geometry is ready, a finite element structural analysis (FEA) is performed to verify the correct behaviour of the component and the steps and the results are explained. The same mesh element type and size is chosen, to make a better comparison with the original design.

Chapter six is focused on the production and the post processing steps. To produce the part, it is necessary to create adequate support structures that help not only with

the manufacturing and physical support of the component, but also with the heat transfer during the building. Some fixtures are included in the model, so that the machining and finishing phases are easier. The component will be tested on a test bench after the production.

A comparison between the original and the optimized component is done in the seventh chapter to show the advantages of using additive manufacturing. Displacements, von Mises stresses, safety factors, materials, geometries and weights are compared.

The results obtained are set out in detail in the conclusion in the eighth chapter.

III. Abstract

The aim of this work is to follow the entire value chain of a mechanical metallic hydraulic module that is produced with the additive manufacturing process called Laser Powder Bed Fusion (L-PBF).

Different software is used: Siemens NX 12 and Altair Inspire 2019 for CAD, Siemens NX Nastran 12 and Altair Inspire 2019 for FEA and topology optimization, and Materialise Magics 21.11 for support structure creation. A comparison between the software used for CAD, FEA analyses and topology optimizations is presented.

The customer provides all the technical information related to the component to perform a structural FEA. After the definition and extension of the design space, loads and constraints are applied on the non-design space and a topology optimization with Solid Isotropic Material with Penalization (SIMP) method is performed. Afterwards it is necessary to rebuild the component with freeform and bionic shapes, making sure that all the parts are connected. After the reconstruction, a further FEA is performed to prove that the optimized part can withstand the loads. The results of this analysis are compared with the results of the analysis of the initial geometry. To make the machining easier, fixtures and stock material are added. The final component will be tested on a bench to prove its efficiency.

In conclusion, all the advantages and disadvantages of both software are compared to better understand which could be the better in the additive manufacturing industry. NX/NX Nastran are the best option for CAD modification and FEA but Inspire can perform topology optimization and reconstruction faster. In addition, additive manufacturing production technology is evaluated for this specific component: it results convenient only for a small production lot.

IV. Introduction to Oerlikon Additive Manufacturing

This thesis has been entirely carried out in the Innovation and Technology Center of Oerlikon AM GmbH (OAM) located in Kapellenstrasse 12, 85622 Feldkirchen, Munich, Germany. Oerlikon AM has six facilities in different cities all over the world: Munich and Magdeburg in Germany and Charlotte, Atlanta, Troy and Plymouth in United States.

This Company, founded in 2016, used the 60 years old Oerlikon experience to focus on AM. As part of the Oerlikon Group, a global powerhouse committed to investing in cutting-edge technologies that deliver superior performance and environmental sustainability, OAM is trusted by some of the biggest names in the manufacturing industry. Oerlikon has specialized in making atomized metal powders used in power generation, automotive and aerospace for more than 40 years. Those industries, both with medical and energy sectors, are those that can get more benefits from this new technology. For example, with the wheel carrier in figure I.IV, 80% weight reduction was achieved, with consistent and better mechanical properties [11].



Figure I.IV - Oerlikon AM, wheel carrier [11]

The Company has a broad range of existing alloys, supported by ongoing research and development. They also know that current off-the-shelf solutions in AM cannot answer every production need. Their R&D teams can rapidly design (figure I.V), optimize, and produce new and custom alloy chemistries for pilot atomization and AM validation in their production facilities.



Figure I.V: Oerlikon AM - Piston head [11]

Oerlikon AM provides a broad range of material and machine options to suit the needs of each prototyping application. They specialize in rapid prototyping of end-use components in metals, polymer, and ceramics (figure I.VI). At Oerlikon AM they also make serial production components for many industries, including power generation, automotive and aerospace.

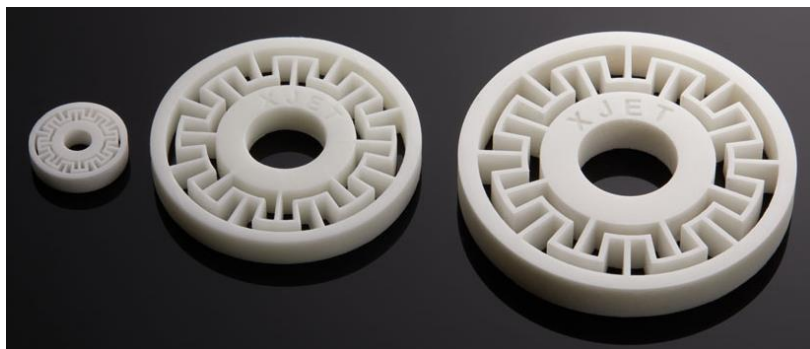


Figure I.VI: Oerlikon AM - Ceramic parts [11]

Among the machines available for metals there are various brands: EOS, SLM, Concept Laser, Trumpf and Arcam. Those machines can print Titanium alloys, Stainless Steel, Tool Steel, Copper alloys, Aluminum alloys and Cobalt Chrome.

Their expertise is such that they can help customers overcome even the most demanding design needs, whatever their industry, and whatever the application. They provide the expertise to choose the right process, machine, and material to make parts manufacturable.



Figure I.VII - Oerlikon AM - Oil filter housing with support structures [11]

They cover all the steps of the complete value chain, from Post-Processing (figure I.VII) to surface engineering, with both thin and thick film coatings and final processing. Hot Isostatic Pressing, vacuum heat treatment, CNC (Computer

Numerical Control) machining, surface finishing, 3D scanning and metallurgical evaluation enable them to provide finished parts (figure I.VIII).



Figure I.VIII - Oerlikon AM - Oil filter housing [11]

This thesis has been conducted entirely in the Application Engineering team, which is specialized in serial production processes. This team of experts assist customers to find the perfect solution for their production, with topology optimization, redesigns, finite element analyses, process simulations, post processing and heat treatments. They are able to do parameter development for new materials and new machines as well.

1. Introduction to Additive Manufacturing

1.1. Additive Manufacturing technology

Additive Manufacturing, most commonly known as 3D Printing, was born in 1984, when Charles Hull first invented Stereolithography [12]. With this new process, designers created 3D models using digital data having the possibility to make it a tangible object (see figure 1.1).

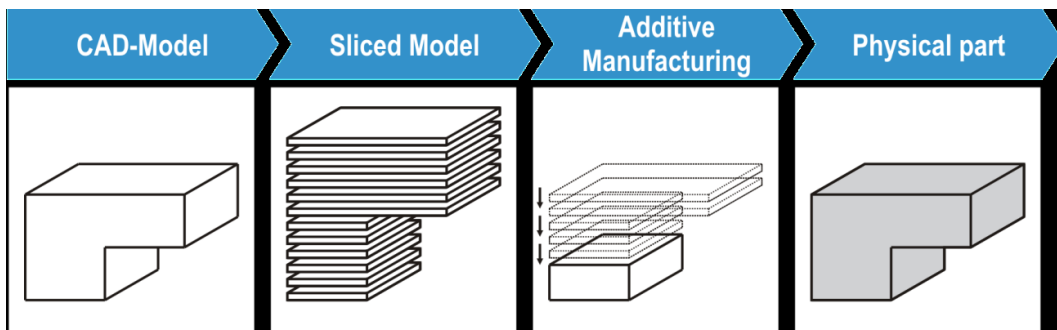


Figure 1.1 - Additive Manufacturing steps [3]

Stereolithography is a production technology that uses a pool filled with liquid photopolymer that solidifies with UV (Ultraviolet) laser beam, with a process called photopolymerization [13]. With this process, building all the component layer after layer was possible for the first time [13].

In 1987 Rapid Prototyping became a commercial reality with the first 3D Systems commercially available AM machine in the world [12].

Start-up DTM (now a part of 3D Systems) produced the world's first Selective Laser Sintering (SLS) machine only in 1992, using a powder instead of a liquid, that solidifies with the heat from a laser [12].

AeroMet developed from 1997 to 2005 a process called laser additive manufacturing (nowadays known as Laser Beam Melting) that used a high-power laser and powdered titanium alloys [12].

More than a hundred of new processes were invented in the Additive Manufacturing field only in the 21st century [14]. Most of their names are trademarks of different machine manufacturers. At the beginning this technology was far from perfect, but the idea of manufacturing something only having its STL file was revolutionary [15]. STL (Standard Triangle Language) file describes only the surface geometry of a three-dimensional object without any representation of colour, texture or other common CAD attributes [16]. They only delineate the coordinates of triangular surfaces vertexes and their normal, according to a Cartesian coordinate system [16].

During the following years, different kinds of Additive Manufacturing technologies were born [14]. Every type has its own advantages and disadvantages but all of them consist in adding material instead of eliminating it with machining.

The first important use of this technology was prototyping: it was faster than the traditional way but at the beginning it was expensive because machinery was patented [17]. With time, there were a lot of innovations that helped with the development of those technologies, so prices became more affordable and the accuracy of products increased [14].

The list of materials that could be used nowadays for AM is still brief compared to all the materials available for traditional manufacturing. As metal alloys it is possible to find Aluminium, Titanium, Inconel, Copper, Cobalt Chrome, Tool steel, Stainless steel, Hastelloy and Gold. Among polymeric materials there are ABS, Polyamide, PEEK, PMMA, Polycarbonate, ULTEM, Polyphenylsulfone and Filled PA. [10] It is also possible to print ceramic materials such as Alumina, Mullite, Silicon Carbide, Zirconia, Plaster and Graphite [10]. There are also a few organic materials: waxes and tissue or cells [10].

1.2. Powder Bed Fusion – Laser Powder Bed Fusion Process

This thesis is focused on the production of a metal component. That is why the technology chosen for this aim is Laser Powder Bed Fusion (L-PBF), most

commonly called Selective Laser Melting (SLM) or Laser Beam Melting (LBM). L-PBF and Electron Beam Melting (EBM) belong to the family of Powder Bed Fusion (PBF) processes. EBM uses an electron beam to melt metal powder while L.PBF uses a laser beam.

Focusing on Laser processes, all L-PBF machines have a build platform, capable of moving on the vertical z-axis direction on which there is metal powder that is spread by a recoater or a blade [3]. The power source (a laser beam) between a complex electromagnetic system, melts and fuses the powder together on the building plate, moving on x and y-axis directions to create the desired shape, section by section (see figure 1.2) [3].

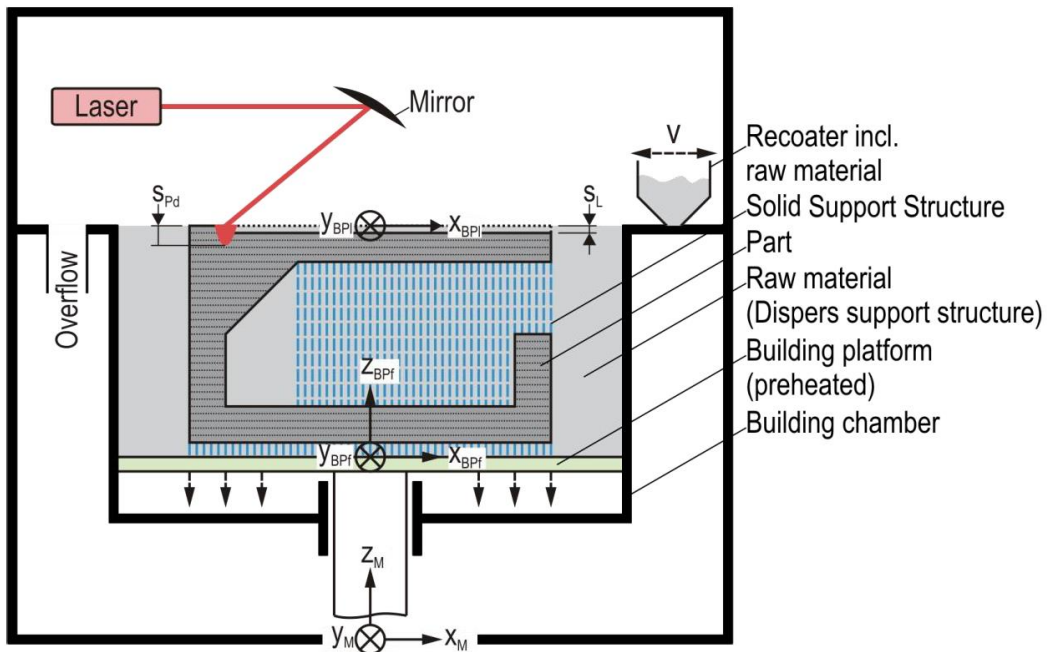


Figure 1.2 - - Laser Powder Bed Fusion process [3]

After solidifying the whole layer, the elevator moves down to an amount called layer thickness and the process is repeated until the whole component is built [18]. In L-PBF powder layer thickness is higher than the fused deposit layer thickness: the depth of penetration is greater than the deposit layer thickness in order to penetrate three or more layers in depth to more totally fuse the deposit (e.g. figure 1.3) [18].

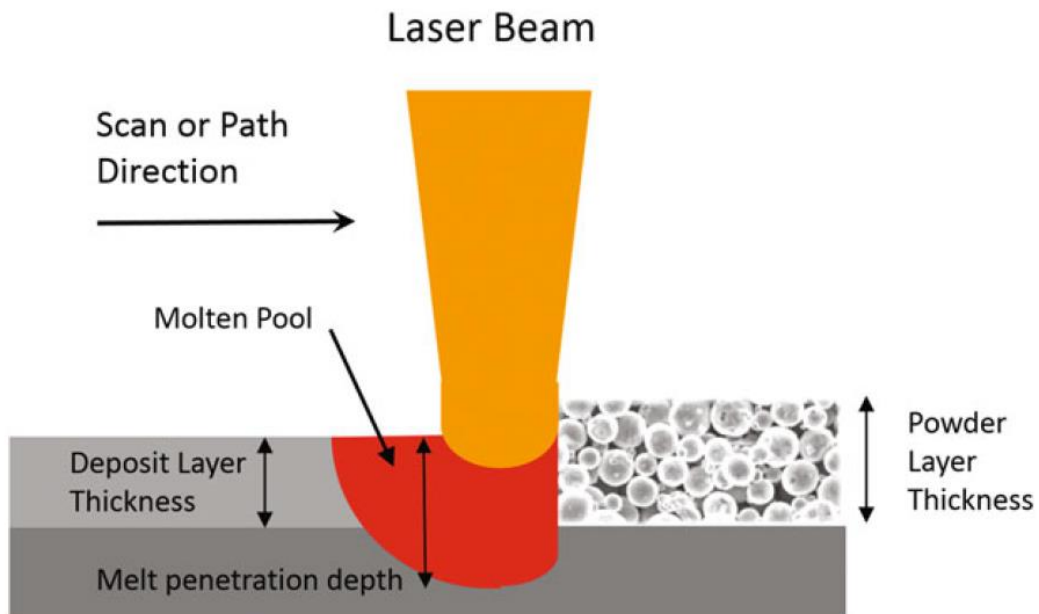


Figure 1.3 - Powder Layer thickness and Deposit Layer Thickness for L-PBF process [18]

At the end of the process, powder must be removed, so that the part is displayed, and heat treatments could be performed. The density obtained with L-PBF is approximately 99.9%, comparable with casting [19]. With further heat treatments such as HIP, the residual porosity could be almost successfully removed [19].

Usually for L-PBF the built part is physically fixed to the build platform, connected by support structures [20]. If not connected with support structures, the component could be fixed to the build platform with an offset of stock material. L-PBF process definitely needs support structures, not only to physically hold the part not to let it fall because of kinematic movements of the machine, but also and mainly to transfer the heat created with melting steps, acting like a heat sink [20]. In fact, one of the disadvantages of L-PBF process is the shrinkage: residual stress and deformation that can occur due to local temperature differences [20].

It is not easy to remove all supports from the component: it is a very delicate procedure that requires manual labour. The reasons why it is rarely done with machines are the complexity of the components and low volumes of production for

AM parts. It is very important to add supports only where needed because a significant use of them will lead to higher material waste, increased risk of build failure and longer production times and higher costs.

One of the biggest advantages of this technology is that parts can be manufactured to near-net shape, no matter how complex they are [21]. Obviously, there will be the need of removing support structures and to finish functioning surfaces if requested. A machining allowance must be provided for post processing finishing. This also means that free-form geometries, infill structures (as honeycomb or lattice) could be easily manufactured but post processing costs and times depend on their complexity.

Among the general advantages of L-PBF in the final product we can find:

- Weight reduction if combined with topology optimization;
- Ergonomic design;
- Freedom of creating complex parts;
- Integrated parts;
- Customization [10].

The advantages of the process are instead:

- Absence of tools;
- Absence of blocking devices;
- Undercuts allowed;
- One single production step;
- One single machine, unlimited shapes;
- Less manual labour;
- Times and costs linked only to dimension and not to geometrical complexity [10].

The disadvantages of the product are:

- Necessity of support structures;
- Surface quality worse than traditional manufacturing (not in all cases);
- Cost of materials;

- Limited number of commercial materials [10].

Among the disadvantages in the process there are:

- Restricted manufacturing volumes;
- Parts dimensions limited by machine dimensions;
- Limited building speed;
- Every machine can work with a limited number of materials [10].

Not all metal materials are available for this process: as mentioned in chapter 1.1., the list is quite short, with less than ten alloy families.

The L-PBF process is carried out in a closed process chamber in an inert gas atmosphere, making Nitrogen or Argon flow in the chamber [21]: this guarantees oxygen levels less than 0.1% that can limit interactions between the powder and the environment [19]. The inert gas removes also fume and weld splatter from the build area.

The size of L-PBF machines range is from 50x50x50 mm up to 800x400x400 mm.

After the manufacturing of the parts, it is possible to do some heat treatments to give them all desired characteristics. First, a stress relieving could be performed to reduce the stresses that were created during the melting process. Among the other heat treatments there could be the annealing, the HIP (Hot Isostatic Pressing), recrystallization or precipitation hardening [18].

The layer thickness used in L-PBF technology is between 15 μm to 100 μm , so the surface quality is almost the same as casting [21]. Post processing may be required, depending on the application.

L-PBF process is not capable of building parts with isotropic characteristics: along the vertical z direction material properties are lower in comparison to x and y ones [1]. This is due to layer-wise build-up and must be considered during process planning [1]. Overall material properties could anyway be selectively configured by locally adjusting process parameters [21].

Since LBM process is different from traditional manufacturing, material properties achieved are a little higher than the ones obtained with other technologies such as forging and casting, but generally elongation is typically lower [22].

Building part costs are still higher than traditional manufacturing for high numbers of part produced, but they can be cheaper for low volumes of production [23]. The cost of a single component also depends on the height [23] (but also on the quantity of the melted material in the layer): to keep it minimum, parts could be orientated in the platform [23]. Another factor that affects costs is the volume platform filling: to increase the efficiency of the job and to minimize the number of jobs run, the available build space should be maximized, also using nesting strategies [23]. Another factor that affects costs is the powder [23]. The one that remains in the system after the job is done, could be partially recycled and reused [23]. This process could affect final part characteristics, because it may change alloy composition (due to oxidation) and powder size distribution [18]. Every part should also be planned with a specified building orientation to increase build success chances and to minimize the use of supports in order to save costs [23]. To reduce costs and to optimize the performance, design for additive manufacturing rules could be used. Parts designed for AM (explanation in detail in chapter 4.1) are more cost efficient compared to parts designed for conventional process [24].

2. Critical analysis of the original component

2.1. Component selection

Not every three-dimensional object benefits from AM. It is very important to evaluate if it is suitable to manufacture using AM. Oerlikon Graziano gave Oerlikon AM the possibility to select which part could be more appropriate for this thesis project.

The part chosen is a small hydraulic module with internal channels. The main advantage of additively manufacturing this part is that there are certain channels that could be closed because they are only useful to hollow the tubes from the full part, so there could be the chance of reducing its weight. It is also possible to change the routing of those channels to make the path shorter, leading to a reduction of pressure losses on hydraulics.

Performing a topology optimisation can be advantageous for this component because it has a high potential for weight reduction. It can lead to a reduction of weight on the entire vehicle were this hydraulic module is mounted. This can bring advantages on the whole system with the reduction of fuel consumption and CO₂ emissions as well.

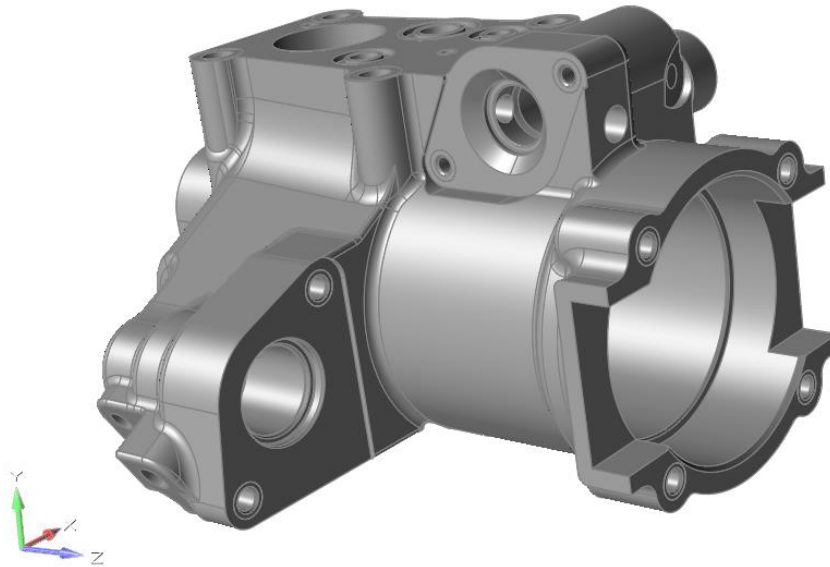


Figure 2.1 - Original component, View number 1, Inspire

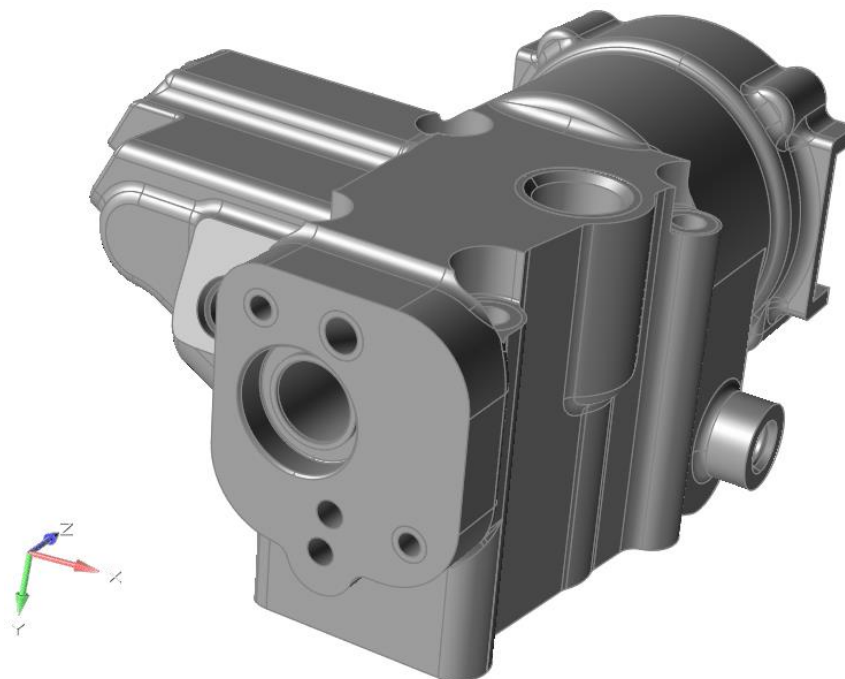


Figure 2.2 - Original component, view number 2, Inspire

Its original material is an Aluminium alloy called Anticorodal 6082, properties at room temperature are presented below in Table 1. This part is originally manufactured by forging. Its functioning temperature is from -40°C to 140°C but,

as the characteristics at those different temperatures were not provided by the customer, the functioning temperature assumed for this piece of work is 20°C.

Name	Symbol	Unity of measure	Value
Young's modulus	E	GPa	69
Poisson ratio	ν	/	0.33
Density	ρ	g/cm ³	2.7
Yield stress	σ_Y	MPa	230
Coefficient of thermal expansion	α	1/K	23.2E-6

Table 1 - Anticorodal 6082 properties

In the picture below the part is showed in its assembly (figure 2.3 and 2.4), the component chosen is in yellow.

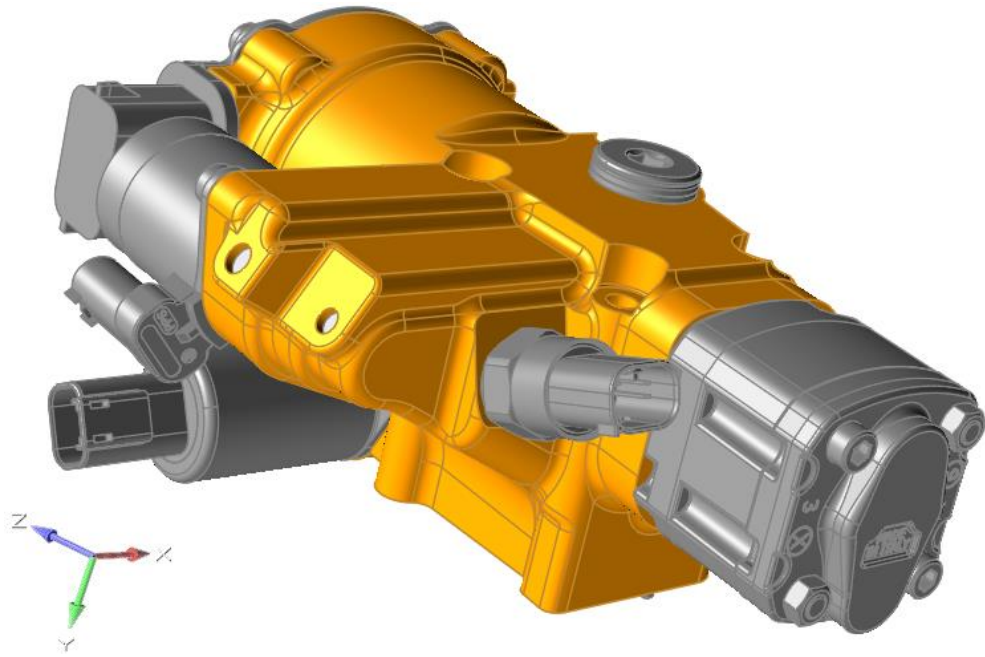


Figure 2.3 - Assembly of the original component, marked in yellow. View number one, Inspire

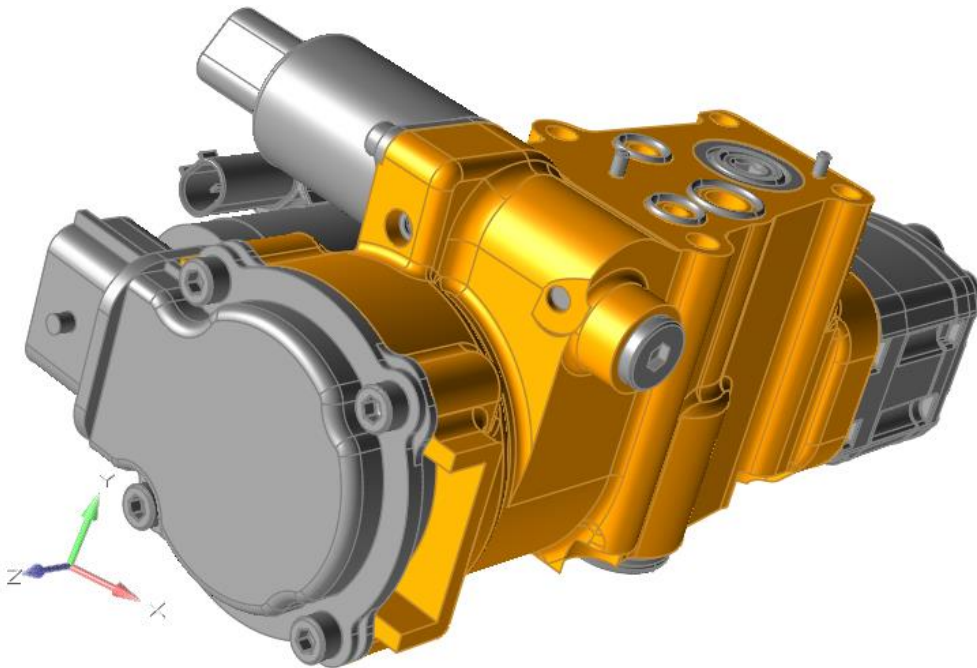


Figure 2.4 - Assembly of the original component, marked in yellow. View number two, Inspire

2.2. Loads, constraints and boundary conditions

The first step, once the geometry is provided, is the application of loads, constraints and boundary conditions. It is very important to have precise instructions to set-up a good model that could represent the real functioning. Theoretically, there should be included also loads due to machining and postprocessing, if data are available. There is also the possibility to add different load cases to see different normal functioning.

The component is fixed in the central four big holes where the screw link it to the rest of the assembly. Since this part is a hydraulic module, a pressure of 4 MPa acts in each inner channel.

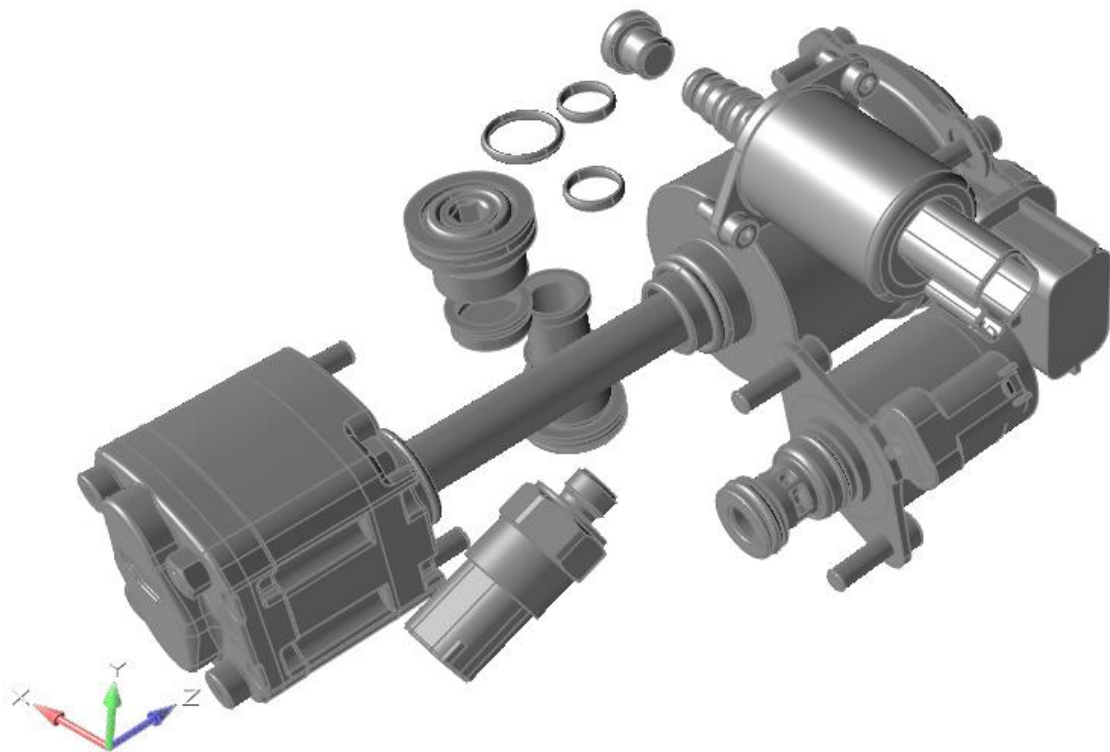


Figure 2.5 - Components linked to the part chosen, Inspire

The component is linked with other parts (motor, pump, valves, solenoid, pressure sensor and caps as shown in figure 2.5). For this reason, the weight of the linked parts (see Table 2) is included in the model, applied in their center of gravity. The

masses were calculated with the assembly file in NX, by knowing the material they are made of. In Table 3 the coordinates of the center of gravity of the masses used are displayed.

	Pump	Motor	Valve	Solenoid	Pressure sensor	Threaded cap	Cap
Mass (Kg)	1	0,28	0,18	0,18	0,03	negligible	negligible
Clamping forces (N)	2634,7	5691,1	5083.1	2634.7	negligible	15639	4289,8

Table 2 - Mass and clamping forces of linked bodies

Coordinates	X [mm]	Y [mm]	Z [mm]
Pump	-5.74	0.008	81.46
Motor	7.019	0.101	-59.44
Valve	-22.79	40.50	58.00
Solenoid	-56.07	-2.17	48.95
Pressure sensor	-31.01	-4.86	-27.59

Table 3 - Coordinates of the center of gravity of the masses.

In this case study two different load cases have been applied. In the first load case, clamping axial forces are applied in outgoing direction only on the inner cylindrical housing of bolts, hypothesizing that there is no contact between part and bolts. In the second load case there is also an equal and opposite force applied in the contact area between component and bolt, see detail in figure 2.6.

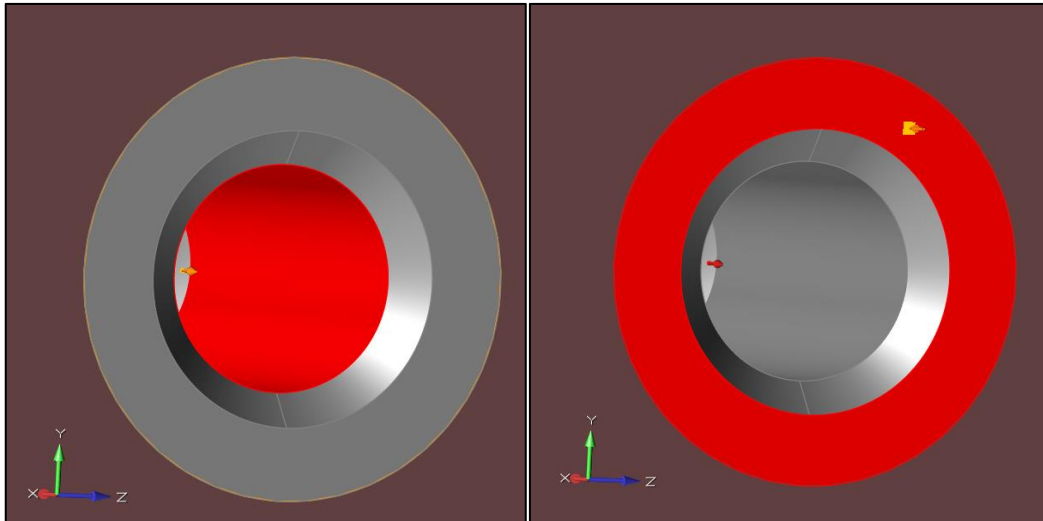


Figure 2.6 - Application of the force. Load case 1 at left, Load case 2 at right, Inspire

A torque of 1,4 Nm, due to motor and pump rotation, is put on the contact/friction area, where the bolts act.

As the customer wanted, it was also considered to add three times the gravitational acceleration (29418 mm/s^2) in negative y axis direction. In figure 2.7 and 2.8 a preview of loads, masses and constraints applied with the software Inspire is presented.

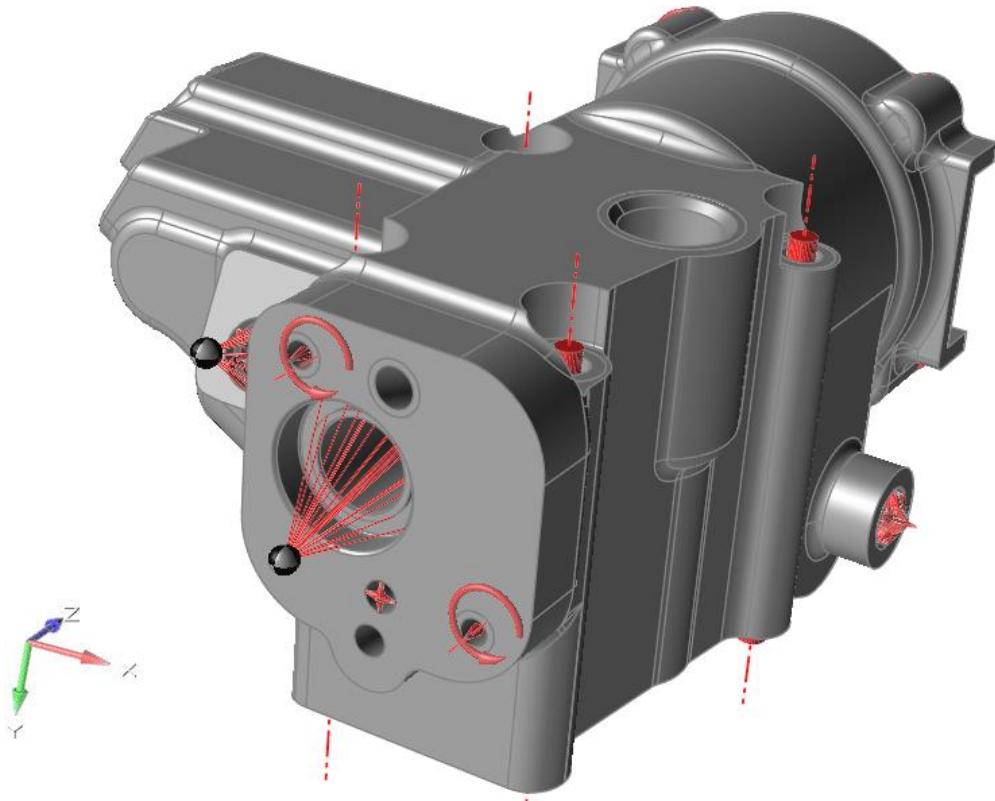


Figure 2.7 - Loads applied on Inspire. Bottom view.

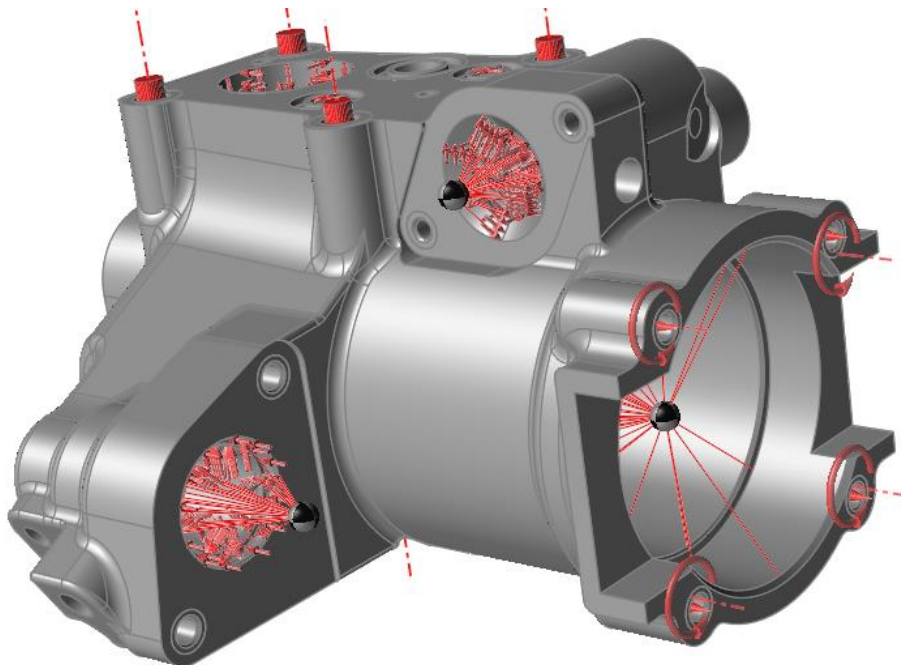


Figure 2.8 - Loads applied on Inspire. Top view.

2.3. Design space identification

Once loads, constraints and boundary conditions are known, they should be applied on the correct surfaces. It is necessary to isolate those parts because they cannot change their topology due to different reasons such as functional surfaces and connections to other parts. These sections are called non-design spaces or frozen areas. [25] It is best practice in topology optimization to add all the loads and boundary conditions to such sections. The rest of the part is called design space or design area.

The Design Space is the area that the software can use to modify the topology of the component. [6] Unlike the Non-Design Space, it has no load, no constraints or boundary conditions applied and no functional surfaces.

To identify the design of the non-design space, NX 12 has been used, because Inspire was not able to handle this operation with the complex geometries in this part. With the command Thicken, a partition of channels has been created. The chosen thickness for channels is 1,5 mm, in certain areas it has been made bigger, in order to increase the functional surfaces. An equation, presented below (1), has been followed to understand which the minimum thickness of pipes is. s_0 is the minimum pipe thickness, p is the maximum pressure applied, d_e is the external diameter of the pipe, σ_{am} is the yield stress, c is the overthickness assumed as zero for aluminium alloys, and a is the manufacturing tolerance assumed as neglectable. The values used in this equation for the smaller pipe are: $p=40$ bar, $d_e=6$ mm, $\sigma_{am}=226$ MPa. The result with the minimum channel is $s_0=0,052$ mm, that is why the thickness chosen is 1,5 mm.

$$s_0 = \left(\frac{pd_e}{20\sigma_{am}+p} + c \right) \cdot \frac{100}{100-a} \quad (1)$$

As displayed in figures 2.9 And 2.10, channel shape could be modified in order to have an additively manufacturable geometry. In those figures, the imprints of the

tools for creating holes in traditional manufacturing are presented. Those imprints will be deleted after in chapter 4.2.

O-rings and dowel pins seats are part of the non-design space because, even if they don't have loads or constraints applied on, it is important to keep their surfaces for connecting other components.

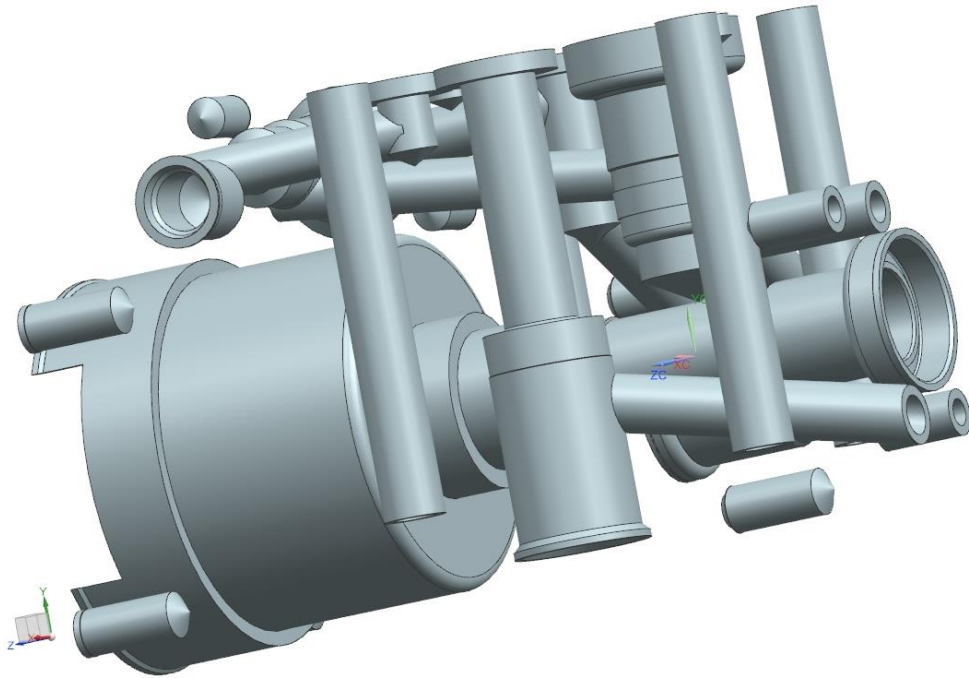


Figure 2.9 - Initial non-design space. View number 1, NX

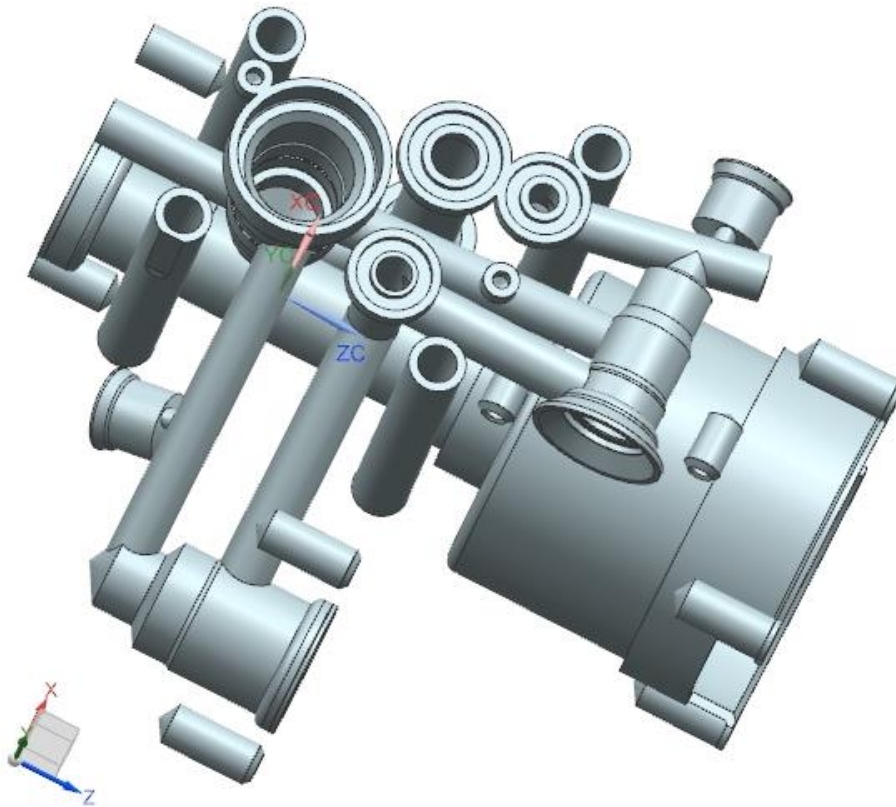


Figure 2.10 - Initial non-design space. View number 2, NX

Initially, a FEM structural analysis is performed on the original component to verify that it can handle the loads applied, so that an optimization may be possible. The results are displayed in chapter 2.4.

After analysing the part, it would be necessary to transform the geometry of the component to make it ready for topology optimization. To do so, all curved surfaces such as fillets and edge blends should be removed in order to simplify the geometry [26]. The Design Space area can be extended to give the material the possibility to position itself in the optimum way in a bigger space [26], keeping in mind the objects that are in the surrounding, being careful that those extension will not intersect other parts.



Figure 2.11 - Complete assembly, part is transparent

This CAD preparation step is very important because it lets the design space increase to give the software the possibility to put the material only where needed to increase its stiffness [26]. The result part, now ready for optimization, after adding loads and boundary conditions, is displayed below in figures 2.12 And 2.13: the yellow area is the design space, the grey section is the non-design space. In some regions there was no possibility to increase the Design Space because the component, in transparency in figure 2.11, is assembled to another part, displayed in dark yellow, that limits its extension.

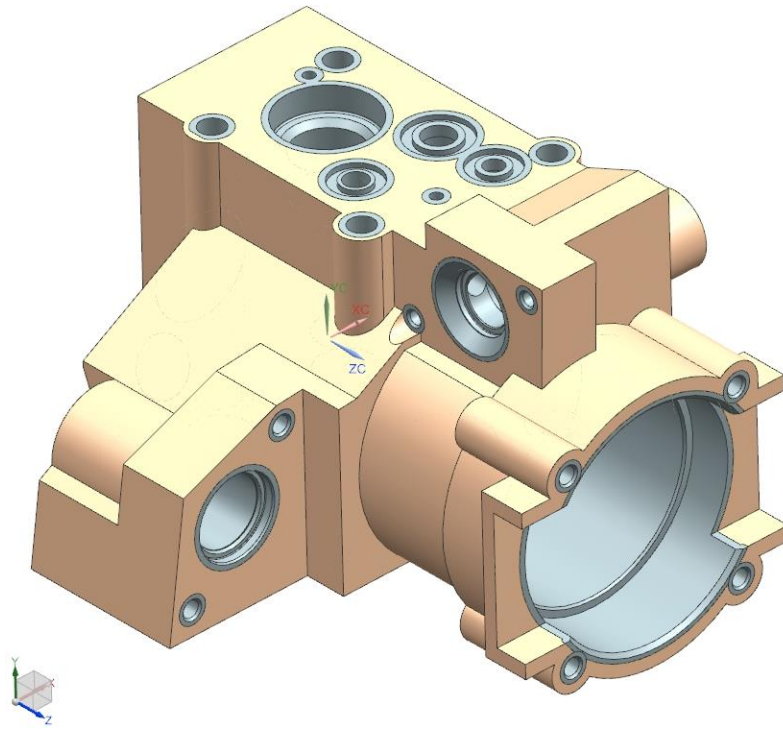


Figure 2.12 - Design space and non-design space. Isometric view 1, NX

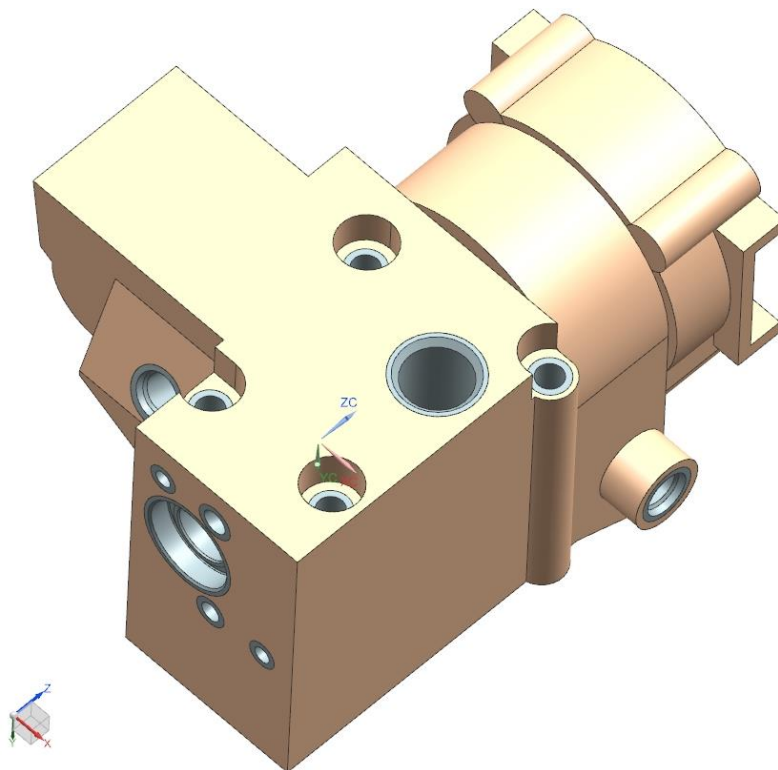


Figure 2.13 - Design space and non-design space. Isometric view 2, NX

To make the part more additively manufacturable, it is also necessary to change the routing of channels. Afterwards other modifications, presented later in detail in chapter 5, will be made to delete sharp edges and points., the new non-design space is shown below in figure 2.14 And 2.15.

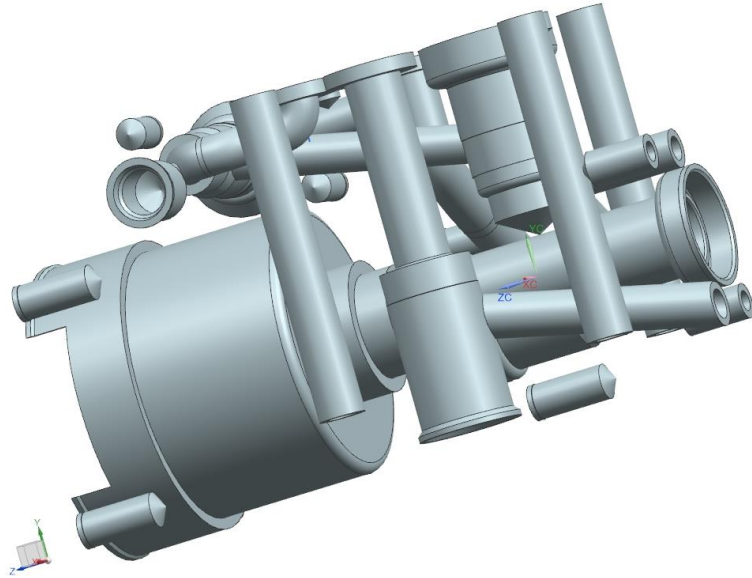


Figure 2.14 - Non-design space, first review. First view, NX

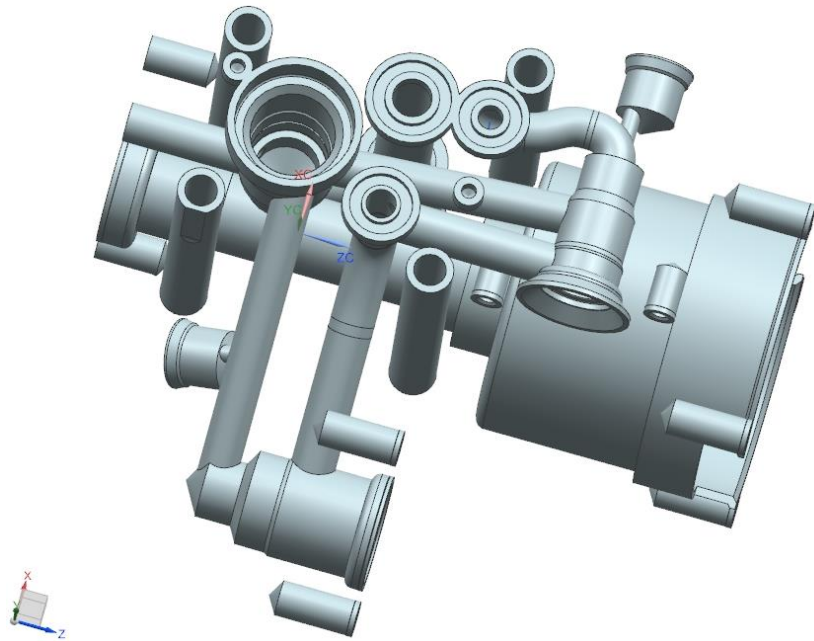


Figure 2.15 - Non-design space, first review. Second view, NX

2.4. Finite element method structural analysis

Following Finite Element Method, a structural static analysis is carried out. Two different software have been used to perform it with the same loads and boundary conditions: Inspire and NX Nastran.

The element size dimension chosen is 1 mm for both software and the type of element is Linear Tetra 4 (first order) for NX Nastran and Inspire. On Inspire you can change the order of the element by selecting *More accurate* (second order) instead of *Faster* (first order) while setting up the analysis, but the computational time is too high, and it needs too much disk space to be performed. The best way of doing these analyses is with parabolic elements Tetra 10 (second order), but it required too much computational cost, because the part is not small, and Inspire software did not manage it. So, first order elements have been used with both software to make the comparison more consistent. The results of these analyses are not only useful to see that the original component can handle the loads, but also to

compare stress levels between the original and the optimized manifold (see more on chapter 7).

This analysis is performed with the original material, which is Anticorodal 6082, an Aluminium alloy. The mechanical properties that are mandatory to perform and review the analyses are the Young's modulus E , the yield stress σ_Y , Poisson ratio ν and the density ρ at the functioning temperature, which is 20°C. These properties are specified in chapter 2.1.

While on Inspire it was easy to apply loads directly on the surfaces by creating rigid connections, with NX the creation of RBE3s are required to add a moment on a surface. It is also required for linking the lumped masses from the centre of gravity of the components around the part (CONM1 elements) to the surfaces where they act.

On Inspire there is the possibility to see the results for both displacements and stresses with Result Envelope mode, that shows the maximum value for each result type across all load cases. Since NX doesn't have this option, the results will be displayed divided by load case. Displacements achieved with Inspire are presented below in figure 2.16 and 2.18 for load case 1 and 2.20 and 2.22 for load case 2. Displacements achieved on NX Nastran are instead presented in figure 2.17 and 2.19 for load case 1 and 2.21 and 2.23 for load case 2. In the different load cases the maximum value is less than three hundredth of a millimeter, which is acceptable.

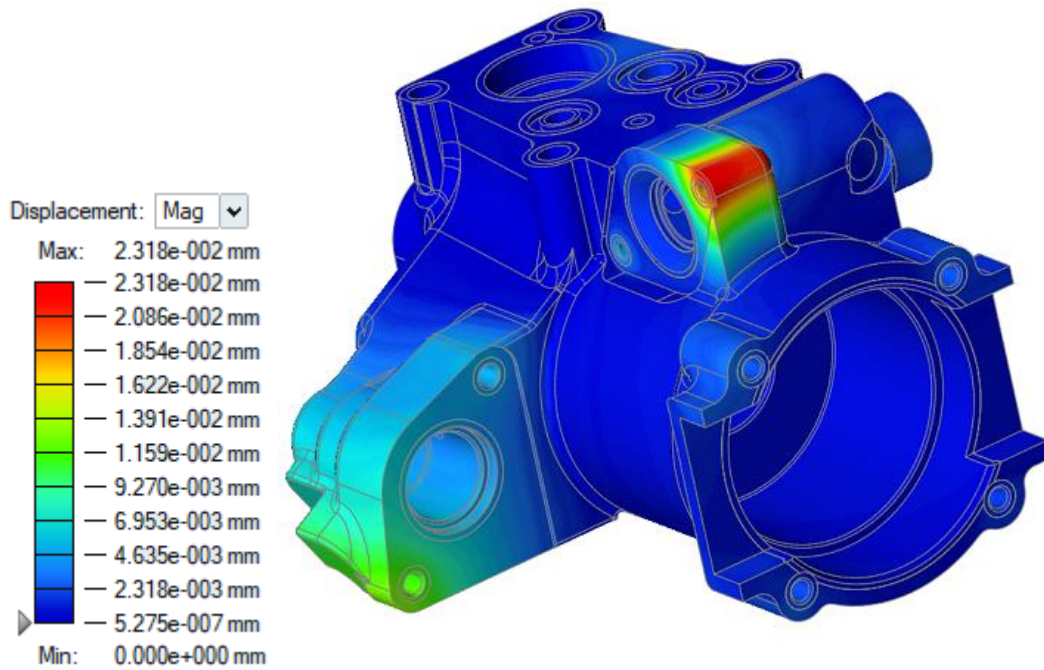


Figure 2.16 - FEA of the original component on Inspire. Displacement load case 1. View 1

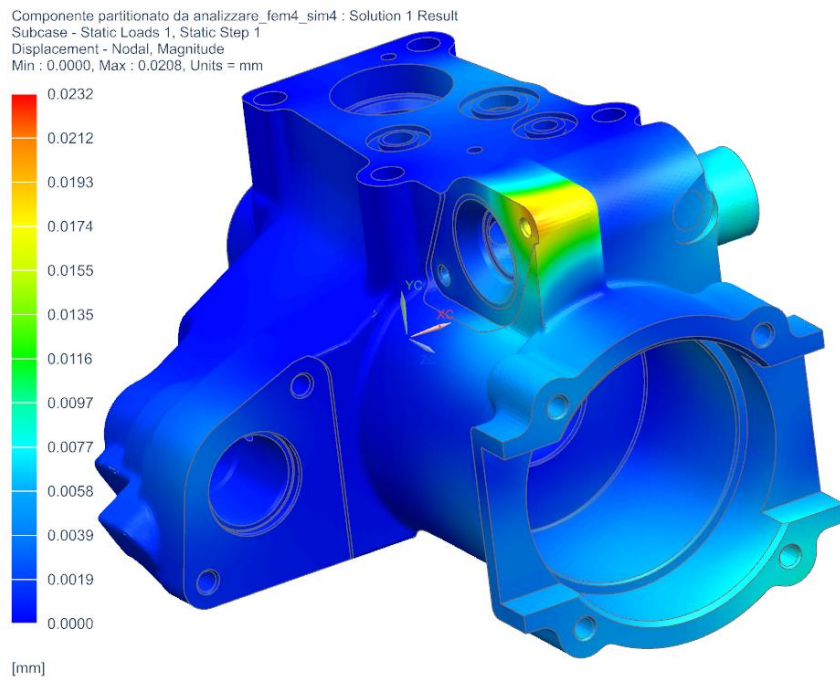


Figure 2.17 - FEA of the original component on NX Nastran. Displacement load case 1. View 1

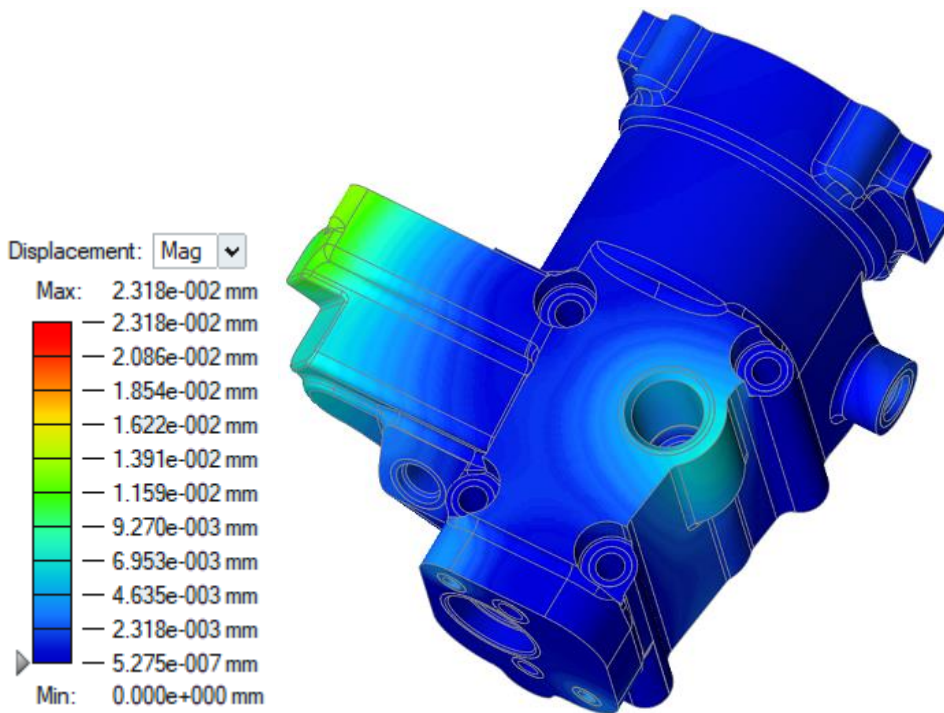


Figure 2.18 - FEA of the original component on Inspire. Displacement load case 1. View 2

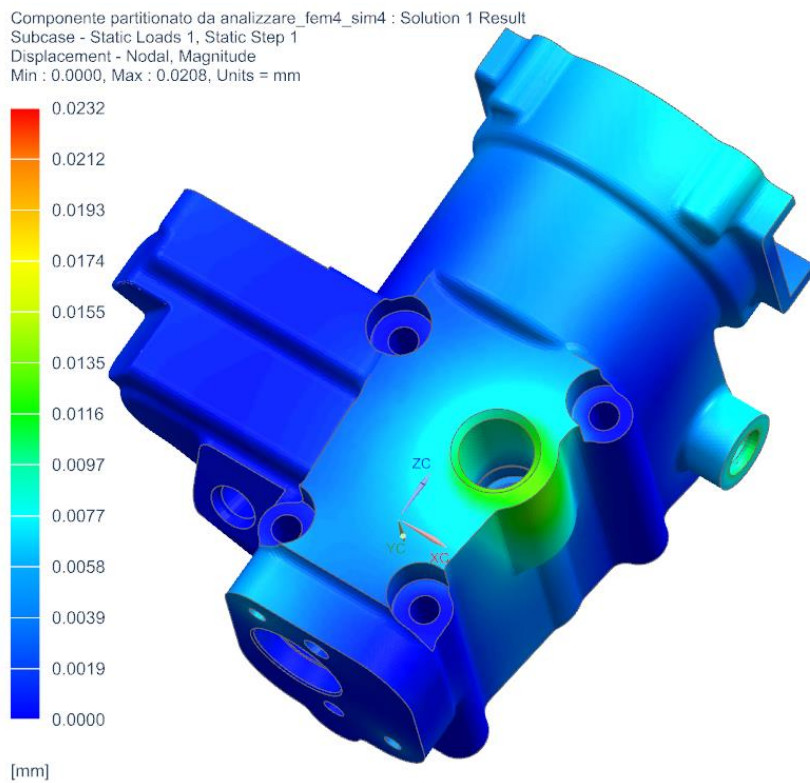


Figure 2.19 - FEA of the original component on NX Nastran. Displacement load case 1. View 2

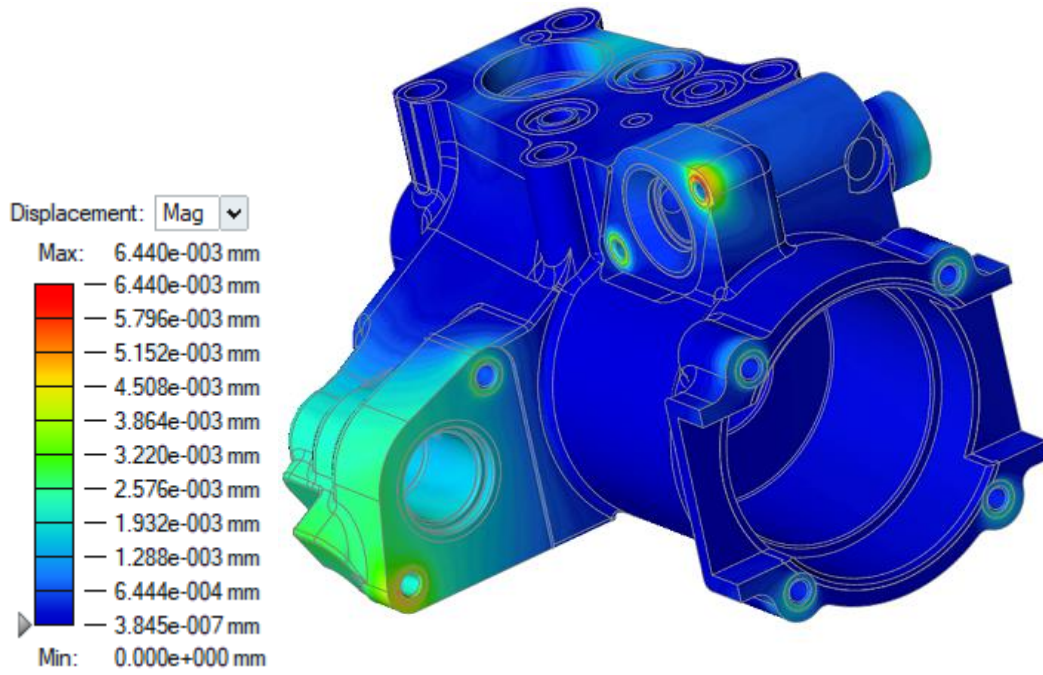


Figure 2.20 - FEA of the original component on Inspire. Displacement load case 2. View 1

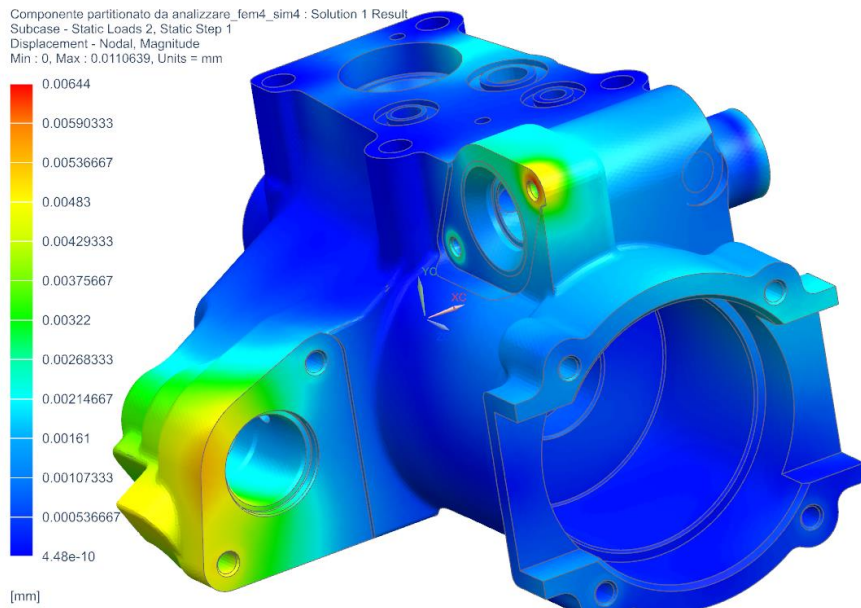


Figure 2.21 - FEA of the original component on NX Nastran. Displacement load case 2. View 1

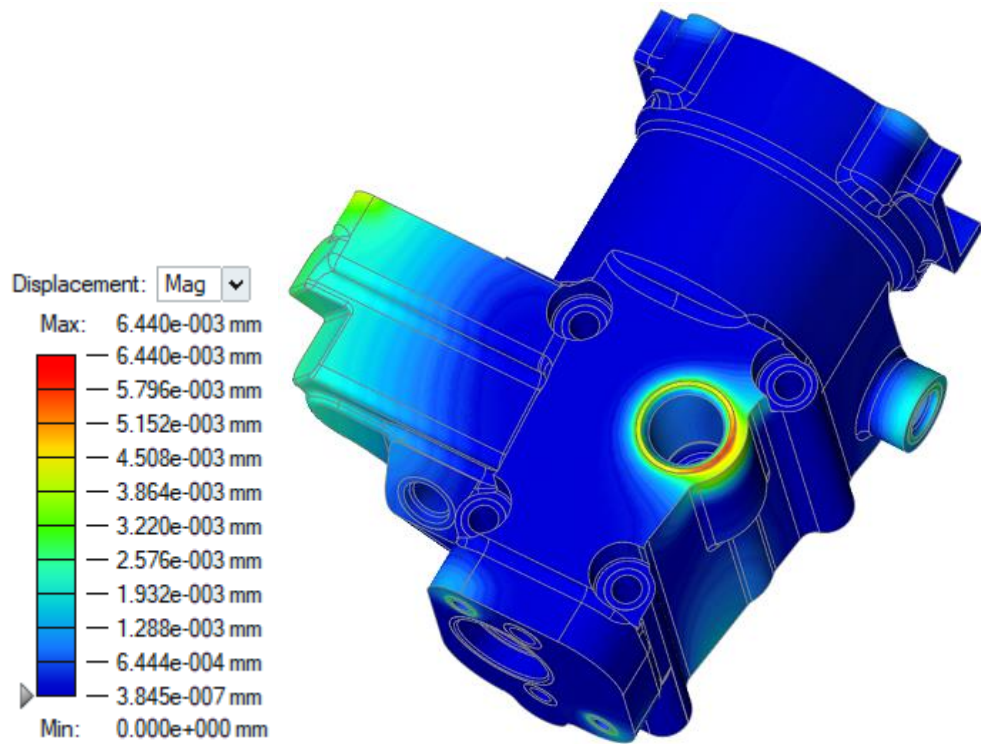


Figure 2.22 - FEA of the original component on Inspire. Displacement load case 2. View 2

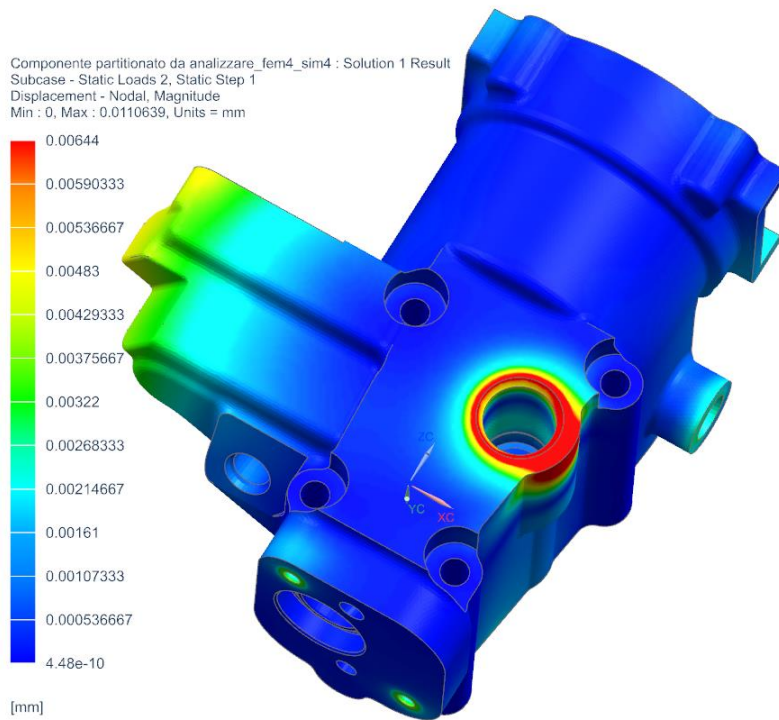


Figure 2.23 - FEA of the original component on NX Nastran. Displacement load case 2. View 2

In the pictures below (figure 2.24, 2.25 and 2.26, 2.27 for Load case 1 and figures 2.28 and 2.23 for Load case 2) Von Mises stress contour plots are displayed with both Inspire and NX Nastran software. Safety factor contour plots could also have been displayed here, but since NX Nastran does not have this option and since a comparison between the two different software could have not be made, it was decided not to include any safety factor contour plot. Safety factor, calculated as yield stress divided performed stress, should never be less than 1.

$$safety\ factor = \frac{yield\ stress}{actual\ stress} \quad (2)$$

The minimum safety factor chosen for these analyses is 1,2. This means that no performed stress should be higher than the yield stress divided by 1,2 (193 MPa for Anticorodal). The minimum factor obtained is almost 1 only in some very small areas, that are negligible due to errors on minimum mesh element size. In the rest of the component, the safety factor is always higher than 1.35, which respects the minimum value defined.

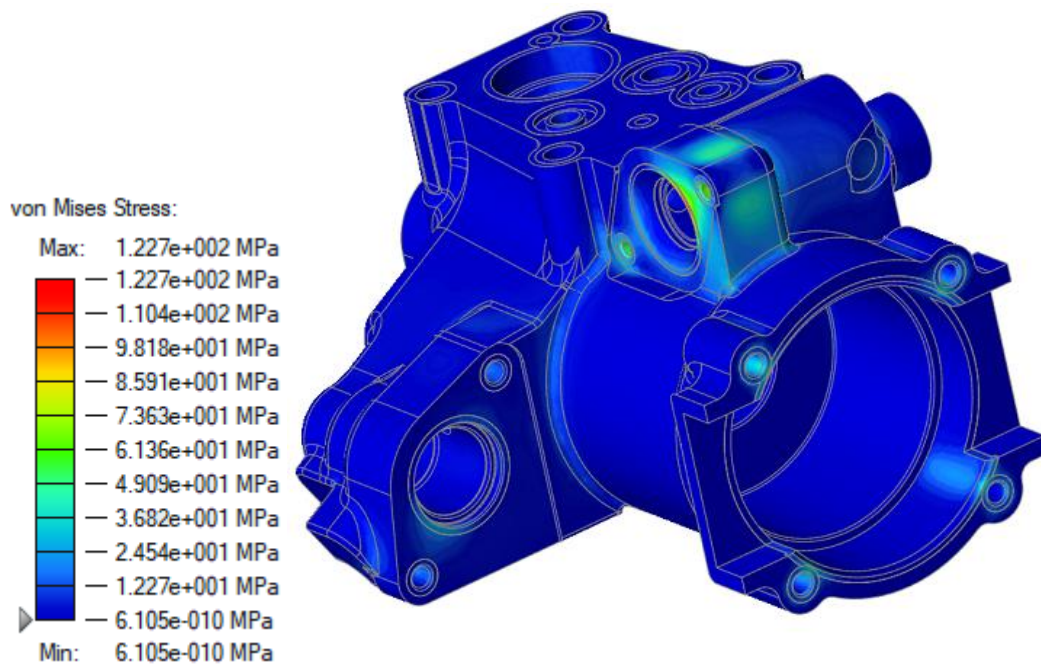


Figure 2.24 - FEA of the original component on Inspire. Von Mises stress load case 1. View 1

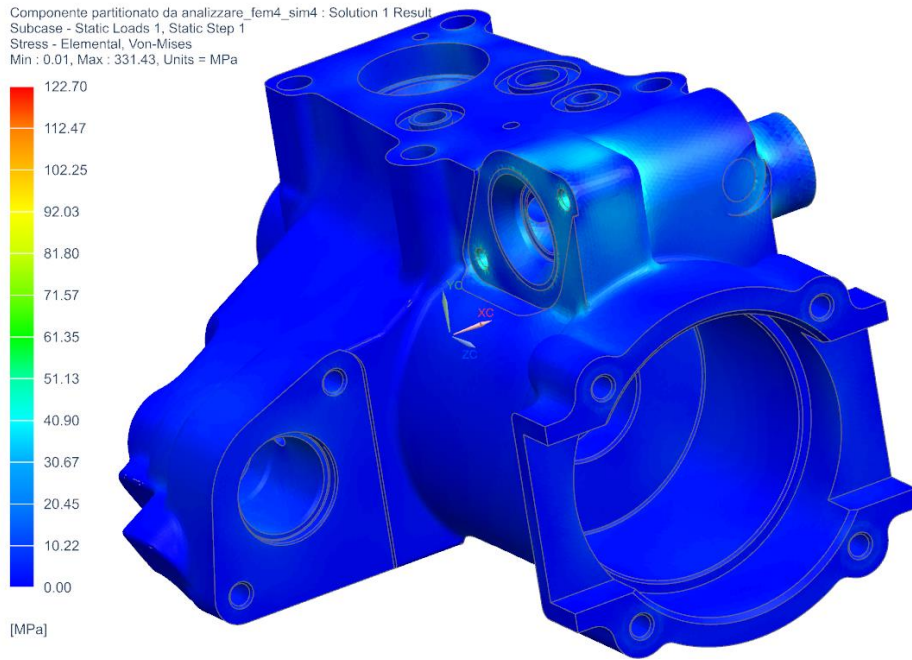


Figure 2.25 - FEA of the original component on NX Nastran. Von Mises stress load case 1. View 1

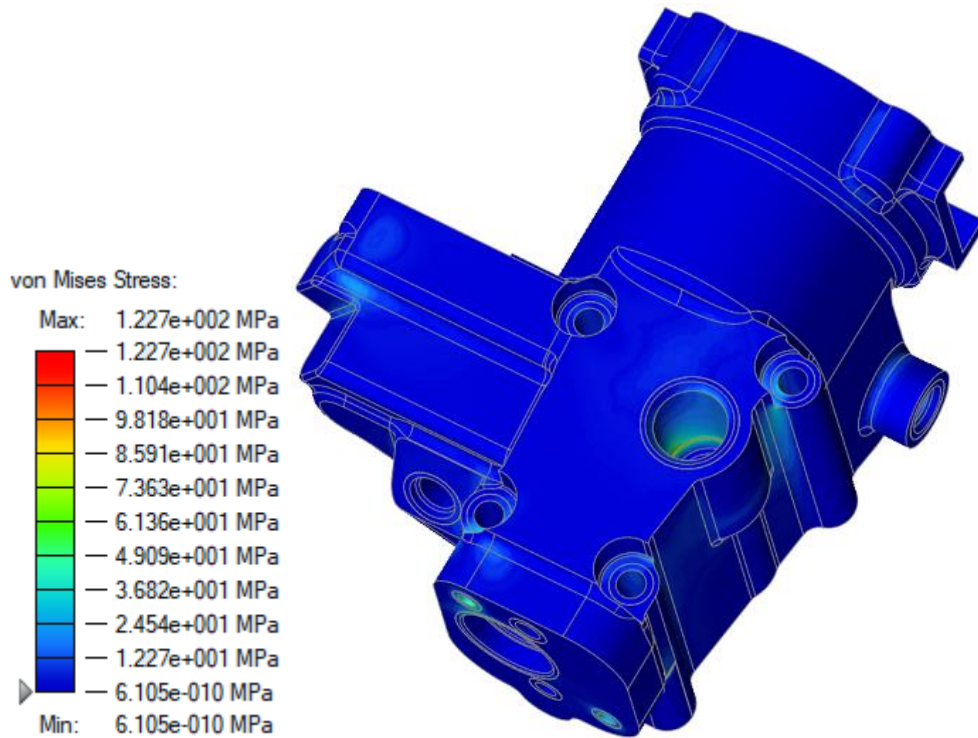


Figure 2.26 - FEA of the original component on Inspire. Von Mises stress load case 1. View 2

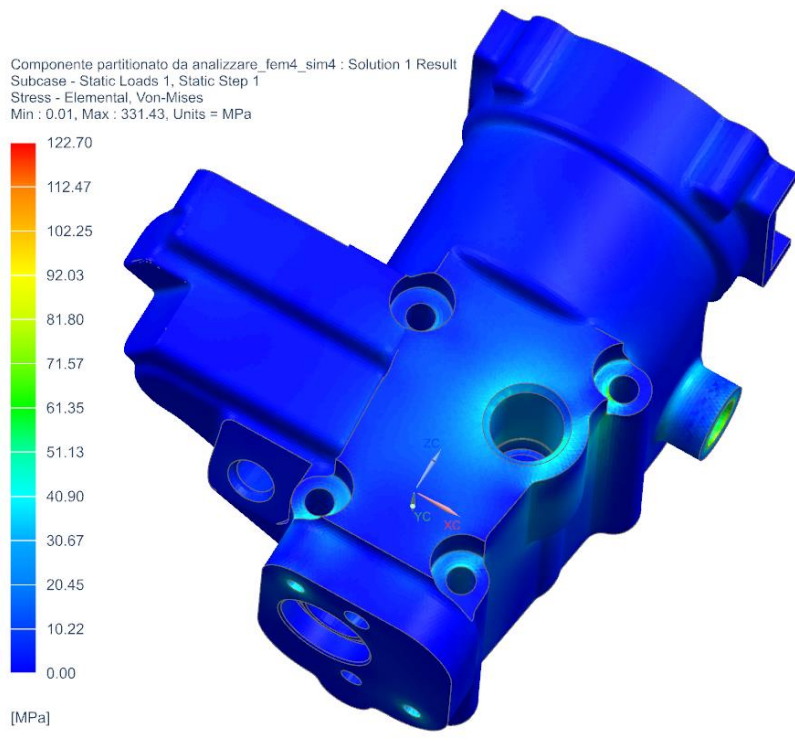


Figure 2.27 - FEA of the original component on NX Nastran. Von Mises stress load case 1. View 2

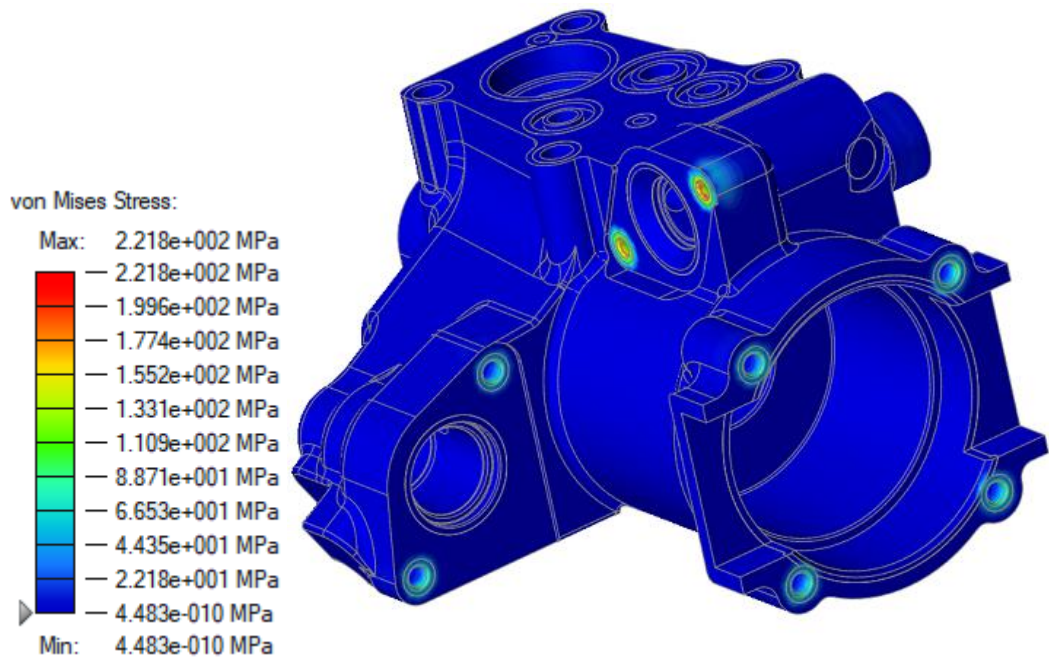


Figure 2.28 - FEA of the original component on Inspire. Von Mises stress load case 2. View 1

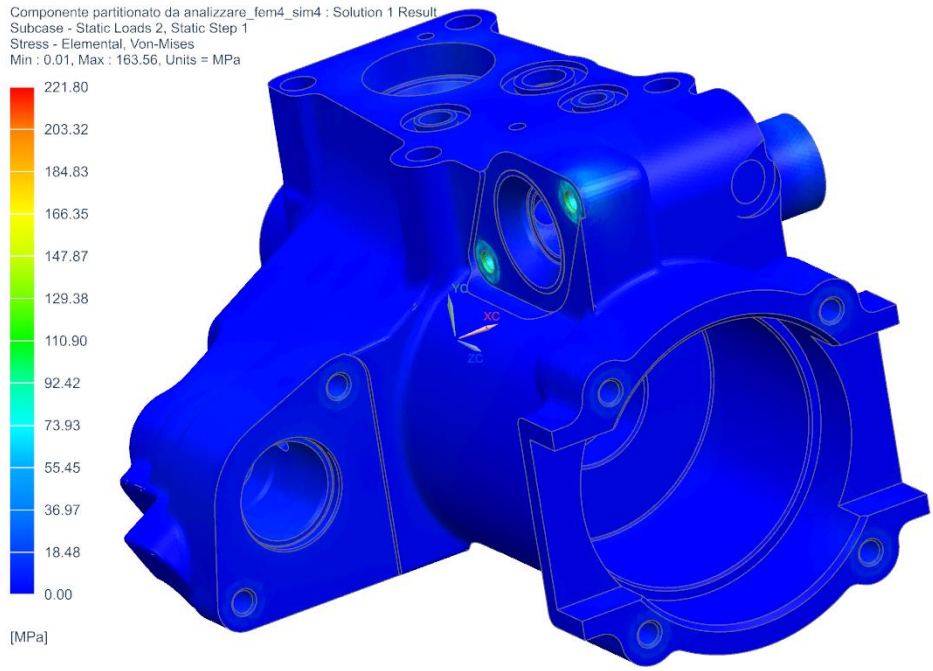


Figure 2.29 - FEA of the original component on NX Nastran. Von Mises stress load case 2. View 1

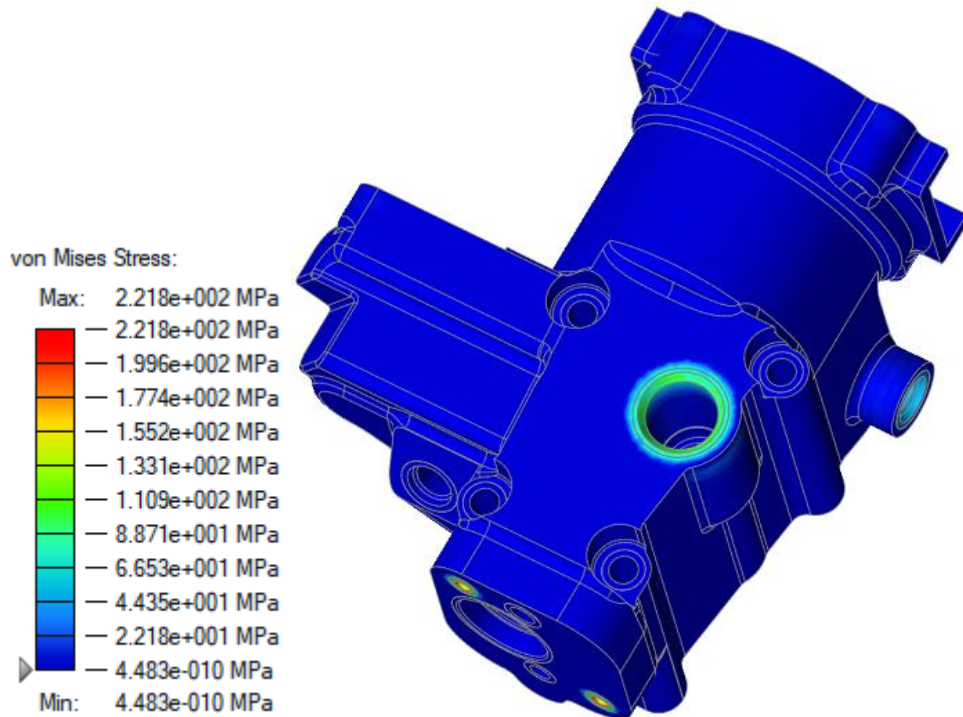


Figure 2.30 - FEA of the original component on Inspire. Von Mises stress load case 2. View 2

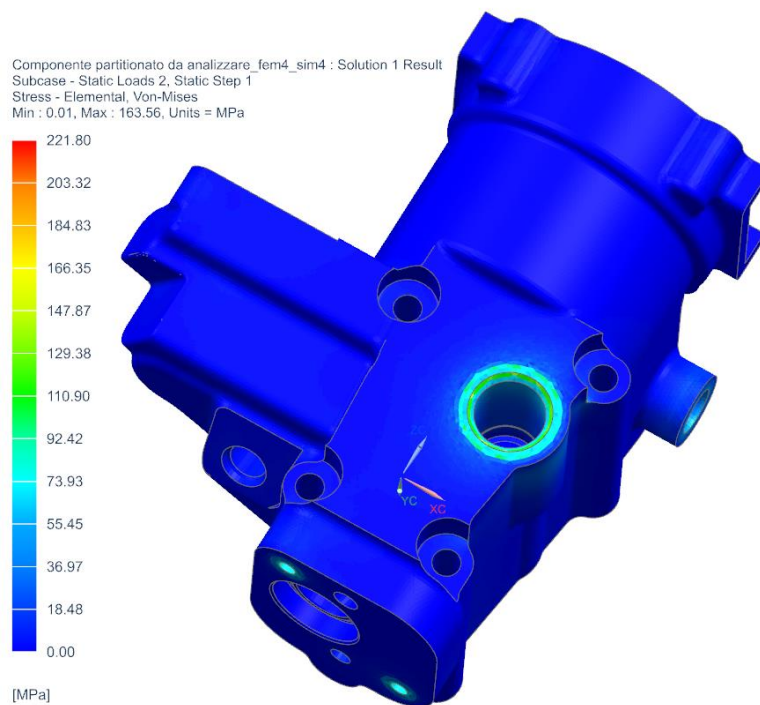


Figure 2.31 - FEA of the original component on NX Nastran. Von Mises stress load case 2. View 2

As already clarified, on NX Nastran it is not possible to have a result envelope that summarizes the results and there is no option to see a safety factor contour plot. On the contrary, there are more options to display stresses and displacements, for example based on their direction, magnitude or if they are referred to a node or to an element.

The results of displacements with NX Nastran are presented below in figures 2.24 to 2.26. Von Mises stresses on NX Nastran are displayed in figures 2.27 to 2.30.

In order to make the comparison more consistent, the scale in the left was modified on NX Nastran, so that the maximum values was settled as the same on Inspire. The minimum value had been considered as zero in all the contour plots. The maximum values achieved on NX Nastran are visible in Table 5. On Nx Nastran the result was presented viewing all the elements in the mesh, but to make the comparison more adequate since on Inspire this is not possible, the mesh was hidden.

Comparing the results of the two software, they look different, especially in the maximum values. But with a closer view to the colour distribution in the images, it is about the same in both cases. Stresses are high in the same areas.

Below a tab that displays the different maximum values.

Displacements [mm]	Inspire	NX Nastran
Load Case 1	0,023	0,021
Load Case 2	0,006	0,011

Table 4 - Maximum values of displacement, Inspire VS NX.

Von Mises Stress [MPa]	Inspire	NX Nastran
Load Case 1	123	331
Load Case 2	222	163

Table 5 - Maximum values of Von Mises stress, Inspire VS NX Nastran

The maximum values of displacements and Von Mises stress in both load cases are extremely different. This could be due to an error in the mesh, because the results would have been more accurate with a second order analysis. Anyway, the maximum values reached are just for small elements, which may be considered negligible.

3. Topology optimization

3.1. Mathematics in topology optimization

In the optimization field it is possible to identify three different types of problems: topology optimization, sizing optimization and shape optimization. [6] Out of these three, topology optimization is the most commonly used method for designing parts for AM, but sometimes it is a combination of the three. In this work Topology Optimization has been used only.

Topology optimization constitutes the first step towards the realization of an optimal structure, from a conceptual point of view. [6] Setting a topology optimization problem requires, as a preliminary data, the definition of a domain of existence [7]. This domain must have a definite shape and represents the space within which the structure is bound to exist [6]. The definition of load and constraint conditions completes the definition of the problem [6]. Assuming that the existence domain is made up of structural material, the optimization process leads to the identification of its optimal disposition, looking for the configuration characterized by maximum rigidity [6]. In this way the objective is to eliminate the useless material and to give the correct form to what is strictly indispensable [6].

Every optimization problem requires the presence of at least one objective to achieve and one or more variables on which it is possible to act to that purpose [6]. For structural optimization problems, objectives are most of times weight, displacements or stresses. Design variables are instead parameters whose value can be varied within a defined range [6]. Optimization problems are also characterized by side constraints, limitations that define the admissibility field of optimization variables, and equality and inequality constraints [6]. Equality constraints are rare, but inequality ones are common and let the subdivision of the solution existing space between feasible and unfeasible solutions [6].

The application of optimization methods on structural field involves the use of objective functions and constraints defined basing on state variables of the analyzed structure [6]. The evaluation of state variables and, indirectly, of the overmentioned functions, is generally assigned to finite element numerical codes [6]. With every modification of the structure proposed by the optimization method, the finite element code evaluates its new state and the optimization problem [6].

There are three different types of methods, depending on the information they need to operate: zero order methods, first order methods and second order methods [6]. Zero order methods are the easiest because they give the possibility to deal with non-convex and non-continue functions and discrete variables [6]. The disadvantage is that they need to evaluate the objective function an extremely high number of times [6]. First order methods need to know the punctual value of the objective function and the value of all his derivatives to identify the research direction of the optimum point [6]. Those methods are more efficient than the previous but calculation costs of derivates are high [6]. In the end second order methods are used rarely because their calculation costs are extremely high. They require to know the punctual value of the objective function, its first and second derivative [6].

In the field of structures, first order optimization methods are more efficient than zero order ones [6]. That is because first order methods require the evaluation not only of the punctual value of the objective and the constraints functions, but also of the value of their derivatives compared to optimization variables [6]. The design sensitivity analysis has the duty to determinate the quantity of those derivatives this requires the evaluation of the derivatives of state variables of which they are a function [6]. Therefore, the calculation of sensitivity coefficients requires the execution of a high number of analysis [6].

In the initial research phases, it was hypothesized that there was a direct link: the determination of state variables and their derivatives was executed in every optimization cycle [6]. This method was not efficient because of the high number of analyses required [6]. Later it was presumed an indirect interface: state variables and their derivative values, coming from the numerical calculation code, used in

the previous analysis, were used to realize an approximated mathematical model of the structure [6]. The obtained model is characterized by several simplifications: it has a reduced validity field, that is why the optimization variables range of variability must be appropriately restricted in order to not make big errors [6]. The model obtained is subjected to optimization: now it is possible to execute more iterations without further structural analysis [6]. The first optimization cycle is closed when the optimization procedures are not anymore able to improve the model obtained [6]. The finite element model is then updated with the optimization results and a new cycle can start with the realization of a new approximate mathematical model [6].

Thus, the solution of a generical optimization problem is obtained through an iterative process made up of different optimization cycles, each one characterized by the iterative application of mathematical optimization procedures to an approximate model type [6].

The convergence of the optimization process is verified two times: first locally with the convergence of optimization procedures applied to the simplified method is checked, second globally with the convergence of the whole optimization process of the structure [6].

The most widespread topology optimization method is SIMP (Solid Isotropic Material with Penalization) [27]. It lets an optimal distribution of the density of the material inside a certain design space, for certain load cases, boundary conditions, production constraints and requirements [27].

The traditional approach to topology optimization provides that the domain is discretized in a grid of finite elements called solid isotropic microstructures [25]. Every element is filled with material in the areas that require it or emptied in the areas where it is possible to remove it, representing voids [7]. The density distribution of the material in a design space is discrete, and each element is assigned a discrete value. If the density is 1, material is required; if it is 0, material is removed.

With SIMP method, introducing a continue density distribution function, the binary problem will be avoided [25]. For every element, density can vary from 1 to a minimum value (ρ_{min}), giving intermediate densities for certain elements [28]. The new mathematical formula that expresses this is presented in the equation below (3) where E is Young's modulus, ρ is the density of the element and p is the penalty factor.

$$E(\rho_e) = \rho_e^p E_0 \quad (3)$$

This formula better represents the behaviour of Young's modulus, since it varies with density. Numerical experiments suggest using $p=3$ [28].

With SIMP method, reducing E leads to a reduction of the rigidity of the element, following the formula below (4), where K_e is the rigidity matrix of the element and N is the number of elements in the design domain [27].

$$K_{SIMP(\rho)} = \sum_{e=1}^N [\rho_{min} + (1 - \rho_{min})\rho_e^p] K_e \quad (4)$$

The SIMP interpolation schemes is well suited for solving stiffness optimization problems [25]. Although, applying it on eigenvalue optimization problems may lead to the appearance of "artificial modes" [29]. For the SIMP schemes this happens as the generalized density goes to zero [29]. Low density regions thus originate low eigenfrequencies [29]. To solve this, one has to use an interpolation scheme that makes sure that the mass to stiffness ratio always is finite as the generalized density vanishes [29]. This method is called Rational Approximation of Material Properties (RAMP), whose scheme is showed below in equation (5) [28].

$$f(\rho(x)) = \frac{\rho(x)}{1+q[1-\rho(x)]} \quad (5)$$

This method is very similar to SIMP method, since q is the penalization factor while p is the penalization factor for SIMP. Having $q=5$ in RAMP is like $p=3$ in SIMP [28]. That is why $q=5$ is set to make the intermediate density approach either 1 (solid) or 0 (void). The relation between the elastic modulus and the material density

at a certain point x is given by the following equation (6), where E^0 is the elastic modulus of the fully solid material [28].

$$E(x) = f(\rho^x)E^0 \quad (6)$$

3.2. Topology optimization of the original component

A topology optimization of the hydraulic manifold has been performed with Inspire 2019 and NX Nastran 12 in order to reduce the weight and to have material only where needed. Thickness constraints selected is 3 mm, which is three times the element size chosen for the FEA [30]. To perform it, material has changed because Anticordal 6082 is not available as a powder in additive manufacturing. The material selected to replace it is AlSi10Mg, an Aluminium alloy, which has slightly better material properties compared to Anticordal 6082 and is a one of the cheapest materials available in the AM industry. Its main average mechanical properties, referred to the *As Built* condition, are:

- Young's module: $E = 65 \text{ GPa}$;
- Yield stress: $\sigma_Y = 240 \text{ MPa}$;
- Poisson ratio: $\nu = 0.3$;
- Density: $\rho = 2.67 \times 10^{-6} \text{ kg/mm}^3$.

Certain mechanical properties, provided by Oerlikon Additive Manufacturing website (<https://www.oerlikon.com/am/en/technologies/am-metal/#31731>), are presented below in figure 3.1.

Material Characteristics	Unit	As Built	Heat-Treated T6
Tensile strength	MPa	410 ± 40	325 ± 20
Yield strength (Rp 0,2%)	MPa	240 ± 40	220 ± 20
Elongation at break	%	5 ± 2	9 ± 2
E-Modulus	GPa	65 ± 5	65 ± 5
Hardness (DIN EN ISO 6506-1)	HBW	120 ± 5	-

Figure 3.1 - Material Characteristics for AlSi10Mg

An overhang angle of 40° has been added as a constraint in the topology optimization: this is the angle at which the part changes from self-supporting to requiring support structures when being additively manufactured. The maximum value of this angle is generally determined by the material and the printer. In order to insert this shape control, a build direction has been identified and can be seen in figure 3.2 and 3.3. The component has been rotated on -45° on x axis and -10° on y axis. This orientation reduces the volume of support structures necessary for the manufacturing process, but it is not optimal for the nesting. An accurate analysis of those aspects is carried out in chapter 6.1.

Design and non-design space have been previously identified in chapter 2.3 and they are displayed in figure 3.2 and 3.3 (design space is in brown, non-design in grey).

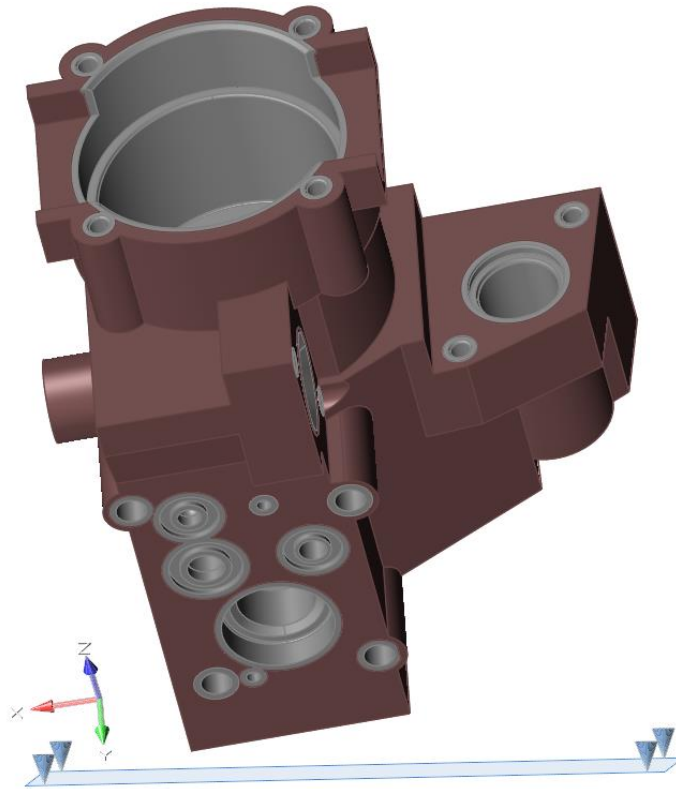


Figure 3.2 - Overhang angle constraint with Inspire. First view

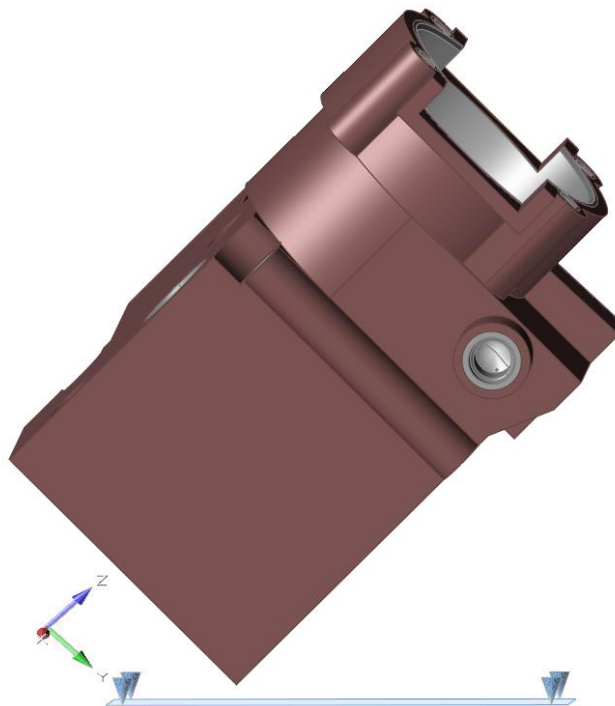


Figure 3.3 - Overhang angle constraint with Inspire. Second view

Different topology optimizations have been run with Inspire 2019 with different objectives. However, the minimum thickness constraint was kept the same at 3 mm, so that it was three times the element size decided during the structural FEA. Furthermore, boundary conditions, constraints and load cases were applied as already showed in chapter 2.4, but the optimization was run with first order elements with the *Faster* option in order to save time. An optimization with second order elements may be possible for components with lesser elements, giving more accurate results, but for this manifold it is not recommended, since it would have taken too much time and disk space.

The first objective of the optimization was the mass reduction, so a minimum safety factor of 1,0 was set. This value may look too low, because the minimum safety factor accepted is 1.2, but, since there are small bad elements in the mesh and since it is a first order analysis, a lower value has been chosen. The results of this topology optimization were not satisfactory because the volume did not seem enough to withstand accidental loads and this solution did not look conservative.

By increasing the minimum safety factor to 1.2, the software could not find a solution to the problem. This is because it was not possible to have such a high safety factor in all the elements of the mesh, because in certain areas it was already lower.

The second type of optimization run with Inspire had maximize stiffness as the objective. A couple of different analysis were run to understand which percentage of the design space could have been ideal to achieve. Reducing volume up to 15% showed that there was the possibility to decrease the volume more. Therefore, the volume was reduced to 5% of the design space lead to a good geometry, even though certain areas needed to be thickened to increase the stiffness. In the pictures below, it is possible to see in grey the design space, in brown the optimized non-design space (see figure 3.3).

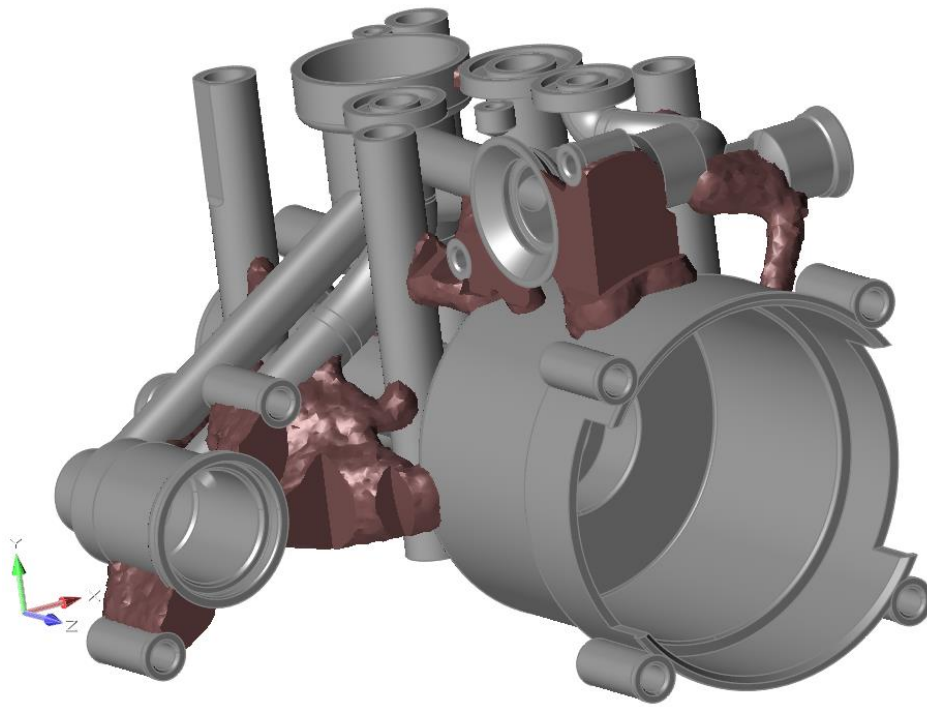


Figure 3.4 - Topology optimization result with Inspire. View 1

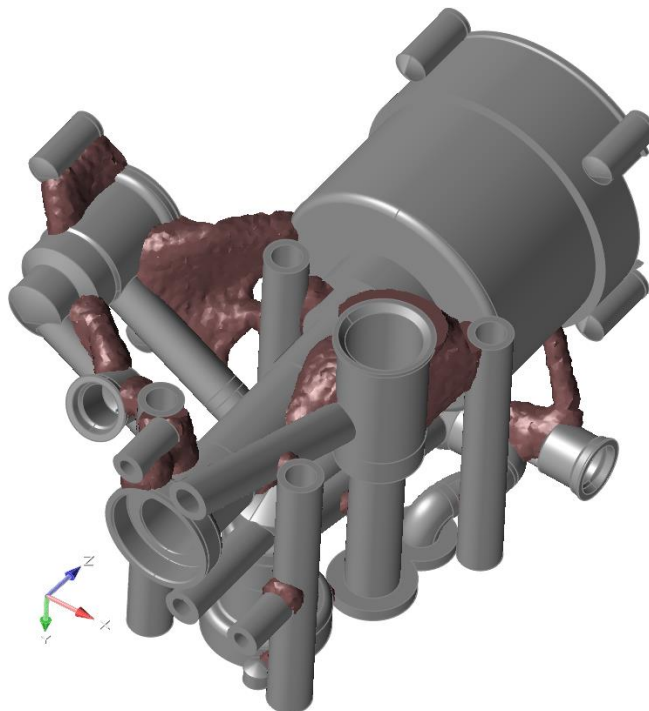


Figure 3.5 - Topology optimization result with Inspire. View 2

It was possible to select more or less material in the non-design space, in brown in the picture, in order to increase or decrease the volume, making the resultant geometry coarser with the *Shape Explorer* function, as displayed below in figure 3.4. Moving the threshold to the right means viewing more elements with a lower density value, making it less smooth, and moving the threshold to the left means viewing more elements with a higher density value, making it smoother. Usually the optimal result for this kind of “*maximize stiffness*” optimization is in the middle of the slider, marked by a star. In this case a different shape has been chosen in order to make the geometry more good looking, closing some holes, created with the mesh triangles, so that the geometry does not have material isolated regions.

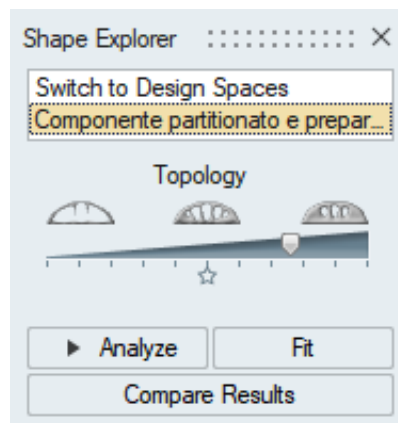


Figure 3.6 - Shape Explorer command on Inspire.

A topology optimization has been run with NX Nastran as well, to compare the different software.

The design objective chosen with NX Nastran is the “*minimum compliance*”. Compliance is the inverse of stiffness, which means that the objective is the same as in the previous case, maximizing stiffness. Design area, load cases and manufacturing constraints (overhang angle and build orientation) are the same as settled on Inspire. The maximum number of iterations selected for this optimisation was set at 40 and the build orientation and the maximum overhang angle have been added as manufacturing constraints.

The results achieved for the 25th design cycle, selected as the optimum, in NX Nastran are presented below in figure 3.6 and 3.7. Just because the process has been terminated does not necessarily imply that a unique and feasible design was found: it is necessary to check all the conditions under which convergence can be achieved. NX rarely converges because of the method it uses, trying to accomplish both the target and the constraint. As shown in the left of the pictures, there is the legend of the density contour plot. On NX Nastran there is the possibility to select the minimum and the maximum values of density, since the density result displayed goes from 0 to 1, where 1 represents the parent material and 0 represents a void. The minimum value has been set to 0.3 in figures 3.7 and 3.8 to show a better optimization result. Usually the minimum value to display should be over 0.5 but in this case the part did not look thick enough with that value, so it was decided to reduce it down to 0.3. On Inspire this option is automatically done with the slider in figure 3.6, but there is no possibility to set and review precise density values. Both software use the SIMP (Solid Isotropic Material with Penalization) method for topology optimization but NX Nastran has also the possibility to use RAMP method.

There is also the option to Laplacian smooth the resulted triangles to make a model that can be better reconstructed with free form structures, creating a .stl file (e.g. figure 3.9 and 3.10).

Componente partizionato e preparato finito V2 fixed_sim1 : Solution 2 Result
Loadcase Independent Results, Design Cycle 25, 25, Iteration 1
Normalized Material Density - Elemental, Scalar
Min : 0.060, Max : 1.000, Units = Unitless

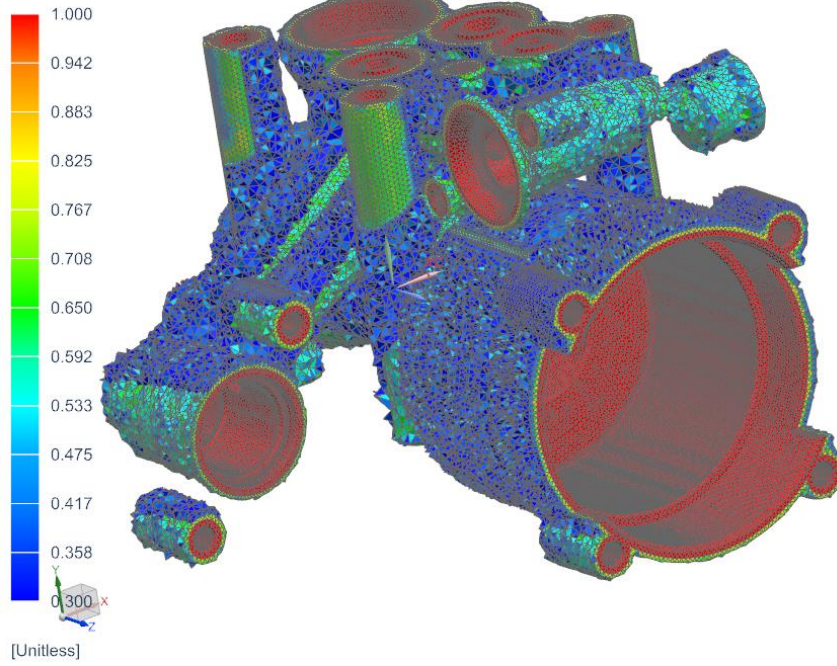


Figure 3.7 - Topology optimization result on NX Nastran. View 1

Componente partizionato e preparato finito V2 fixed_sim1 : Solution 2 Result
Loadcase Independent Results, Design Cycle 25, 25, Iteration 1
Normalized Material Density - Elemental, Scalar
Min : 0.060, Max : 1.000, Units = Unitless

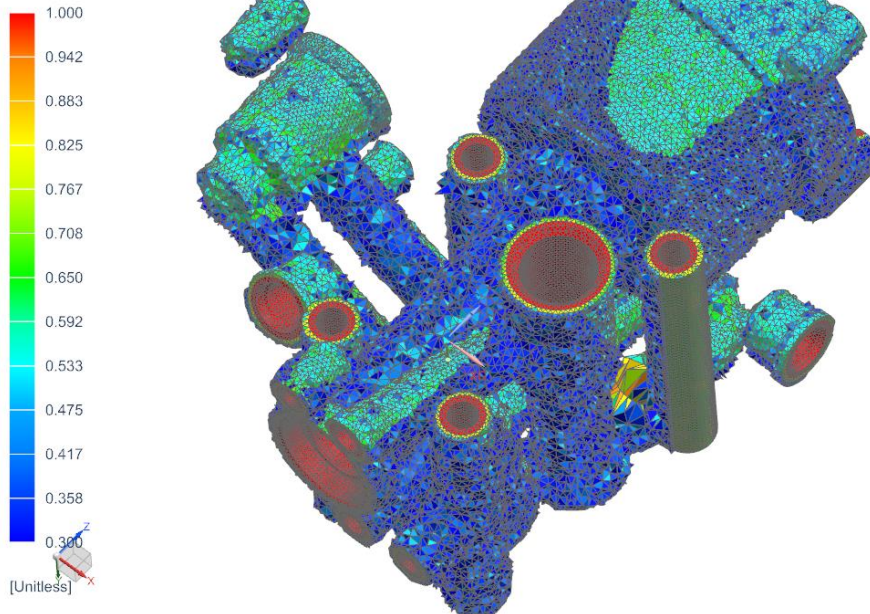


Figure 3.8 - Topology optimization result on NX Nastran. View 2

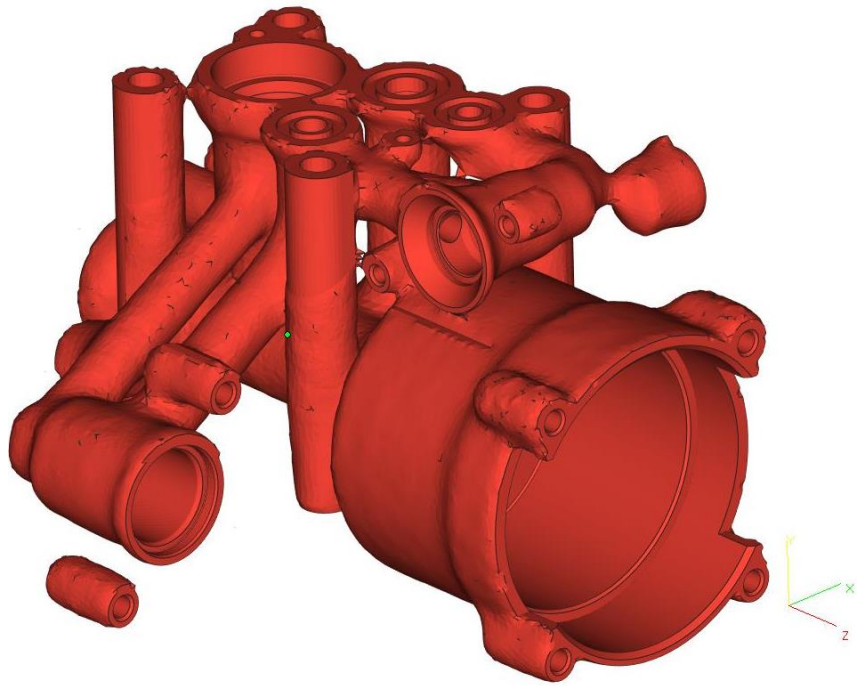


Figure 3.9 - Laplacian smooth. View 1, Magics

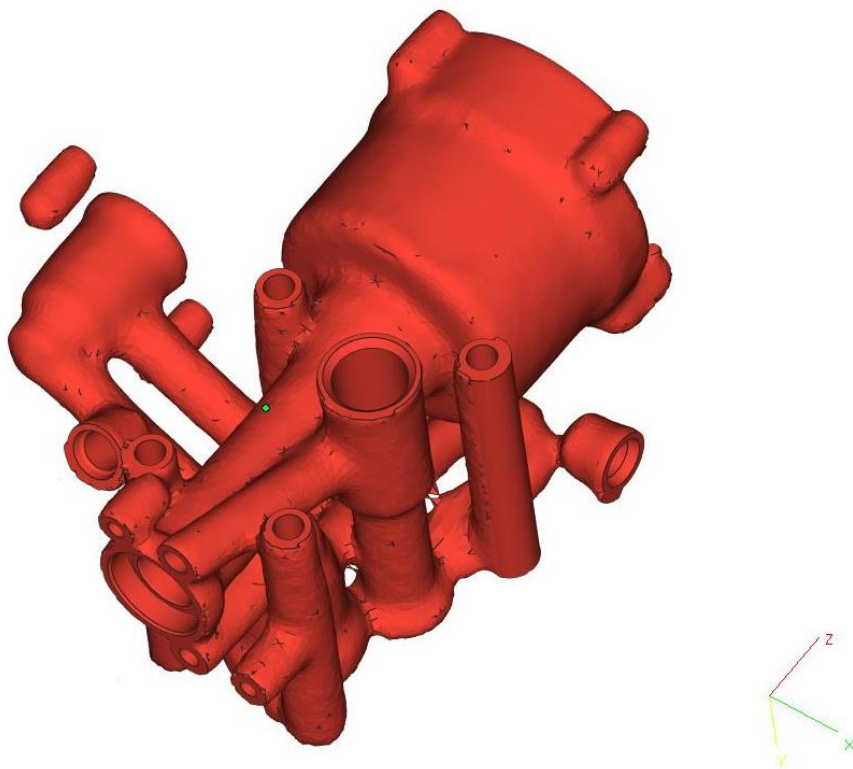


Figure 3.10 - Laplacian Smooth. View 2, Magics

The idea of having the possibility to decide which density value to use to review the results is functional, because the user can easily decide it in order to customize the results.

In figures 3.7 and 3.8 the topology optimization results on NX Nastran are shown. In red it is possible to see the part with full density (100%) while, changing colors, there are the lower densities, down to 30% displayed in blue. With lower levels of density, the part looked too similar to the original, which is why the minimum value chosen is 30%.

The results of the optimizations run with different software are completely different. This is due to the different convergence method the programs use. While NX tries to achieve both the object and the constraint, sometimes not converging with an optimum, Inspire only tries to achieve the object, always finding an optimum solution. Looking at the optimization results with the different software (figures 3.4,3.5,3.7 and 3.8), it is clear that Inspire created some beams to link some parts in the design space to increase the stiffness. NX instead tried to make the design space thicker, adding elements on it, but leaving some floating shells not connected with the rest of the component. The algorithm behind topology optimization in NX Nastran is not ideal in this specific case. That is why topology optimization result achieved with NX Nastran does not look optimal.

The maximum number of iterations can be decided on NX, but not on Inspire: Inspire iterations just stop when the optimization has converged and the optimum is found. Another difference is that on NX the weight target must be set as a value while on Inspire you can decide it by giving a percentage of the total volume that one wants to achieve.

The advantages and disadvantages of both software just discussed, are summarized below in Table 6.

	Inspire	NX Nastran
Maximum number of iterations	X	✓
Optimization methods	SIMP	SIMP and RAMP
Weight target	percentage	value
Result components linked	✓	X
Definition of beams in the design	✓	X
Non-floating loaded areas in non-design space	✓	X
Reconstruction with free forms	Easy	Complicated
<i>Wrap</i> feature for free forms remodeling	✓	X

Table 6 - Comparison between Inspire and NX Nastran topology optimizations

It is mandatory to remember that the optimization run with any software only proves that the component will withstand the loads included in the optimisation and that it can't prove that the component will not break or bend if subjected to other additional loads.

Since the component to effectively produce should be just one, it was necessary to decide which of the optimization results to pick to reconstruct the geometry into a solid body. Both the software could have been used to do this operation, but for simplicity Inspire was chosen. The reconstruction with NX is possible as well, but it is a little more tedious than Inspire, since it does not have the feature *Wrap*. A

comparison between the two will be shown later in chapter 4.2, but the final part will be manufactured using Inspire's topology optimization results.

4. Component redesign

4.1. Design for Additive Manufacturing

Design for Additive Manufacturing guidelines are those used to improve the component and to make it more suitable for AM process [26]. This means not only the cost will be saved, but also that there will be some improvements that could help with the build process. Design guidelines strongly depend on chosen material, machine concept and process parameters [26]. A few of these design guidelines are included below.

One of the factors to consider when designing part is the orientation dependency of the achievable surface roughness in L-PBF [31]. In general, the smaller the angle between the build plate and the surface of the part, the higher the roughness [31]. Overtaking a critical angle leads to an increased droplet effect on down facing surfaces, also called downskin, and in the end to an erroneous build-up of the layers due to a reduced heat flux into the powder bed compared to completely solidified metal [2]. Generally, the result is a failure of the process, as shown in figure 4.1 [31]. To neutralize this behaviour, support structures can be used and are recommended above the highly material and manufacturing machine dependent critical angle [2]. Often, the angle limit is between 30° and 45° , but it depends on the processed material, the melting strategy, and also the part features (thickness, shape etc.) above the regarded face [2]. When orientating a part, it is also important to remember that the surface roughness of the upskin surfaces will be better than downskin [2]. Depending on the customer requirements, there is the possibility to decide the orientation based on the quality of the surfaces.

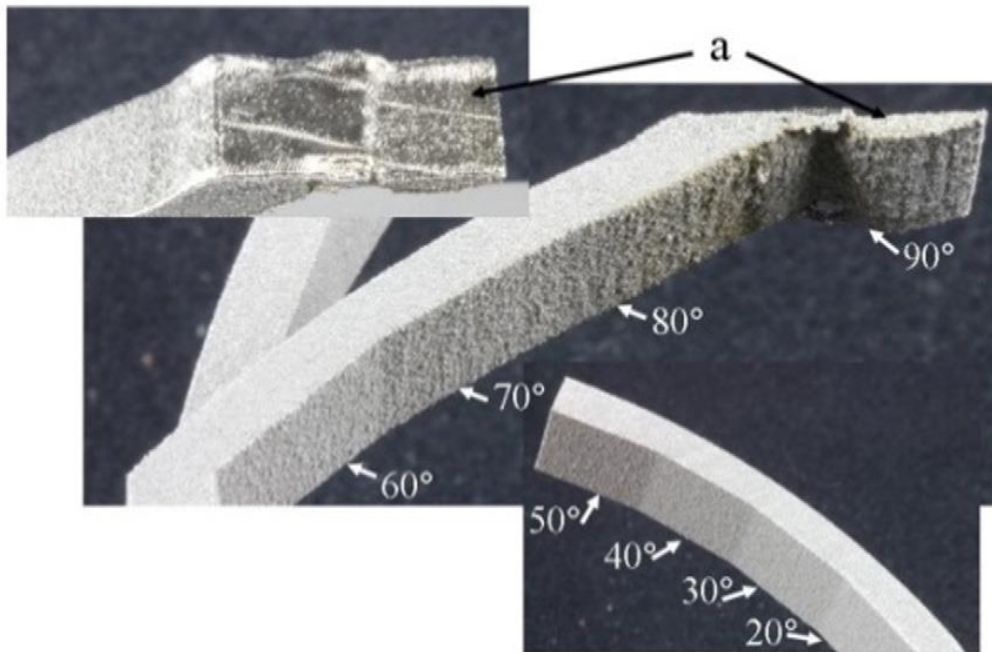


Figure 4.1 - Bridge for downfacing surfaces (a=plane of process failure) [2]

Horizontal holes are also a problem to be faced. They require the use of support structure if they have a diameter larger than approximately 8 mm (for some materials this value is even smaller or higher) [2]. To avoid that, it is possible to modify the shape of the hole and to make it drop shaped (e.g. figure 4.2) [31].

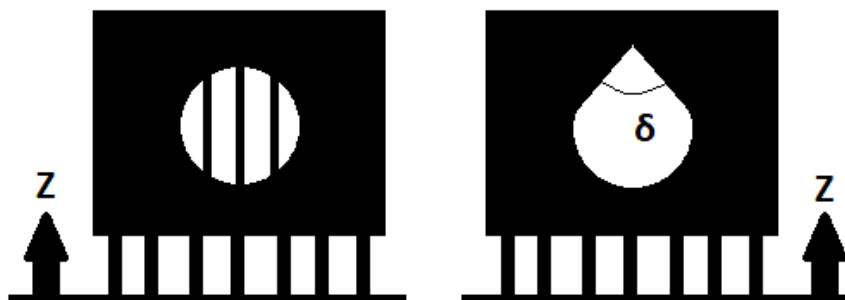


Figure 4.2 - Vertical holes, left with support, right with drop shape. δ is the downskin angle

Moreover, vertical, horizontal or angled holes cannot be produced with this technology if their diameter is smaller than a certain value, from 0.7 to 2 mm, depending on the material and the inclination [2].

One of the first things to do with a part is to orientate, position and arrange it to minimize the frictional forces generated during the movement of the recoater [31]. This is done to avoid the recoater possibly rupturing due to the collision between the building parts [33]. Longitudinal geometries should be oriented in the coating direction, not parallel to the recoater. In general, critical geometries should not be built against coating direction (e.g. figure 4.3) [34].

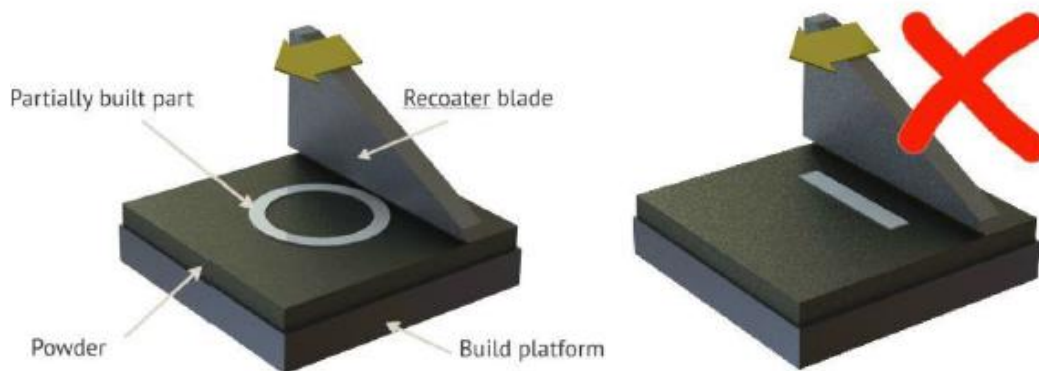


Figure 4.3 - Direction of build to avoid recoater collision [34]

The orientation of a part could affect significantly the extent of the warping effect [35]. To counter it, it is better to avoid fusing large part surfaces during a single step wherever possible [31]. Deformation of large part surfaces may be impeded using appropriate designed support structures and the application of heat [31]. In this way, exposure of the large surface can be divided between different layers throughout a build.

Parts built with AM do not also have isotropic mechanical properties such as yield strength and tensile strength: usually they are worse in the z direction [22]. In order to make a component more resistant to the loads applied, it is possible to orient it in the best way [36]. This anisotropy could be slightly reduced with heat treatments [36].

Properly orienting a part on the build platform means also finding the best option to reduce the amount of support structures [5]. Those structures are needed not only to not to let the part fail when manufacturing a downfacing surface, and especially

for exchanging the heat [5]. The ideal orientation would not let the component need support structures, which leads to reduce material waste, production time and manual labour and to increase the surface quality [5]. This is most of the times a utopia but, once the orientation is defined, some modifications in the design can be done to decrease the amount of supports. For example, there is the possibility to create solid beams, instead of support blocks or lines, that can directly link the component to one of its features [5].

Finding the best orientation is not always easy: there is the need to find a good compromise between support structures, surface roughness, limitations of the process, distortions, efficiency, process stability and part quality, which all lead to costs [31].

Another factor to be considered, is the wall thickness. The minimum wall thickness in L-PBF depends on the process parameters which affect the melt pool dimensions [31].

In order to test the proposed orientation and support structures, software simulations can be performed. With those, there is the possibility to forecast shrink lines, deformations, breaking of the recoater and part failure. There is also the possibility to compensate them, adding some material or changing the part orientation and/or support structures.

4.2. Redesign

With Siemens NX software, some design modifications have been performed on the component to make it more suitable for AM. At the beginning, the routing of channel was modified in order to avoid sharp edges and to make the geometry more fluent, keeping in mind that the customer wanted the channel to be as short as possible in case of modifications.

In figure 4.4 it is possible to see the junction that has been created with the feature *Sweep along guide* using spline curves as a guide and the pipe section as start and end sections. The diameter of the channel has been kept as the original.

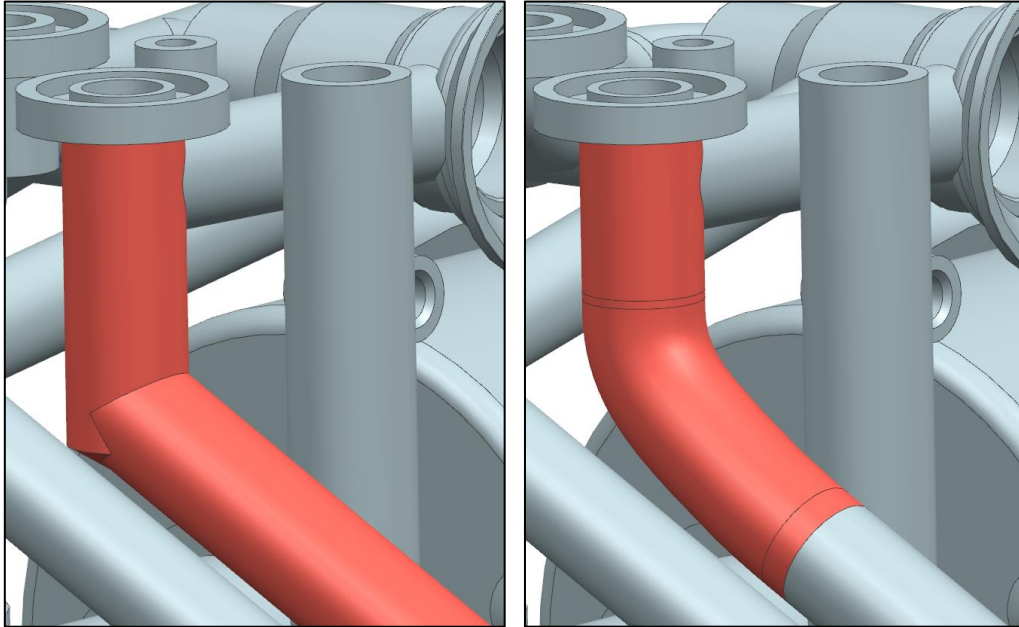


Figure 4.4 - Channel n.1. Left original, right new routing, NX

In figure 4.5 the channel is modified to make a better component for AM, showed in figure 4.6. The channels have been deleted with *Delete Face* and rebuilt using *Revolve* to make junctions and *Sweep along guide* to link them. The guide is made by creating a *Datum plane* on where both the axis of the starting and ending sections lie. The sensor is linked with a small tube, that has been moved going from the initial and the final configuration to make it shorter.

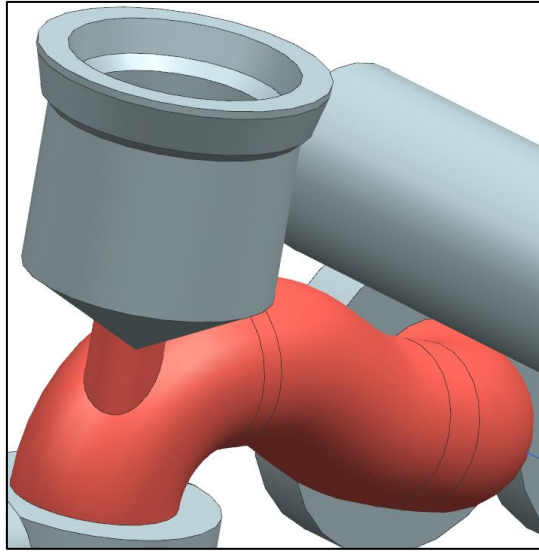


Figure 4.5 - Channel n.2 original, NX

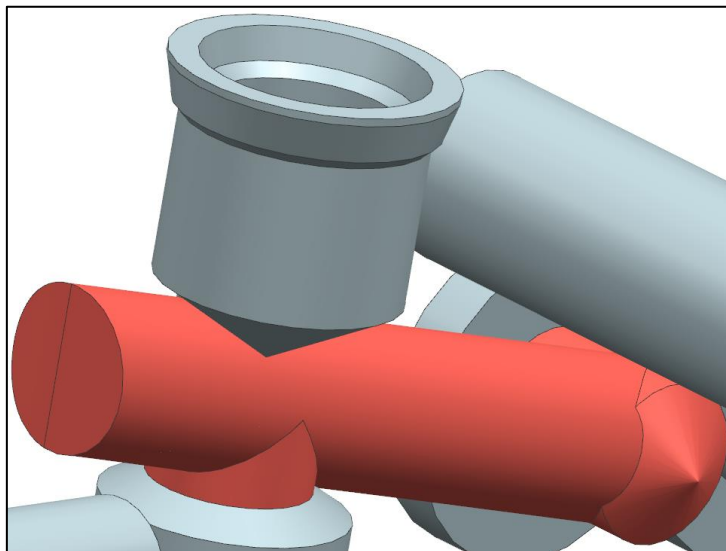


Figure 4.6 - Channel n.2 new routing, NX

In figure 4.7, on the bottom left of the image, one channel has been reshaped in order to avoid sharp edges. Initially the channel has been deleted with *Delete Face* feature, than a new pipe with a different inclination has been created with the command *Cylinder*. The edges have been cut with *Trim Body* command. The result is presented in figure 4.8.

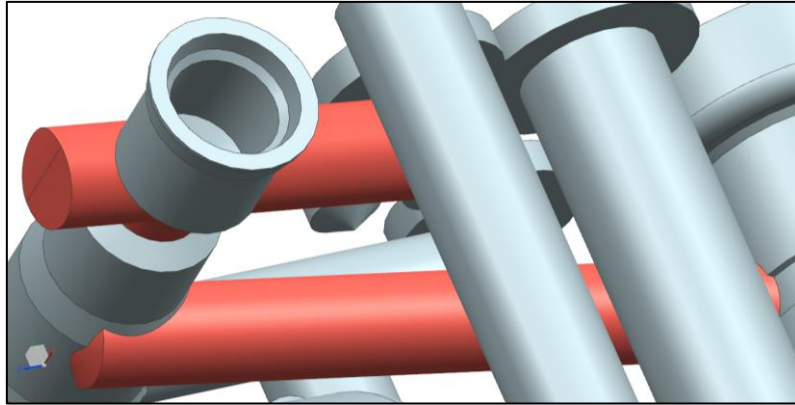


Figure 4.7 - Channel n.3 original, NX

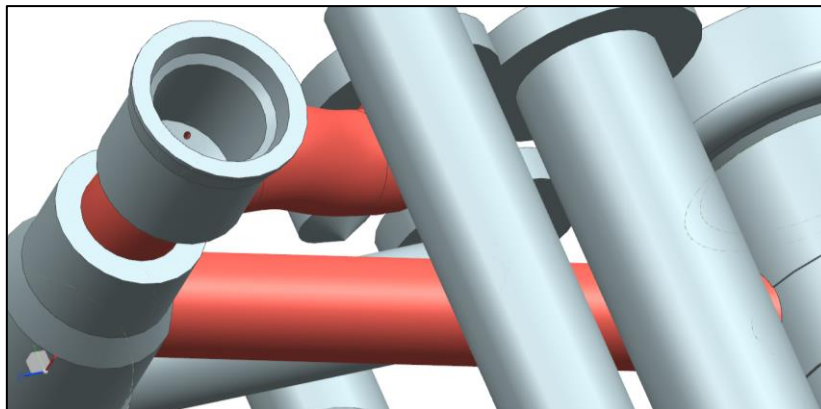


Figure 4.8 - Channel n.3 new routing, NX

With those modifications, non-design space was changed. Usually non-design space is kept as defined in the beginning, but in this case the customer gave his approval to make some modifications to the initial geometry, reminding not to modify the functional surfaces. Some attention has been put not to make the thickness of the part smaller than the minimum printable thickness. All those changes were done before topology optimization.

Moreover, sharp edges and points have been removed, because it is not possible to produce them with this technology, since they are zones with high concentration of stresses.

Since topology optimization results, displayed in chapter 3.2, are in STL format, it was necessary to redesign the geometry to obtain a solid body, by using the results as a reference. Freeform geometries, just as *polyNURBS* on Inspire and *Realize Shapes* on NX have been used to create the final design. There is the possibility on Inspire to automatically convert the result of the optimization, generally displayed as a very coarse mesh, into surfaces. This feature called *Fit* unfortunately does not create solid bodies, making the reconstruction more difficult. For this reason, *polyNURBS* are the best option. Comparing *polyNURBS* on Inspire with *Realize shapes* on NX, Inspire tool is more fast and functional, since it has the *Wrap* tool, that quickly generates a solid geometry by clicking on a section, trying to automatically estimate its diameter. Meanwhile, on NX, the *Realize shape* must be translated and rotated in the desired position, being less time efficient. In both software, the free forms can be directly manipulated from their cage, by pushing and pulling faces, points or edges. The result in both software showed some areas in the design space were not linked to the rest of the component because they did not have loads or constraints applied on them. For this reason, they have been connected with free forms.

To make this thesis more efficient, Inspire software has been used to reconstruct the geometry obtained with the optimization in figure 3.4 and 3.5. After the reconstruction phase was done, *polyNURBS* redesigned body needs to be cut with the Boolean operation *Subtract*, so that they do not intersect the design space and they do not extend over the non-design space.

In the end, using NX, fillets have been added with the *Edge Blend* feature to avoid sharp edges (see figure 4.9 and 4.10) and stock material of 1 mm has been included in order to machine the component in the areas that need to be finished, as provided by the customer. Those operations have been done with NX and not Inspire because the geometries were too complex and Inspire was not able to add the desired fillets. As requested by the customer, further material has been added to increase the functional surfaces even if it was not necessary according to the FEA results.

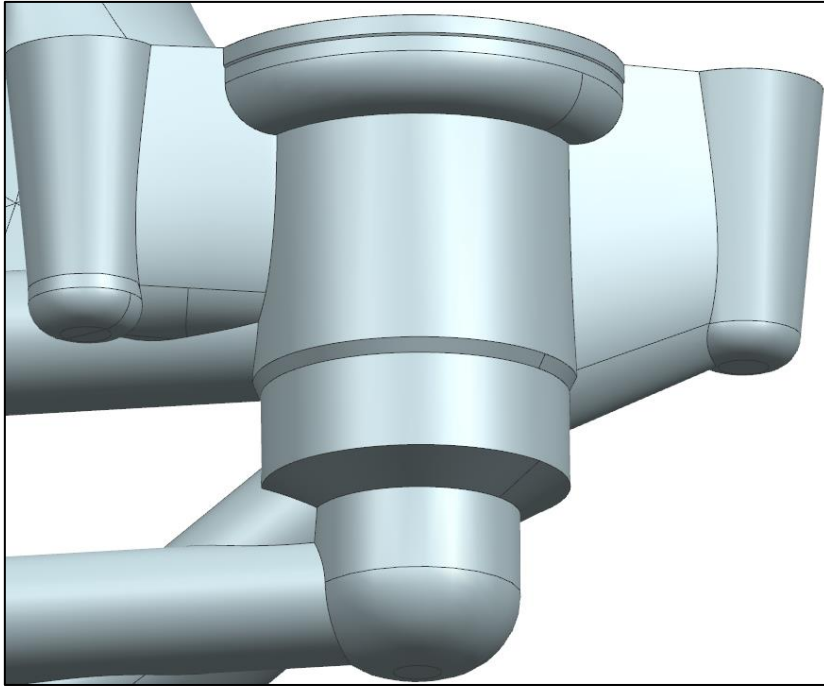


Figure 4.9 - Fillets n.2 original, NX

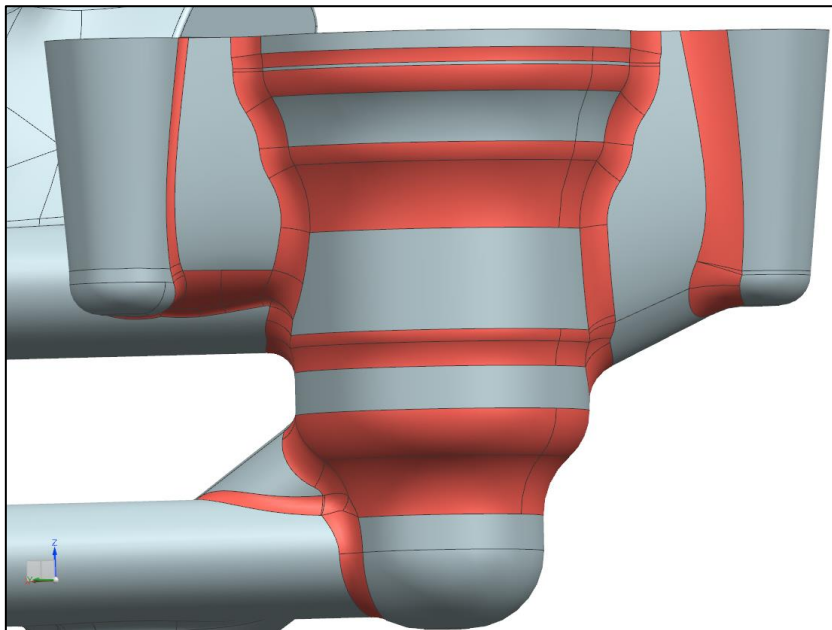


Figure 4.10 - Fillets n.2 new, NX

The final design, without stock material, is presented below in figure 4.12 and 4.14. In figure 4.11 and 4.13 there are the topology optimization results, so that the redesign can be easily reviewed.

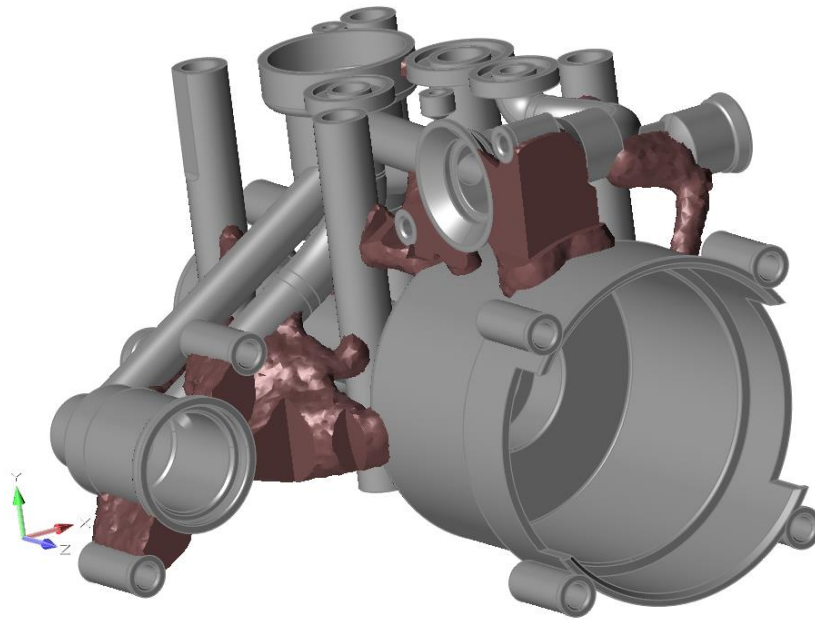


Figure 4.11 - Topology optimization result. View 1, Inspire

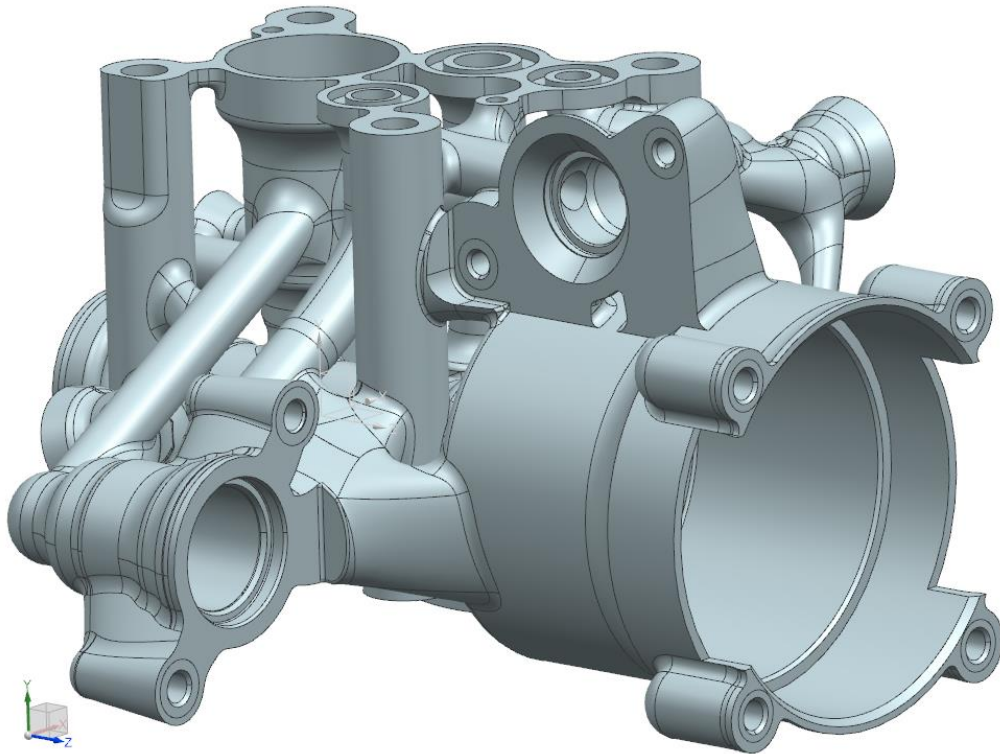


Figure 4.12 - Final design. View 1, NX

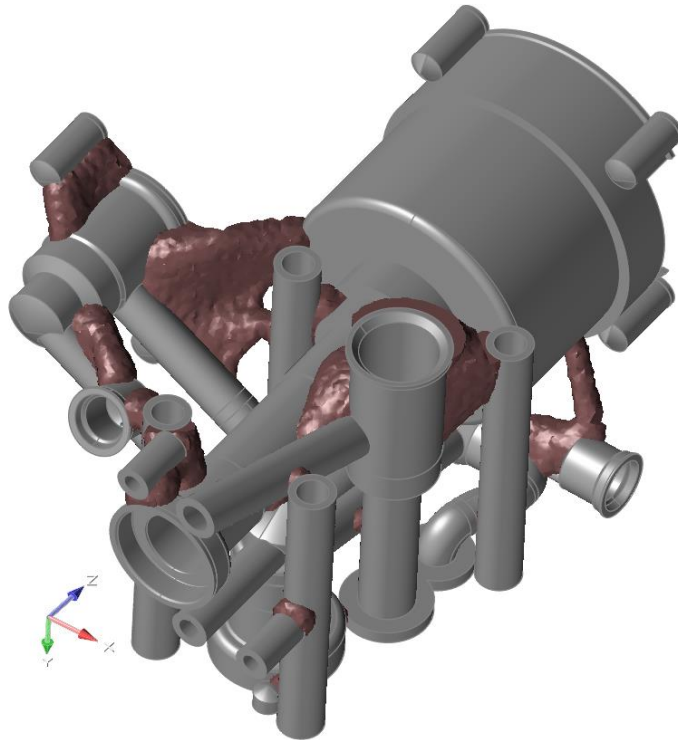


Figure 4.13 - Topology optimization result. View 2, Inspire

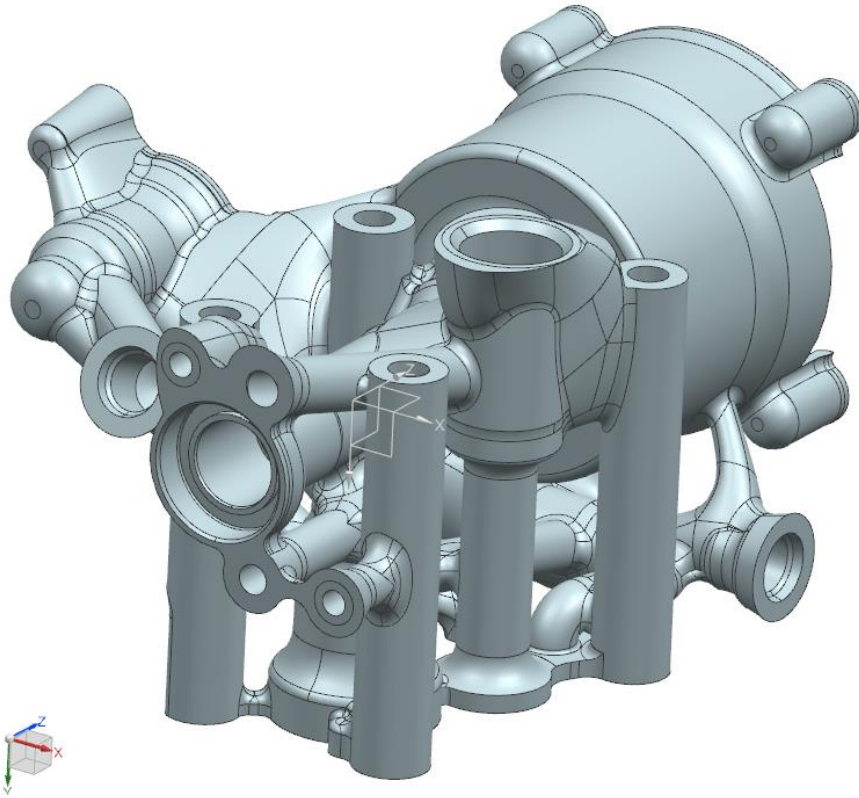


Figure 4.14 - Final design. View 2, NX

5. Design verification – structural analysis

To prove that the optimized and redesigned component can withstand all the applied loads, it is necessary to perform a FEM structural static analysis. It is important to compare the results of this analysis with the original calculation showed in chapter 2.4.

In order to improve the performance of the component (for example to reduce weight or to increase stiffness), the material was changed. Another cause is that there are not so many materials available for this technology, compared to traditional manufacturing. The material chosen for this component is AlSi10Mg as already specified in detail in chapter 3.2. The same load presented in the chapter 2.2 were applied to perform this structural static FEA with Inspire. The element size settled is 1 mm and the analysis was performed with first order elements. The results of displacement contour plots are presented in the figures below in figure 5.1 and 5.2 for load case 1 and 5.3 and 5.4 for load case 2. Von Mises stress contour plots are shown later in figure 5.5 and 5.6 for load case 1 and 5.7 and 5.8 for load case 2.

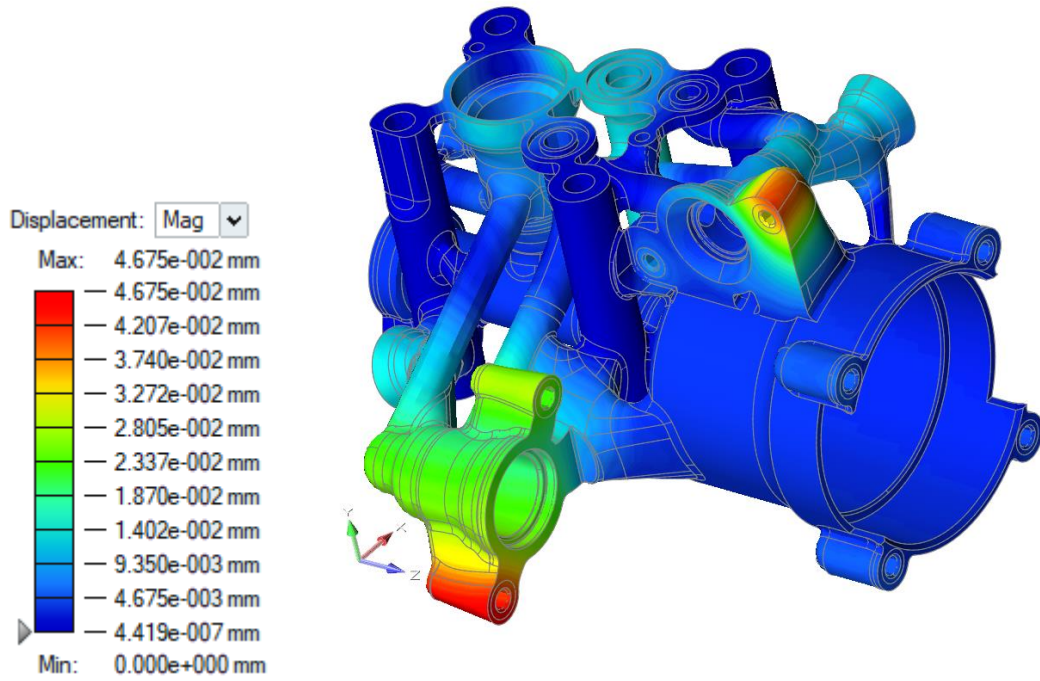


Figure 5.1 - FEA of the final component on Inspire. Displacement contour plot for load case 1. View 1

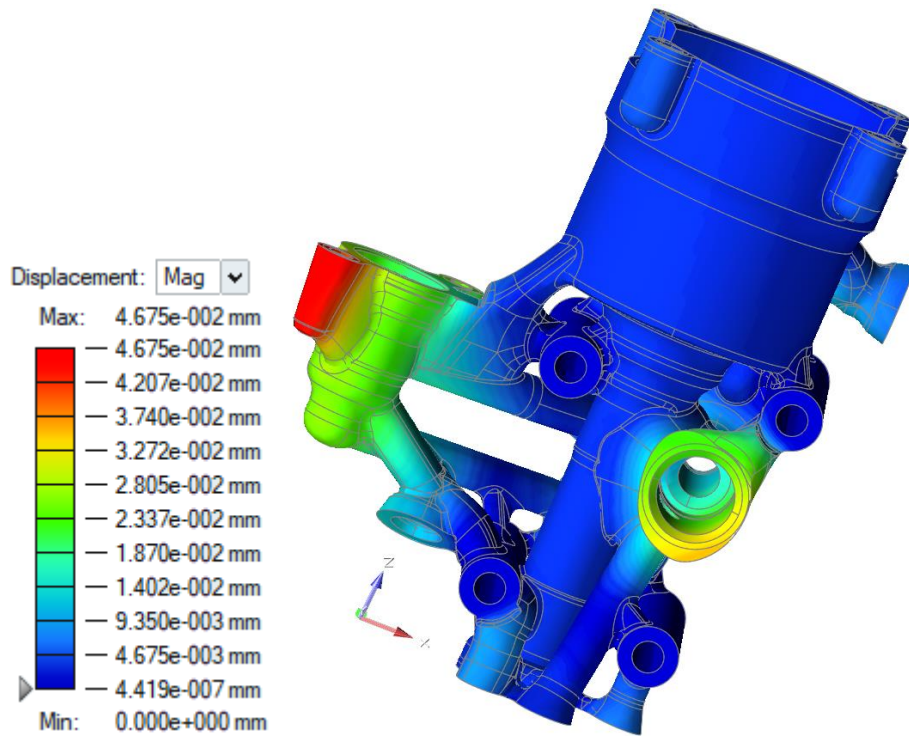


Figure 5.2 - FEA of the final component on Inspire. Displacement contour plot for load case 1. View 2

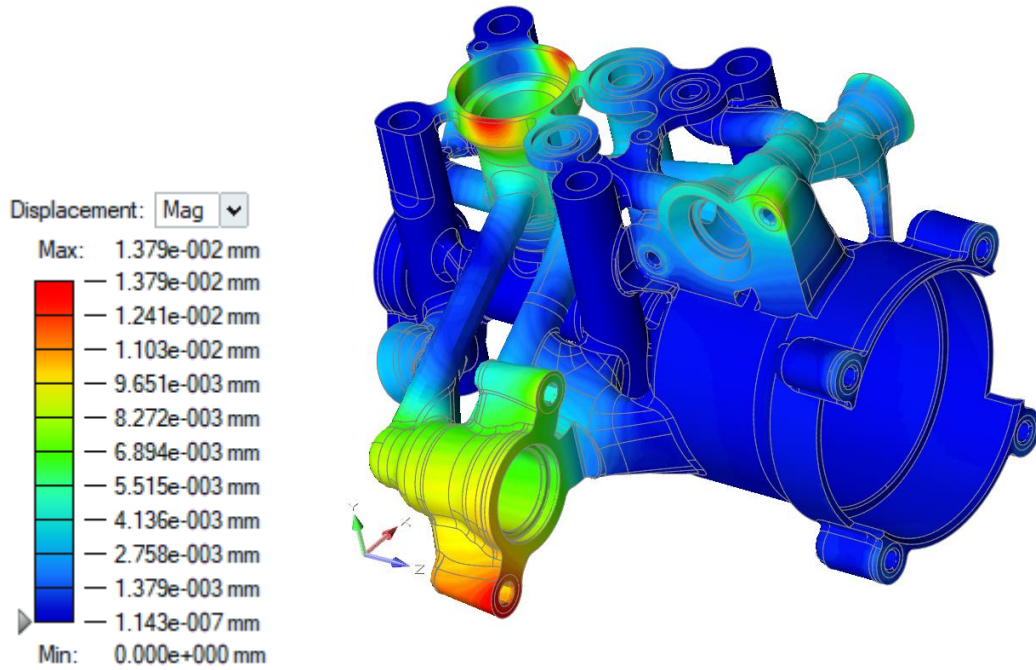


Figure 5.3 - FEA of the final component on Inspire. Displacement contour plot for load case 2. View 1

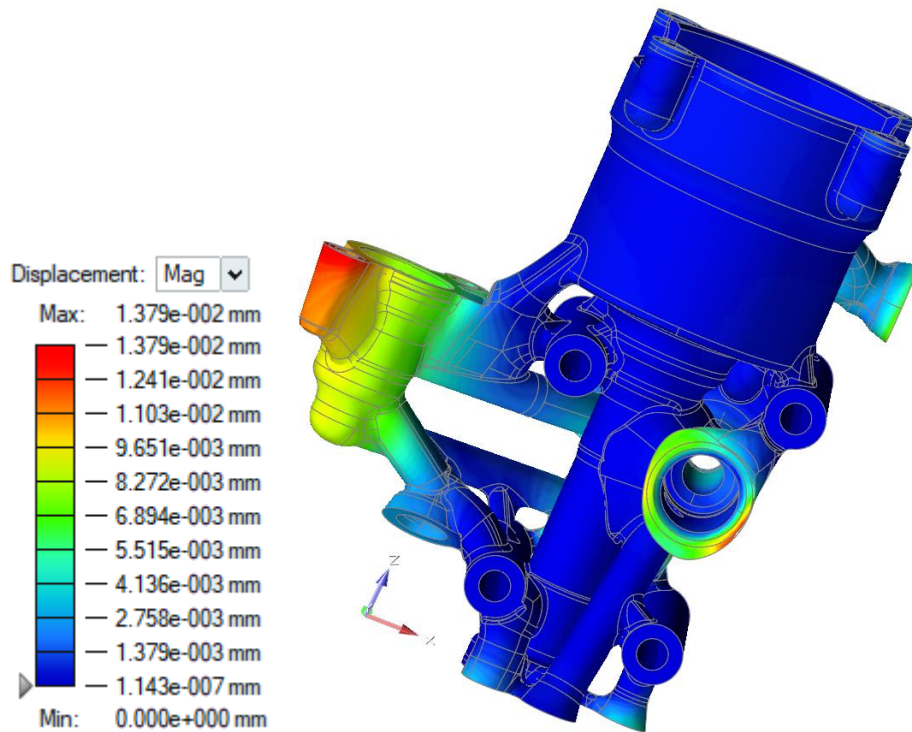


Figure 5.4 - FEA of the final component on Inspire. Displacement contour plot for load case 2. View 2

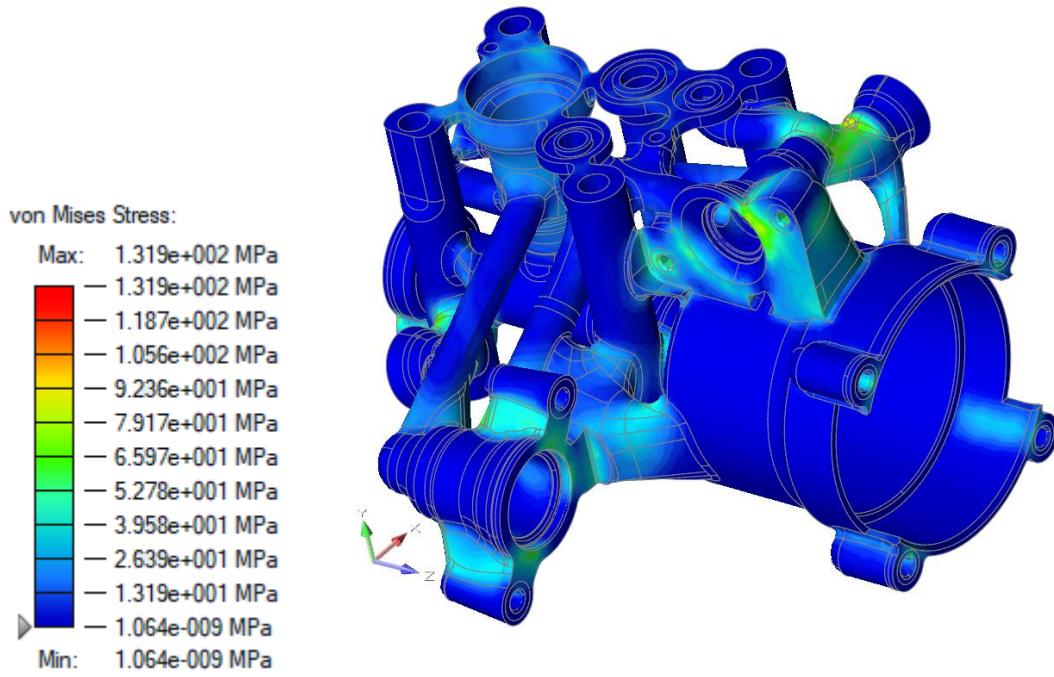


Figure 5.5 - FEA of the final component on Inspire. Von Mises stress contour plot for load case 1. View 1

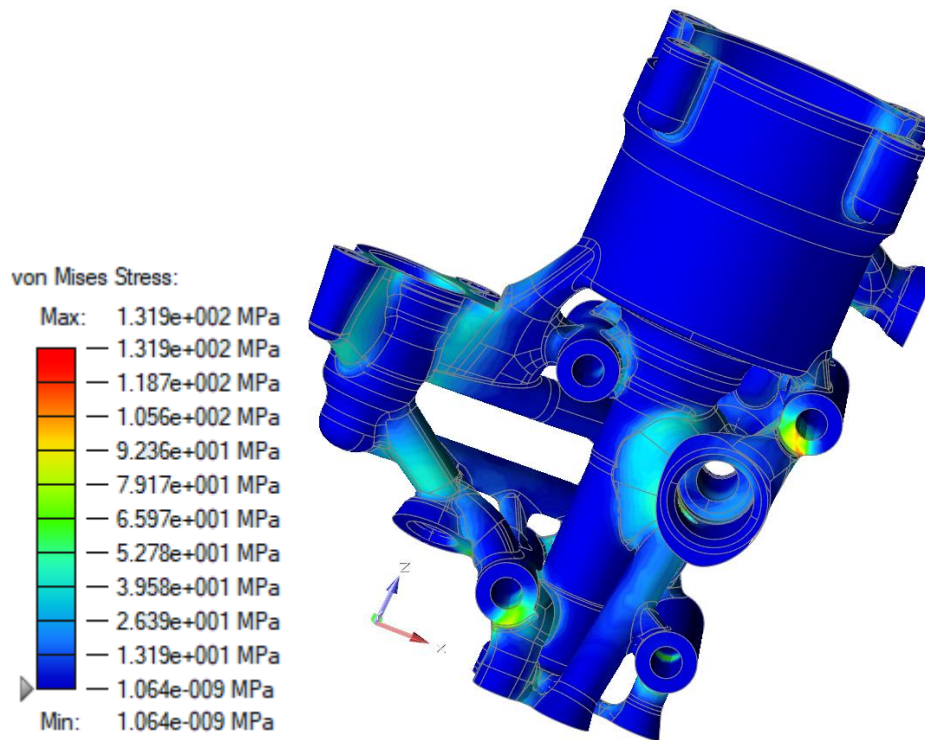


Figure 5.6 - FEA of the final component on Inspire. Von Mises stress contour plot for load case 1. View 2

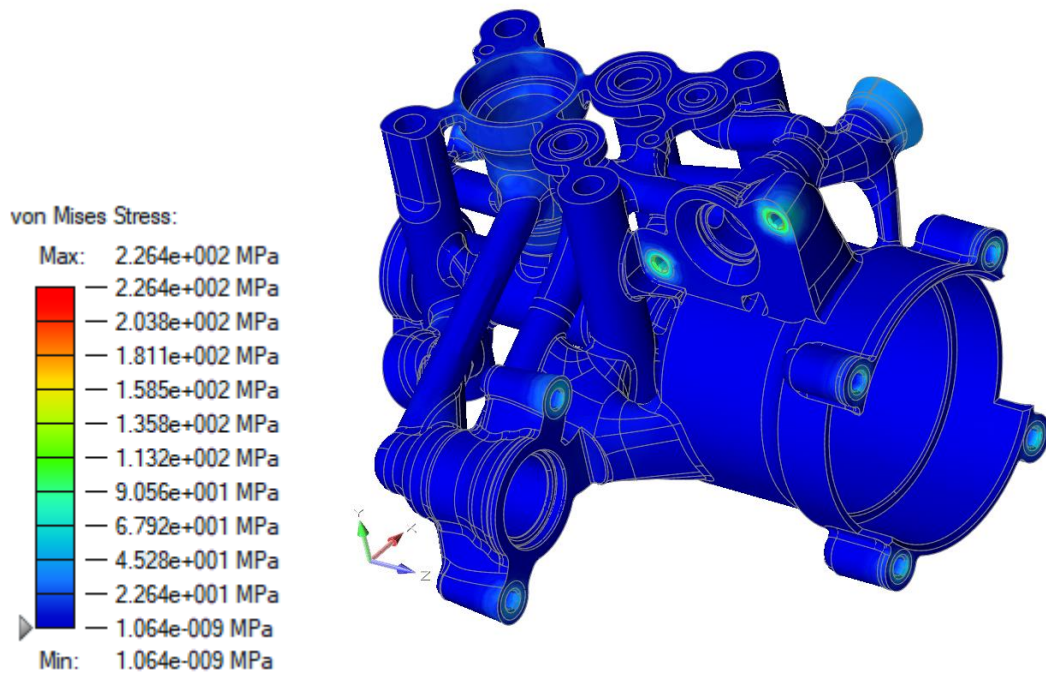


Figure 5.7 - FEA of the final component on Inspire. Von Mises stress contour plot for load case 2. View 1

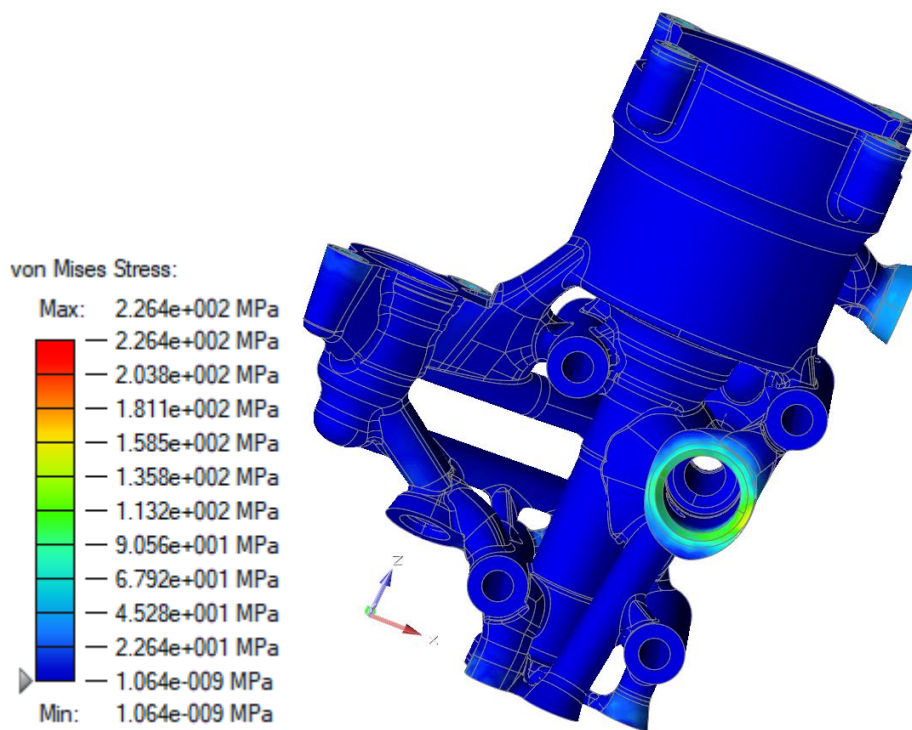


Figure 5.8 - FEA of the final component on Inspire. Von Mises stress contour plot for load case 2. View 2

Since the Yield stress value for AlSi10Mg is 240 MPa at room temperature, looking at the contour plots it is possible to confirm that the part can perfectly withstand the loads and it will not deform, with a minimum safety factor of 1.06 (for load case 2) only in a few small bad elements in the mesh. The maximum displacement is 0.0468 mm (achieved in load case 1), less than five hundredths of a millimeter, which is acceptable. Unfortunately, those analyses are made with first order elements, only because Inspire could not perform an analysis with second order elements, due to the bad conversion from step file to stmod format, since Inspire internally uses the parasolid geometry kernel.

6. Manufacturing and post processing

6.1. Building orientation and support structure generation

The building orientation of the component was decided before the topology optimization, so that the software could optimize the geometry of the hydraulic module in a way that the component needs none or very few support structures. Two different configurations of building orientation looked advantageous. The first orientation is in vertical (with a build platform parallel to x-y plane), as presented below in figure 6.1. In this configuration, supports are required in some of the channels that would anyway be machined. Some of those channels have instead a diameter smaller than 8 mm, so they don't need support structures in the inside [34]. The advantage of this build orientation is that the component does not take too much time to be produced, because it develops itself on plus z direction and the build job height is 136 mm. The main disadvantage is that support structures make up a lot of volume. However, this is the best orientation for optimizing the nesting since the most number of parts can be placed on the building platform.

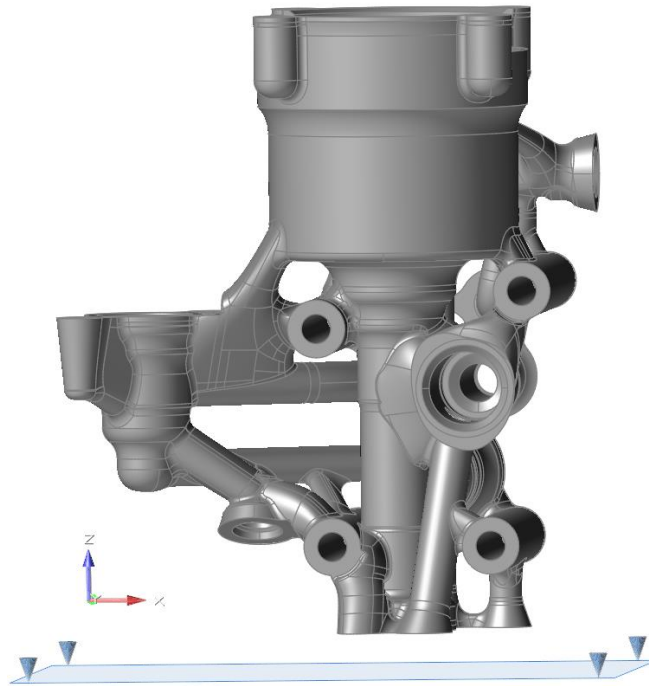


Figure 6.1 - Possible orientation, vertical, Inspire

In the second orientation, which in the end was chosen as definitive, the component is inclined at 45 degrees on the minus x axis and 10 degrees on the minus y axis. Here support structures are only present inside the channels where it can be machined, but the build job takes longer, since the build job height is 148 mm. However, the number of horizontal channels in this orientation is smaller than the previous: thus, reducing the machining cost. This is also the only orientation in which none of the inner channels need support structures inside. With this configuration a lower volume of support structures is achieved. But because the part is a little tilted, a lesser number of components will fit on the build plate, thus reducing nesting capabilities.

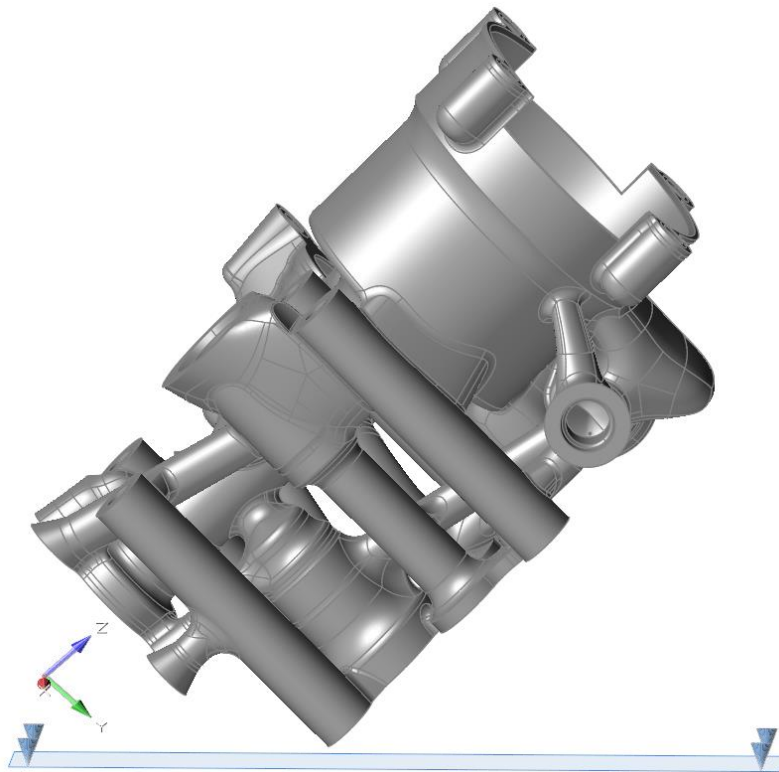


Figure 6.2 – Orientation decided, inclined, Inspire

In Table 7 below there is a summary of all the above-mentioned advantages and disadvantages of both part orientations.

	Unity of measurement	Vertical orientation	X45 y10 orientation
Volume of supports	mm ³	99970	65611
Build time	h	5,06	5,53
Component's height	mm	136	148
Precision of channels		Worse	Better
Surface quality		Worse	Better
Parts in the platform		More	Less

Table 7 – Advantages and disadvantages for different part orientations

Since the component needs to be machined on certain functioning surfaces, an offset was added on those particular functioning surfaces and some fixtures were created. Two different machining positions, presented in figures 6.3 and 6.4, were decided with the help of the machining team. In the first machining position in figure 6.3, the component is fixed with four M5 screws to the machining platform, which will be added after the additive manufacturing of the component. After the upper surface will be machined, the big square platform will be removed, and the component will be fixed on the four fixtures, as shown in the pictures, that will be removed afterwards. The four small fixtures will be additively manufactured with the component itself.

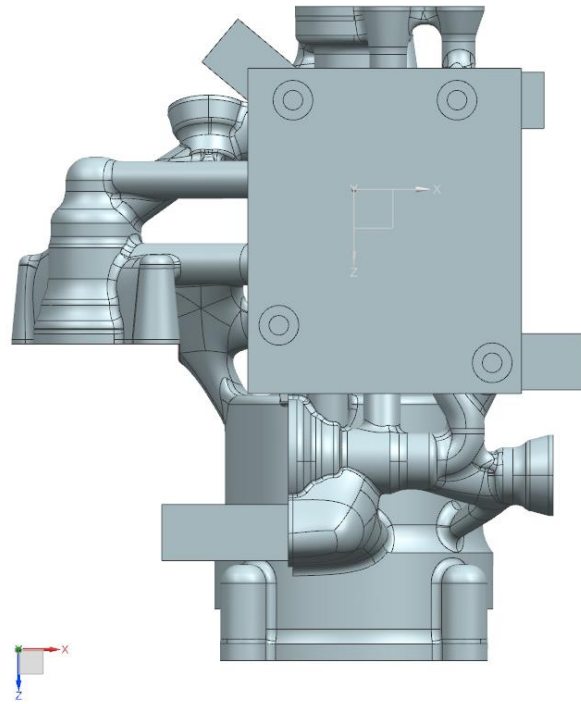


Figure 6.3 – Machining position 1, NX

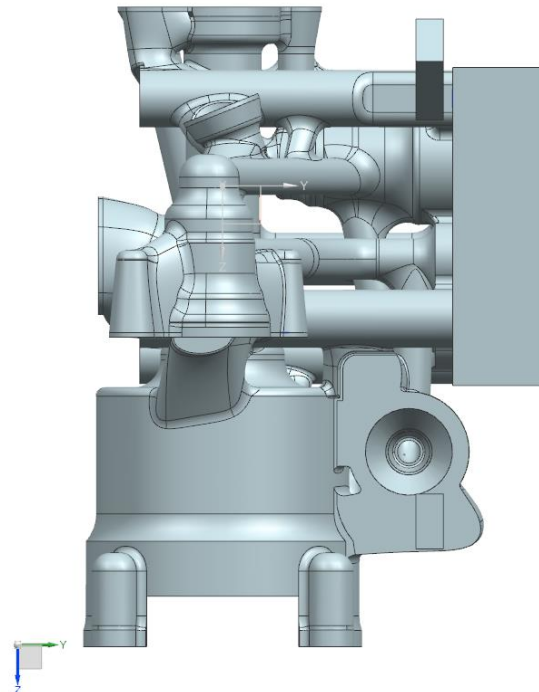


Figure 6.4 – Machining position 2, NX

After the choice of the building direction and the sacrificial fixtures, the component has been imported on Materialise Magics 21.11 [37] as an stl file, to create appropriate support structures.

The first thing to do in Magics is to fix the geometry, because there could be problems like overlapping triangles or shells. After the geometry is fixed, an automatic supports creation is performed. This is not the final version; more support structures will be created manually, while some will be deleted and remodelled. Since the material is an Aluminium alloy, a lot of support structures are not needed as in the case of Titanium or Inconel, also because its critical overhang angle is smaller than 35 degrees.

The machine chosen is a Trumpf TruPrint 3000. The recoater goes from plus to minus x axis, so the part was oriented on the platform in order to avoid any possible recoater collisions.

Different types of support structures could be used for this purpose: there are point supports, line supports, contour supports, and volume supports. Deciding which support to use mainly depends on the surface to support. With downfacing edges, contour supports with a thickness of 0.5 mm were added, while, in the remaining downfacing surfaces, block supports were preferred.

The distance between the build platform and the lowest point of the part has been set to 7 mm. As shown in figures 6.5 and 6.6, the support structures added are displayed in red, while the component is in green. Some supports have been angled or rescaled a little to decrease the amount of waste material during the process. As already mentioned, with this orientation, support structures are not inside the inner channels, but they are in the areas that will be machined for adding threads.

As shown in pictures 6.5 and 6.6, some support structures are not linked to the build platform but to the part itself. This reduces the amount of support structures but can also make the surface quality of the part in that particular area worse after the support is removed. In this case, the customer did not require the outer surface to have a high quality in the non-functional surfaces, but they required a low cost per part. Therefore, some supports are made shorter.

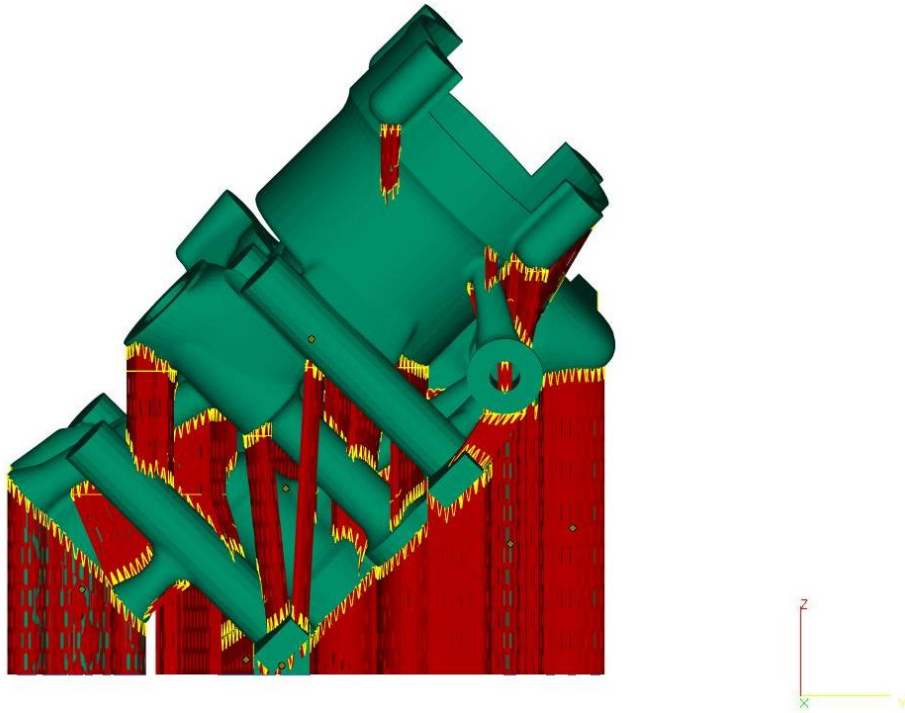


Figure 6.5 - Support structures, first view, Magics

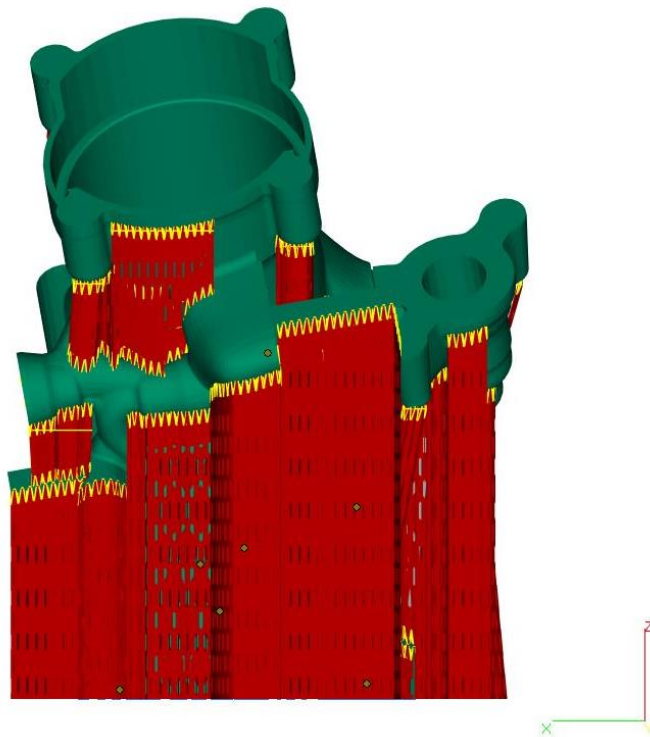


Figure 6.6 - Support structures, second view, Magics

Looking closer at figure 6.7, there are some blue and red lines that represent contour and line supports. Those lines have been added for those unsupported downfacing edges or in some areas where the exposure increases significantly from layer to layer. There could have been also the possibility to decrease the amount of support structures, adding some solid pins instead of supports. Those pins would have stayed in the part itself, in order to reduce support removing costs and times. In the end this option was not considered because it would have meant a increment of weight of the part, reducing only partially the amount of supports.



Figure 6.7 - Support structures, bottom view, Magics

6.2. Part production

The dimensions of the component are 136x120x89 mm³. The orientation was decided before the topology optimization, so the bounding box of the oriented component measures 104x133x144 mm³. As already specified, the production material will be AlSi10Mg. With all information it is possible to decide on which available machine in the facility of Magdeburg, Germany (ex Citim GmbH) the part will be produced. Initially, only one prototype will be delivered to show the customer the design and the properties, so that it could be tested.

In automotive field, price is a factor to seriously consider when deciding which machine to use. That is why the best machine for the creation of the prototype would be Trumpf's TruPrint 3000 [38] because it has a low hourly rate, even if the build volume is too big for producing only one component. Adding different components in the same job is advantageous for the production of a single part, while *TruPrint 3000* is anyway a better machine for nesting, since it is the biggest among Trumpf machines, and more parts can fit inside.

Eight test coupons (four cubes and four cylinders) were added as well in order to validate the density of the component in the four quarters of the building platform.

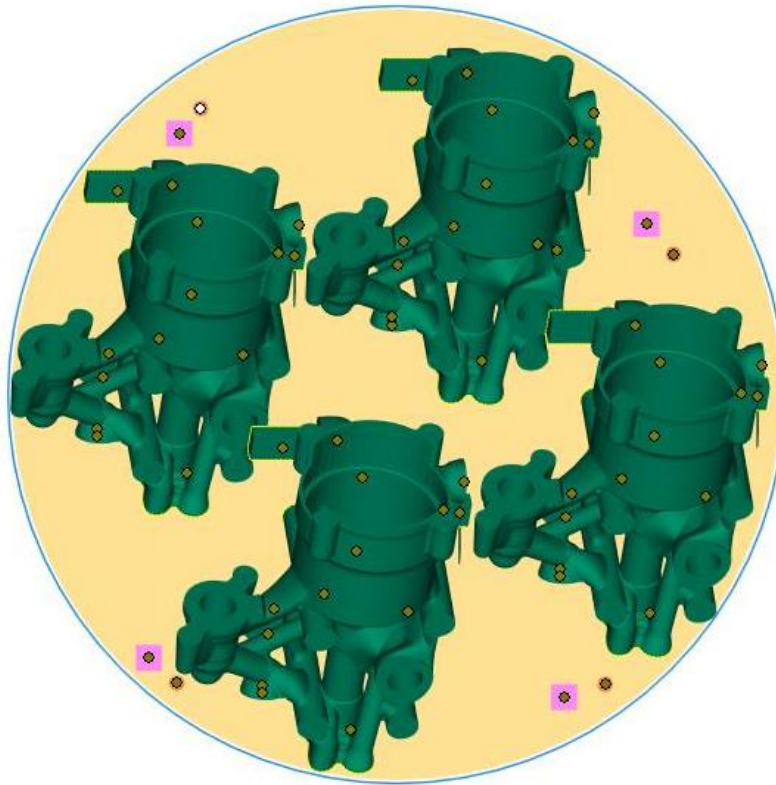


Figure 6.8 - Nesting on TruPrint 3000, front view. Magics

On this machine it is possible to do a nesting: four parts can fill the build volume (as shown in figure 6.8), that will increase production rate. Unfortunately, the machine is higher than needed for this component, as visible in figure 6.9. Since there is still some remaining space in the building platform, these four components can be printed with other small parts, so that the job could be more efficient.

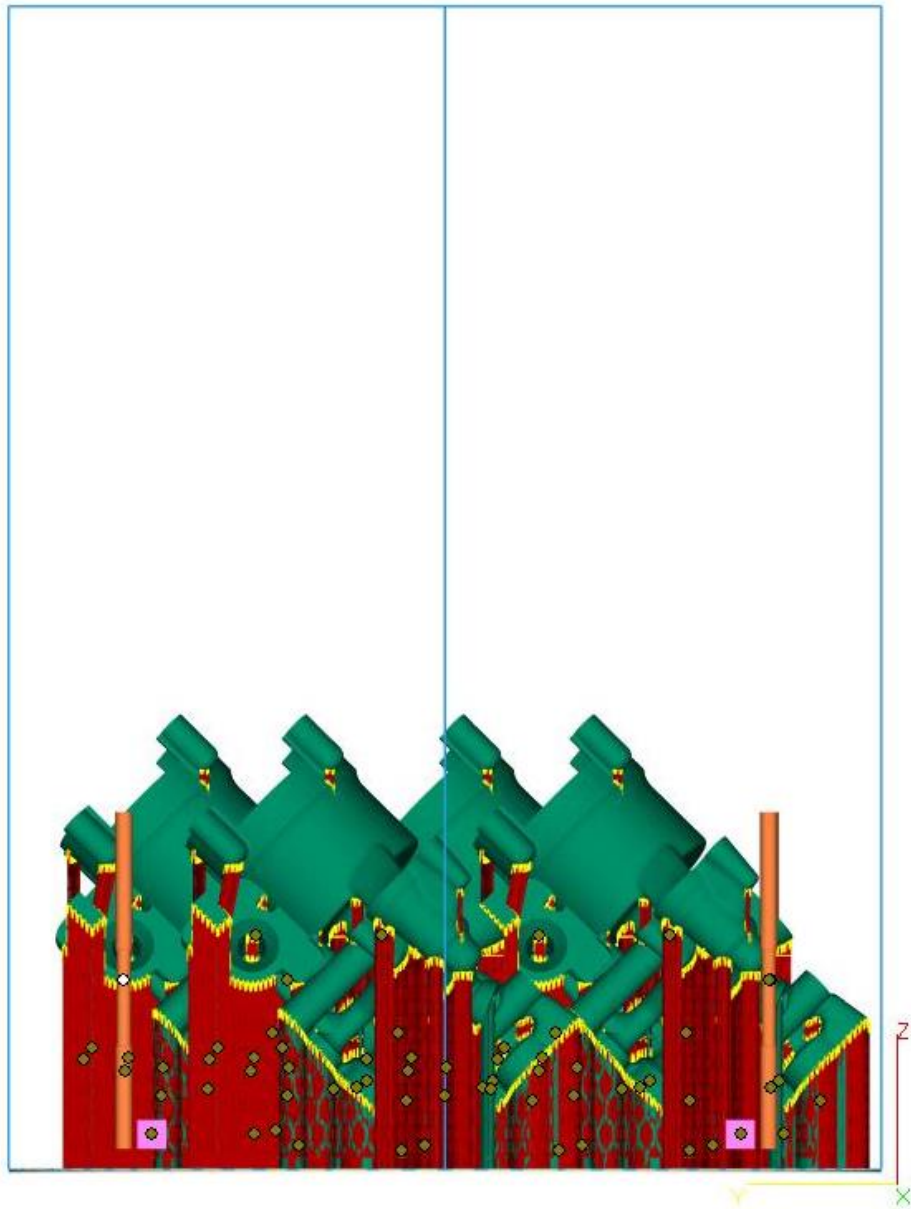


Figure 6.9 - Nesting on TruPrint 3000, lateral view. Magics

6.3. Post processing

On every functional surface, an additional allowance is required to machine that areas. The areas that need to be finished are indicated by the customer and are the functional surfaces and holes that need threads. The allowance dimension depends

not only on the processed material and its geometry, but also on the surface quality requirement.

In figure 6.10 and 6.11 the area to be machined and where the allowances have been added are marked in light blue. Additionally, the smaller holes have been removed and will be obtained directly from machining.

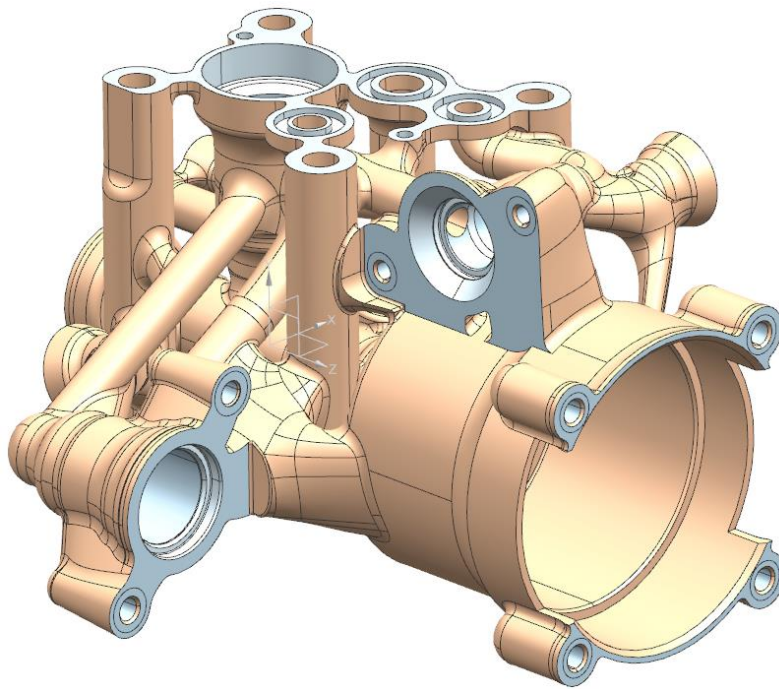


Figure 6.10 – Final component, in light blue the areas that need to be machined. View 1, NX

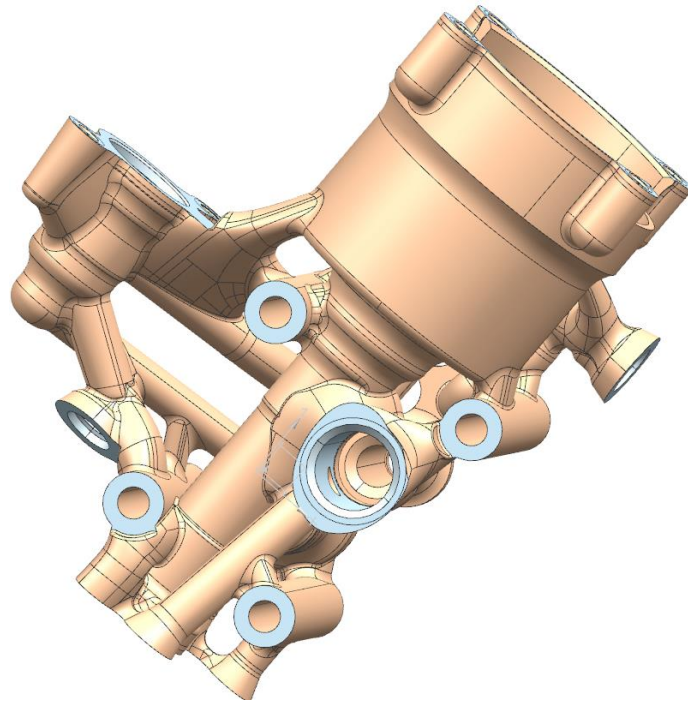


Figure 6.11 – Final component, in light blue the areas that need to be machined. View 2, Inspire

A machining strategy is required to finish the part, as described in the previous paragraph. There was the necessity to design and include some fixtures and latches to block the part in order to machine it in two steps.

Another way to post process this component could be by the new technology called Hirtisation®, by Hirtenberger [39]. This process is based on electrochemical pulse methods, trying to eliminate mechanical finishing [39]. With this technology, support structures are dissolved and the surface roughness is significantly reduced, both from the inside and the outside of the part [39]. This is a huge advantage for this component, because it presents a lot of inner channels that are hardly machinable in traditional ways and they are also difficult to access for cleaning from the remaining powder from the process.

7. Comparison between original and optimized component

The weight of the original component is 1,022 kg. The weight of the final part is 0,309 kg, after removing offsets, fixtures and support structures. The overall weight saving is 69%, comparing the final component produced in AlSi10Mg with the original manifold in Anticorodal 6082.

The most important difference between the two components is the design. The design space is kept as it originally was, with certain changes only in the routing of the channels, but the non-design space has been drastically modified.

Since the analysis on the optimized part has been carried out with Inspire, this comparison is between the analyses of the original and optimized components in Inspire.

In table 8 it is possible to observe the differences in the values of weight, volume, material, displacement, von Mises stress and safety factor, between original and optimized components.

The minimum safety factor has been calculated following equation (2), the ratio of the yield stress of the adopted material to the maximum von Mises stress achieved for the selected load case. This value does not represent the actual level stress in the component, since the maximum von Mises stress is present only in a few small bad elements (almost punctual) in the mesh.

Comparing the original with the optimized component, it is possible to see how the weight has decreased remarkably, with slightly increasing stresses and displacements.

Since the Yield stress of AlSi10Mg is a little bit higher than Anticorodal 6082, even if stresses and displacements are higher, the minimum safety factor calculated is approximately the same in both the versions of the component. For load case 2, the minimum safety factor is even a bit higher in the optimized version.

It is interesting to notice that, even if both the structures can withstand the loads, with a significant decrease of weight, achieved via topology optimisation, it is possible to obtain similar stresses and deformation behaviours, making the part more efficient.

	Unit of Measurement	Original	Optimized
Weight	kg	1,022	0,309
Volume	m ³	3,784E-04	1,157E-04
Material		Anticorodal 6082	AlSi10Mg
Max displacement LC1	mm	0,023	0,047
Max Von Mises stress LC1	MPa	123	132
Min safety factor LC1		1,87	1,82
Max displacement LC2	mm	0.0064	0.0138
Max Von Mises stress LC2	MPa	222	226
Min safety factor LC2		1,03	1,06

Table 8 – Comparison between original and optimized component

In the pictures below (from figure 7.1 to 7.8) displacement contour plots and Von Mises stresses contour plots are compared between the original and the optimized component.

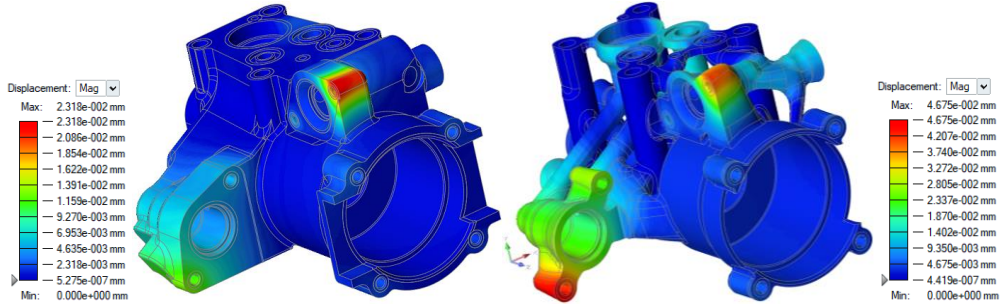


Figure 7.1 – Original (left) and optimized (right) component. Displacement, load case 1, view 1. Inspire

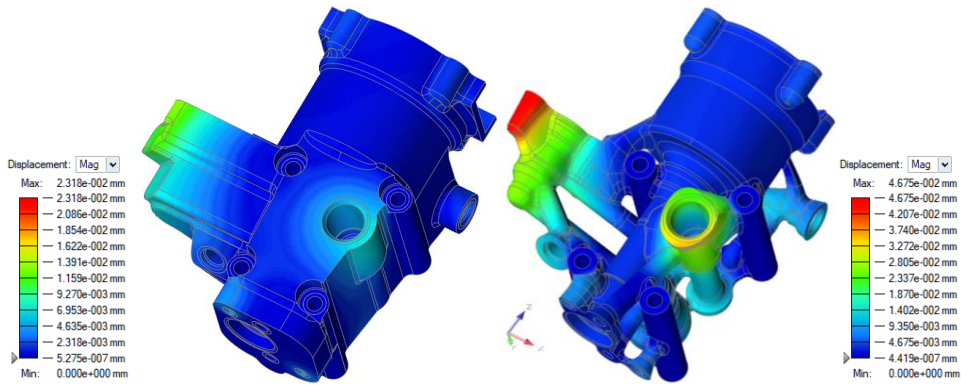


Figure 7.2 - Original (left) and optimized (right) component. Displacement, load case 1, view 2. Inspire

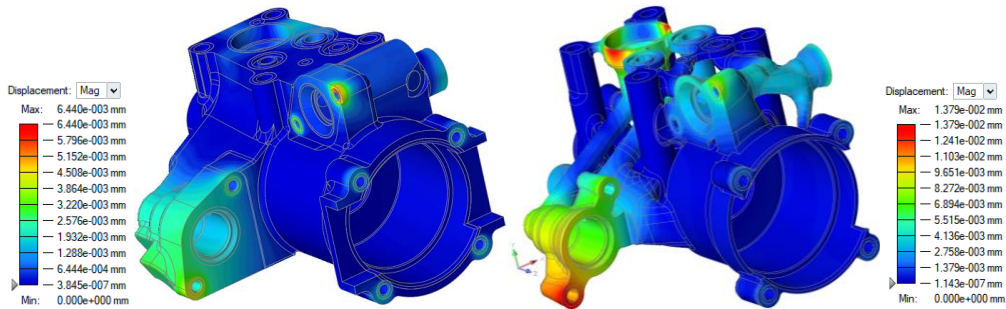


Figure 7.3 - Original (left) and optimized (right) component. Displacement, load case 2, view 1. Inspire

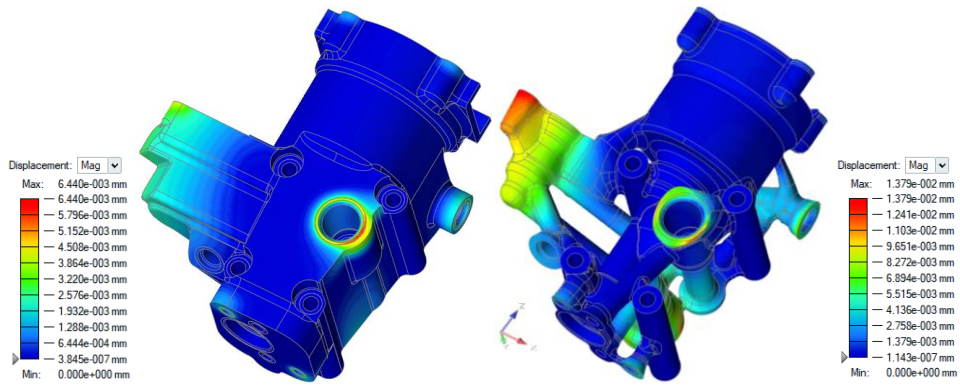


Figure 7.4 - Original (left) and optimized (right) component. Displacement, load case 2, view 2. Inspire

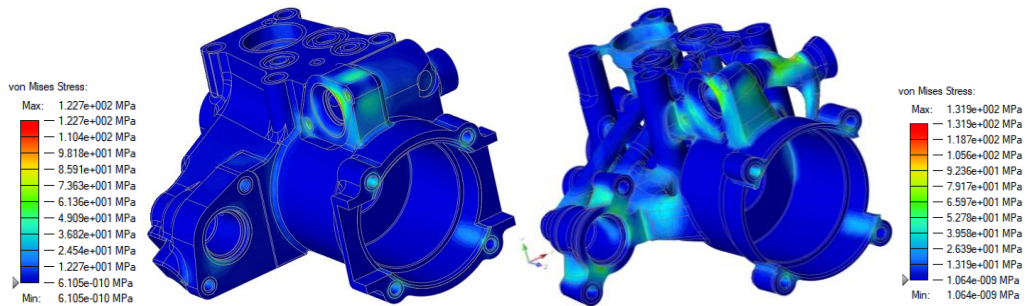


Figure 7.5 – Original (left) and optimized (right) component. Von Mises stresses, load case 1, view 1. Inspire

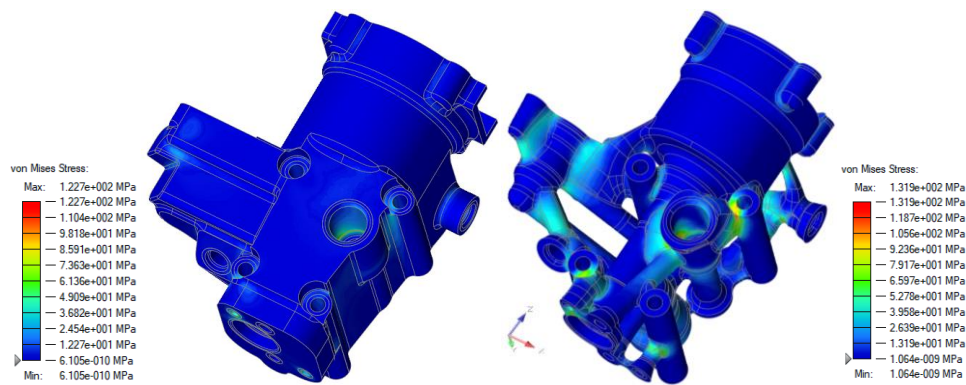


Figure 7.6 - Original (left) and optimized (right) component. Von Mises stresses, load case 1, view 2. Inspire

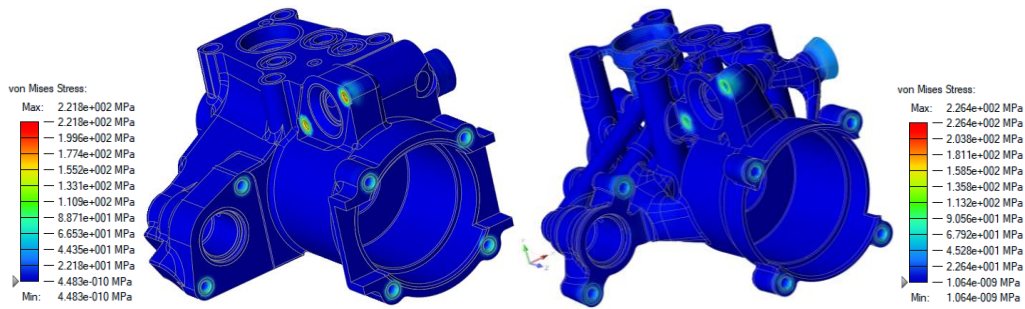


Figure 7.7 - Original (left) and optimized (right) component. Von Mises stresses, load case 2, view 1. Inspire

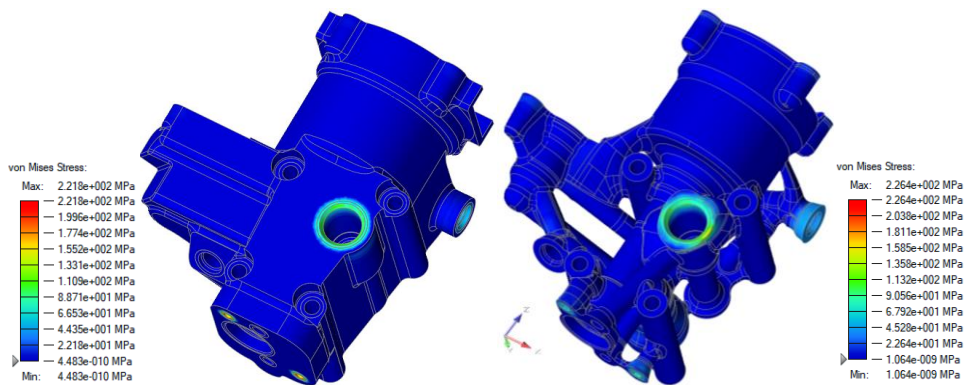


Figure 7.8 – Original (left) and optimized (right) component. Von Mises stresses, load case 2, view 2. Inspire

In the figures from 7.11 to 7.16, the safety factors of the original and the optimized component are compared for different load cases. It was decided to show in the pictures the component with a safety factor lower than 1.5 as well in order to check that the performed stresses of the component are below the allowable limit.

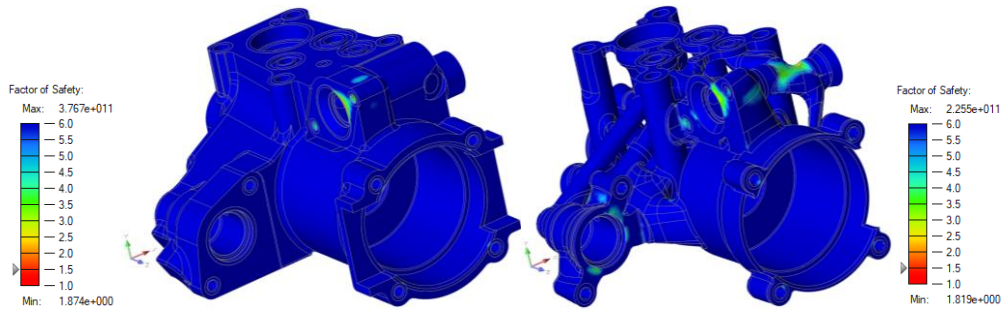


Figure 7.9 - Original (left) and optimized (right) component. Safety factor, load case 1, view 1. Inspire

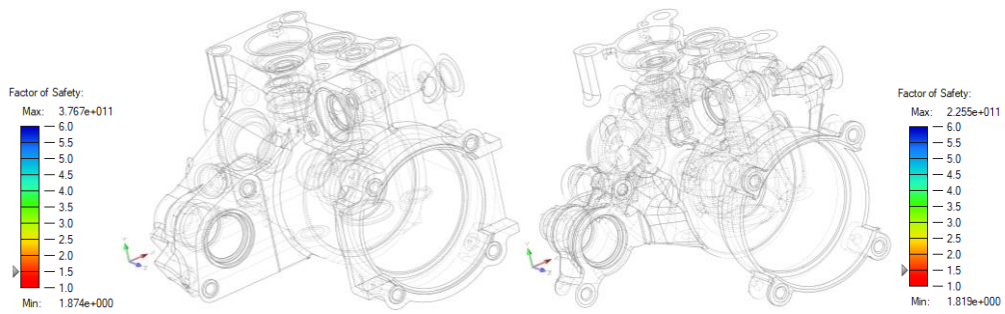


Figure 7.10 - Original (left) and optimized (right) component. Safety factor less than 1.5, load case 1, view 1. Inspire

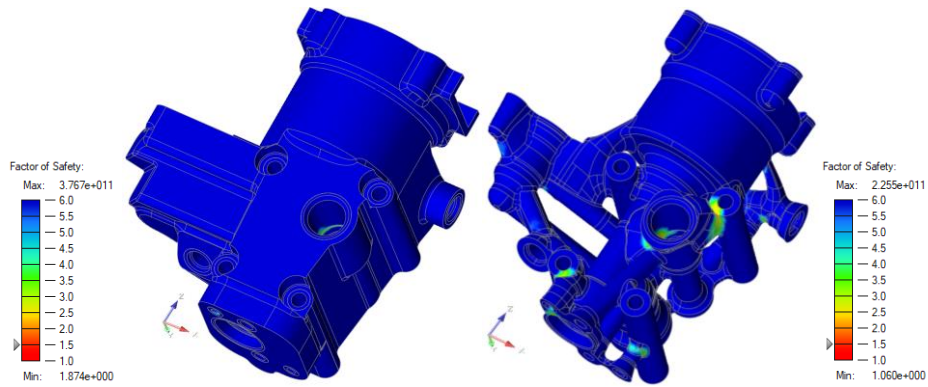


Figure 7.11 - - Original (left) and optimized (right) component. Safety factor, load case 1, view 2. Inspire

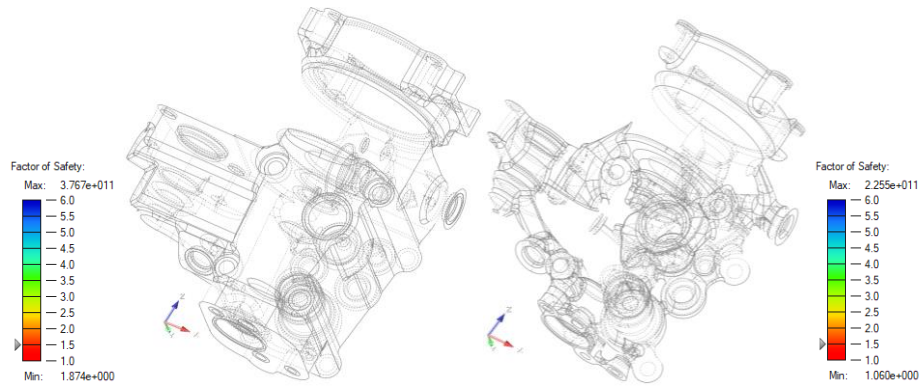


Figure 7.12 - - Original (left) and optimized (right) component. Safety factor less than 1.5, load case 1, view 2. Inspire

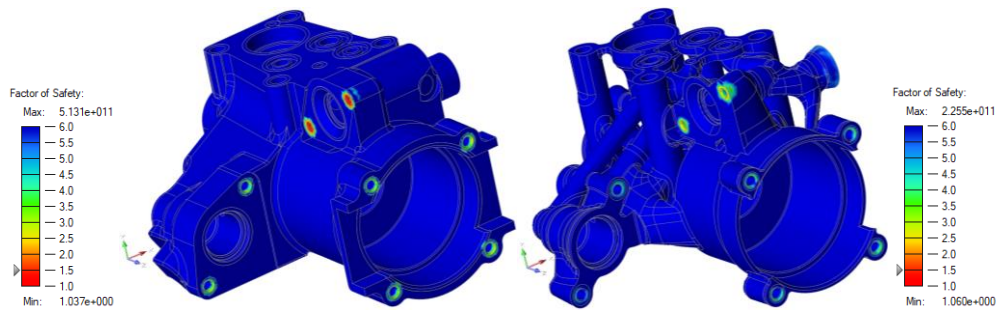


Figure 7.13- Original (left) and optimized (right) component. Safety factor, load case 2, view 1. Inspire

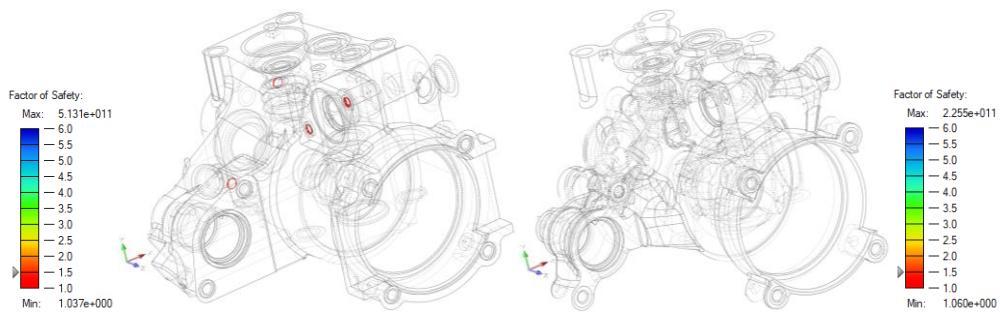


Figure 7.14 - Original (left) and optimized (right) component. Safety factor less than 1.5, load case 1, view 1. Inspire

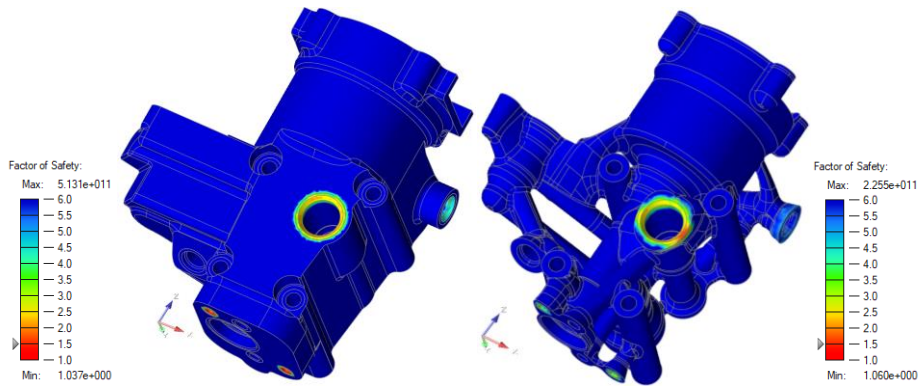


Figure 7.15 - Original (left) and optimized (right) component. Safety factor, load case 2, view 2. Inspire

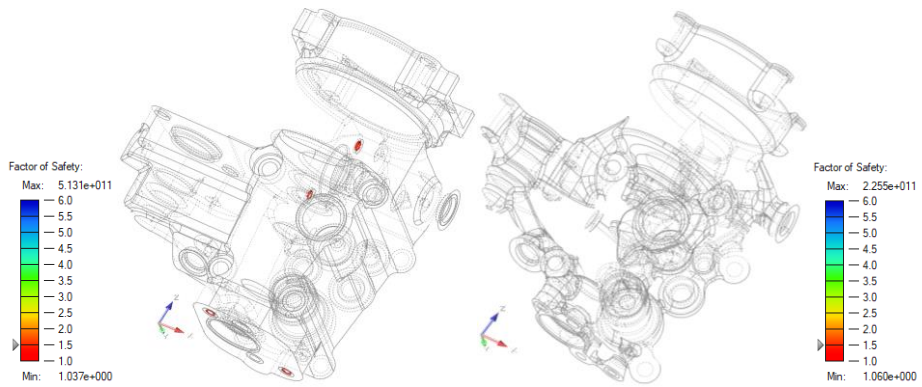


Figure 7.16 – Original (left) and optimized (right) component. Safety factor less than 1.5, load case 2, view 2. Inspire

As explained previously, few elements showed a safety factor less than 1.5 and a small area that could be assumed as a singularity. Therefore, the results of this analysis are considered satisfactory.

8. Conclusion

This piece of work has been performed not only to show the advantages and disadvantages of a complete series production of an automotive component, but also to compare two different software: Altair Inspire and Siemens NX for CAD and Altair Inspire and NX Nastran for FEA and topology optimization.

For the first comparison, it is shown that additive Manufacturing is, despite all, still advantageous for this case study: the price of the component is not economical because its dimensions are too big (since only four components can be built in the same machine), and the production volumes required are too high. AM is the better option to produce the prototype: the cost for a single component with AM is 850 € while the price of the original part is 1100 €. While in traditional manufacturing the cost goes strongly down with the increase of the number of parts to manufacture, in AM the descent is less pronounced. The cost to produce 3000 parts per year with traditional manufacturing is 48 € for each part, plus 25000 € for machining tooling (less than 9 euros for each part). With AM, if the production lot is 3000 parts, the price for each will be around 450 €.

The best advantage is instead the weight reduction: with topology optimization the weight has been reduced up to 69% even though weight reduction is not a major factor in the automotive industry. Since the component is mounted on a car, weight reduction can although lead to several advantages like a small reduction of the consumptions of fuel and CO₂ as well. The break-even point that makes AM advantageous obviously depends on the production volume required, but there are also those other factors that cannot be considered. Therefore, for a lower number of parts requested, additive manufacturing would be the best technology to produce this specific component.

For the second comparison, the comparison between the two different software, it is not possible to say which is more suitable for AM, since both have their advantages and disadvantages in all the steps in the production chain.

The more complete software for visualization, design and CAD modifications is Siemens NX, because it allows the manipulation of surfaces, points and volumes in a more precise and efficient way. Obviously, it is mandatory to know how to use this software to enjoy the advantages, because it is not intuitive and user friendly as compared to Inspire: which is why it was important and necessary to participate in trainings to perform this thesis.

NX is obviously a valid option also because it is a more complete software, not only for CAD work, but also capable of modifying complex geometries, and with the possibility to perform the three steps of topology optimisation, redesign and FEA of the process flow all in the same GUI (Graphic User Interface), without switching in between different file formats. NX-Nastran, used to perform the FEA, offers a wide range of options for meshing the component, with different types of elements, generally having more options for every feature, making it more customizable. No problems were encountered to perform analyses with first or second order tetra elements with NX Nastran.

Inspire is instead a very powerful software, even if it has a lot of bugs, even in the last updated version of 2019. Being a simplified and all-in-one program of the more complex Altair's HyperWorks, it is really user friendly and it is quick and easy to set-up optimization run, but this does not work all the time, especially for second order elements. Numerous problems have been found, so the support team was contacted different times, sometimes not finding a solution, because it is not possible to modify the mesh in Inspire itself. Another problem is the conversion from step file, provided by the customer, to stmod file format, since surfaces were created instead of solids. Furthermore, the partition tool was not able to create an offset to divide the complex geometry of the inner channels, that is why a proper CAD tool has been used to accomplish that. Despite all of this, in this particular case, Inspire is the better option to perform a topology optimisation on this component and to reconstruct the resulting geometry. Because of its Wrap feature, *polyNURBS* is an easier tool & quicker method to create the final solid part. Unfortunately, not being able to make difficult modifications, its use remains only marginal.

In the end, the results in the comparison between Altair and Siemens software show that the ideal option would be to use both during the engineering steps: Inspire for topology optimization and geometry reconstruction and NX for CAD modifications and NX Nastran for the FEA.

Nevertheless, changing the software multiple times is not recommended because of the loss of information that it can lead to, going from one file format to another. That is why it is always preferable to use the same software to perform all the steps. This is possible with NX but not with Inspire.

In conclusion, it is possible to assert that the redesigned component, shown in figure 8.1 and 8.2, leads to undoubted advantages for quality, waste material and engineering time, especially in automotive field, for the reduction in fuel consumption and CO₂ emissions. Despite this, one should remember that for serial production this component is still on a preliminary stage as the effective production time is still too slow for big production volumes. However, for small production numbers, this is a solution to seriously consider, because it can be more advantageous compared to conventional manufacturing.

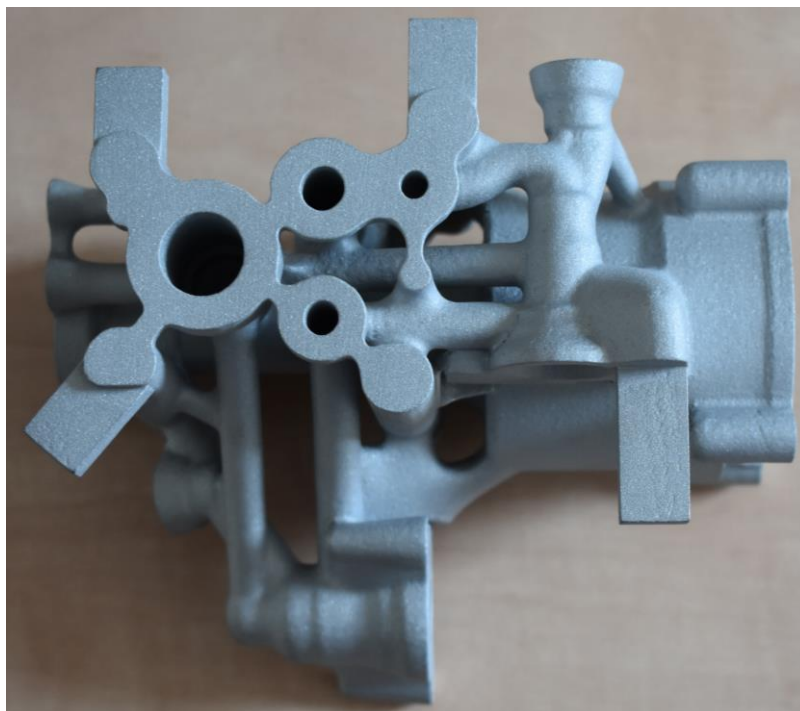


Figure 8.1 - Manufactured component. View 1

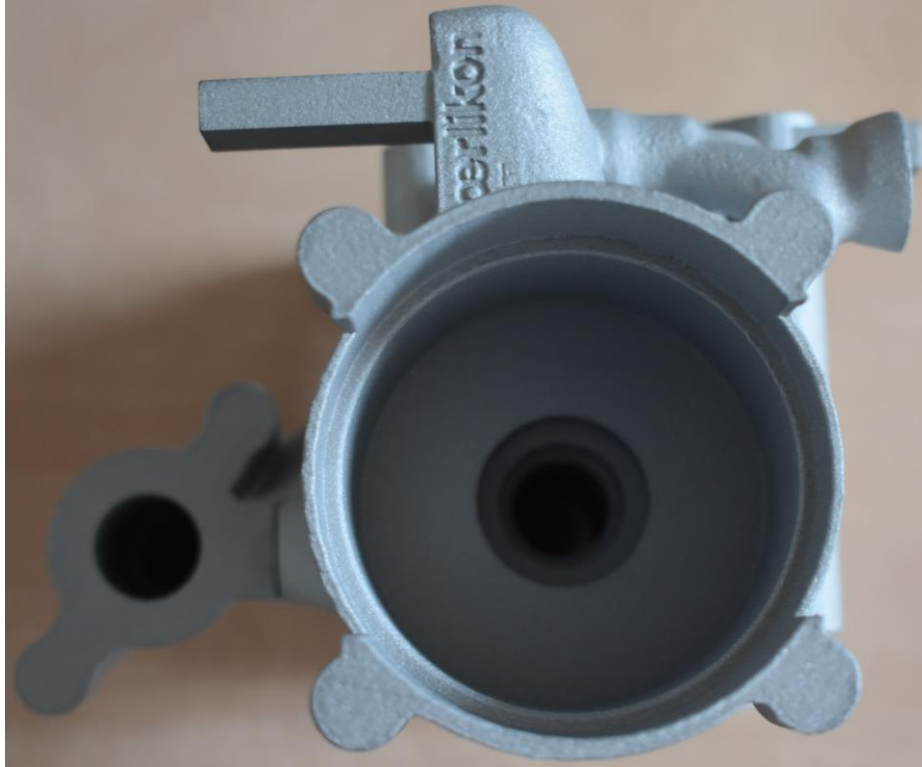


Figure 8.2 - Manufactured component. View 2

A recommendation for future further researches could be to compare the few software available in the market that are able to perform topology optimizations (including redesign and FEA). This can help companies and researchers in the additive manufacturing field to find the best solution, improving design and analyses, with the possibility to decrease time and costs.

A. List of figures

<i>Figure 1.1 - Additive Manufacturing steps [3]</i>	20
<i>Figure 1.2 - - Laser Powder Bed Fusion process [3]</i>	22
<i>Figure 1.3 - Powder Layer thickness and Deposit Layer Thickness for L-PBF process [18]</i>	23
<i>Figure 2.1 - Original component, View number 1, Inspire</i>	28
<i>Figure 2.2 - Original component, view number 2, Inspire</i>	28
<i>Figure 2.3 - Assembly of the original component, marked in yellow. View number one, Inspire</i>	30
<i>Figure 2.4 - Assembly of the original component, marked in yellow. View number two, Inspire</i>	30
<i>Figure 2.5 - Components linked to the part chosen, Inspire</i>	31
<i>Figure 2.6 - Application of the force. Load case 1 at left, Load case 2 at right, Inspire</i>	33
<i>Figure 2.7 - Loads applied on Inspire. Bottom view.</i>	34
<i>Figure 2.8 - Loads applied on Inspire. Top view.</i>	34
<i>Figure 2.9 - Initial non-design space. View number 1, NX</i>	36
<i>Figure 2.10 - Initial non-design space. View number 2, NX</i>	37
<i>Figure 2.11 - Complete assembly, part is transparent</i>	38
<i>Figure 2.12 - Design space and non-design space. Isometric view 1, NX</i>	39
<i>Figure 2.13 - Design space and non-design space. Isometric view 2, NX</i>	39
<i>Figure 2.14 - Non-design space, first review. First view, NX</i>	40
<i>Figure 2.15 - Non-design space, first review. Second view, NX</i>	41
<i>Figure 2.16 - FEA of the original component on Inspire. Displacement load case 1. View 1</i>	43
<i>Figure 2.17 - FEA of the original component on NXNastran. Displacement load case 1. View 1</i>	43
<i>Figure 2.18 - FEA of the original component on Inspire. Displacement load case 1. View 2</i>	44
<i>Figure 2.19 - FEA of the original component on NXNastran. Displacement load case 1. View 2</i>	44

<i>Figure 2.20 - FEA of the original component on Inspire. Displacement load case 2. View 1</i>	45
<i>Figure 2.21 - FEA of the original component on NX Nastran. Displacement load case 2. View 1</i>	45
<i>Figure 2.22 - FEA of the original component on Inspire. Displacement load case 2. View 2</i>	46
<i>Figure 2.23 - FEA of the original component on NX Nastran. Displacement load case 2. View 2</i>	46
<i>Figure 2.24 - FEA of the original component on Inspire. Von Mises stress load case 1. View 1</i>	47
<i>Figure 2.25 - FEA of the original component on NX Nastran. Von Mises stress load case 1. View 1</i>	48
<i>Figure 2.26 - FEA of the original component on Inspire. Von Mises stress load case 1. View 2</i>	48
<i>Figure 2.27 - FEA of the original component on NX Nastran. Von Mises stress load case 1. View 2</i>	49
<i>Figure 2.28 - FEA of the original component on Inspire. Von Mises stress load case 2. View 1</i>	49
<i>Figure 2.29 - FEA of the original component on NX Nastran. Von Mises stress load case 2. View 1</i>	50
<i>Figure 2.30 - FEA of the original component on Inspire. Von Mises stress load case 2. View 2</i>	50
<i>Figure 2.31 - FEA of the original component on NX Nastran. Von Mises stress load case 2. View 2</i>	51
<i>Figure 3.1 - Material Characteristics for AlSi10Mg</i>	58
<i>Figure 3.2 - Overhang angle constraint with Inspire. First view</i>	59
<i>Figure 3.3 - Overhang angle constraint with Inspire. Second view</i>	59
<i>Figure 3.4 - Topology optimization result with Inspire. View 1</i>	61
<i>Figure 3.5 - Topology optimization result with Inspire. View 2</i>	61
<i>Figure 3.6 - Shape Explorer command on Inspire.</i>	62
<i>Figure 3.7 - Topology optimization result on NX Nastran. View 1</i>	64
<i>Figure 3.8 - Topology optimization result on NX Nastran. View 2</i>	64

<i>Figure 3.9 - Laplacian smooth. View 1, Magics</i>	65
<i>Figure 3.10 - Laplacian Smooth. View 2, Magics</i>	65
<i>Figure 4.1 - Bridge for downfacing surfaces (a=plane of process failure) [2]</i>	70
<i>Figure 4.2 - Vertical holes, left with support, right with drop shape. δ is the downskin angle</i>	70
<i>Figure 4.3 - Direction of build to avoid recoater collision [34]</i>	71
<i>Figure 4.4 - Channel n.1. Left original, right new routing, NX</i>	73
<i>Figure 4.5 - Channel n.2 original, NX</i>	74
<i>Figure 4.6 - Channel n.2 new routing, NX</i>	74
<i>Figure 4.7 - Channel n.3 original, NX</i>	75
<i>Figure 4.8 - Channel n.3 new routing, NX</i>	75
<i>Figure 4.9 - Fillets n.2 original, NX</i>	77
<i>Figure 4.10 - Fillets n.2 new, NX</i>	77
<i>Figure 4.11 - Topology optimization result. View 1, Inspire</i>	78
<i>Figure 4.12 - Final design. View 1, NX</i>	79
<i>Figure 4.13 - Topology optimization result. View 2, Inspire</i>	79
<i>Figure 4.14 - Final design. View 2, NX</i>	80
<i>Figure 5.1 - FEA of the final component on Inspire. Displacement contour plot for load case 1. View 1</i>	82
<i>Figure 5.2 - FEA of the final component on Inspire. Displacement contour plot for load case 1. View 2</i>	82
<i>Figure 5.3 - FEA of the final component on Inspire. Displacement contour plot for load case 2. View 1</i>	83
<i>Figure 5.4 - FEA of the final component on Inspire. Displacement contour plot for load case 2. View 2</i>	83
<i>Figure 5.5 - FEA of the final component on Inspire. Von Mises stress contour plot for load case 1. View 1</i>	84
<i>Figure 5.6 - FEA of the final component on Inspire. Von Mises stress contour plot for load case 1. View 2</i>	84
<i>Figure 5.7 - FEA of the final component on Inspire. Von Mises stress contour plot for load case 2. View 1</i>	85

<i>Figure 5.8 - FEA of the final component on Inspire. Von Mises stress contour plot for load case 2. View 2</i>	85
<i>Figure 6.1 - Possible orientation, vertical, Inspire</i>	88
<i>Figure 6.2 – Orientation decided, inclined, Inspire</i>	89
<i>Figure 6.3 – Machining position 1, NX.....</i>	91
<i>Figure 6.4 – Machining position 2, NX.....</i>	91
<i>Figure 6.5 - Support structures, first view, Magics</i>	93
<i>Figure 6.6 - Support structures, second view, Magics</i>	93
<i>Figure 6.7 - Support structures, bottom view, Magics</i>	94
<i>Figure 6.8 - Nesting on TruPrint 3000, front view. Magics</i>	96
<i>Figure 6.9 - Nesting on TruPrint 3000, lateral view. Magics</i>	97
<i>Figure 6.10 – Final component, in light blue the areas that need to be machined. View 1, NX.....</i>	98
<i>Figure 6.11 – Final component, in light blue the areas that need to be machined. View 2, Inspire</i>	99
<i>Figure 7.1 – Original (left) and optimized (right) component. Displacement, load case 1, view 1. Inspire.....</i>	102
<i>Figure 7.2 - Original (left) and optimized (right) component. Displacement, load case 1, view 2. Inspire.....</i>	102
<i>Figure 7.3 - Original (left) and optimized (right) component. Displacement, load case 2, view 1. Inspire.....</i>	102
<i>Figure 7.4 - Original (left) and optimized (right) component. Displacement, load case 2, view 2. Inspire.....</i>	103
<i>Figure 7.5 – Original (left) and optimized (right) component. Von Mises stresses, load case 1, view 1. Inspire</i>	103
<i>Figure 7.6 - Original (left) and optimized (right) component. Von Mises stresses, load case 1, view 2. Inspire</i>	103
<i>Figure 7.7 - Original (left) and optimized (right) component. Von Mises stresses, load case 2, view 1. Inspire</i>	104
<i>Figure 7.8 – Original (left) and optimized (right) component. Von Mises stresses, load case 2, view 2. Inspire</i>	104

<i>Figure 7.9 - Original (left) and optimized (right) component. Safety factor, load case 1, view 1. Inspire</i>	105
<i>Figure 7.10 - Original (left) and optimized (right) component. Safety factor less than 1.5, load case 1, view 1. Inspire</i>	105
<i>Figure 7.11 - - Original (left) and optimized (right) component. Safety factor, load case 1, view 2. Inspire</i>	105
<i>Figure 7.12 - - Original (left) and optimized (right) component. Safety factor less than 1.5, load case 1, view 2. Inspire</i>	106
<i>Figure 7.13- Original (left) and optimized (right) component. Safety factor, load case 2, view 1. Inspire</i>	106
<i>Figure 7.14 - Original (left) and optimized (right) component. Safety factor less than 1.5, load case 1, view 1. Inspire</i>	106
<i>Figure 7.15 - Original (left) and optimized (right) component. Safety factor, load case 2, view 2. Inspire</i>	107
<i>Figure 7.16 – Original (left) and optimized (right) component. Safety factor less than 1.5, load case 2, view 2. Inspire</i>	107
<i>Figure 8.1 - Manufactured component. View 1</i>	110
<i>Figure 8.2 - Manufactured component. View 2</i>	111

B. List of equations

- (1) – Minimum thickness of pipes
- (2) – Safety factor
- (3) – Young's modulus with SIMP method
- (4) – Rigidity with SIMP method
- (5) – RAMP scheme
- (6) – Young's modulus with RAMP method

C. List of tables

<i>Table 1 - Anticorodal 6082 properties</i>	<i>29</i>
<i>Table 2 - Mass and clamping forces of linked bodies.....</i>	<i>32</i>
<i>Table 3 - Coordinates of the center of gravity of the masses.</i>	<i>32</i>
<i>Table 4 - Maximum values of displacement, Inspire VS NX.</i>	<i>52</i>
<i>Table 5 - Maximum values of Von Mises stress, Inspire VS NX Nastran</i>	<i>52</i>
<i>Table 6 - Comparison between Inspire and NX Nastran topology optimizations</i>	<i>67</i>
<i>Table 7 – Advantages and disadvantages for different part orientations.....</i>	<i>90</i>
<i>Table 8 – Comparison between original and optimized component</i>	<i>101</i>

D. Abbreviations

AM - Additive Manufacturing

ASTM – American Society for Testing and Materials

CAD – Computer Aided Design

CAE – Computer Aided Engineering

CNC – Computer Numerical Control

DFAM – Design for Additive Manufacturing

DMLS – Direct Metal Laser Sintering

EBM – Electron Beam Melting

FEA – Finite Element Analysis

FEM – Finite Element Method

GUI – Graphic User Interface

HIP – Hot Isostatic Pressing

L-PBF – Laser Powder Bed Fusion

LBM – Laser Beam Melting

OAM – Oerlikon Additive Manufacturing GmbH

OG – Oerlikon Graziano S.p.a.

PBF – Powder Bed Fusion

RAMP – Rational Approximation of Material Properties

R&D – Research and Development

SIMP – Solid Isotropic Material with Penalization

SLA – Stereolithography

SLM – Selective Laser Melting

STL – Standard Triangulation Language

UV – Ultraviolet

E. Bibliography

- [1] D. Herzog, V. Seyda, E. Wycisk and C. Emmelmann, “Additive manufacturing of metal,” Elsevier Ltd., 2016.
- [2] J. Kranz, D. Herzog and C. Emmelmann, “Design guidelines for laser additive manufacturing of lightweight structures in TiAl6V4,” Laser Institute of America, 2014.
- [3] D. Zimmer and G. Adam, “Direct Manufacturing Design Rules,” Universitaet Paderborn, 2013.
- [4] I. Gibson, D. Rosen and B. Stucker, “Additive Manufacturing Technologies,” Springer.
- [5] G. Strano, L. Hao, R. Everson and K. Evans, A new approach to the design and optimisation of support structures in additive manufacturing, International Journal of Advanced Manufacturing Technology , 2013.
- [6] G. Chiandussi, “Metodi di ottimizzazione applicati a problemi ingegneristici, Introduzione ai metodi di ottimizzazione,” 2017.
- [7] J. Brennan, 20 Years of Topology Optimization: Birth and Maturation of a Disruptive Technology, Altair Hyperworks website, 2014.
- [8] P. Kurup, T. Remo, J. Cotrell, S. D. Jenne and P. O’Connor, Analysis of Supply Chains and Advanced Manufacturing of Small Hydropower Systems, Clean Energy Manufacturing Analysis Center, 2018.
- [9] M. S., Topology optimisation for 3D printing, 3dnatives, 2018.

- [10] L. Iuliano and M. Galati, *Materiale didattico - Tecniche per la fabbricazione additiva*, 2017.
- [11] Oerlikon.AM, "<https://www.oerlikon.com/am/en/>".
- [12] T. Wohlers and T. Gornet, "History of additive manufacturing," 2016.
- [13] P. Bartolo and G. Mitchell., Stereo-thermal-lithography: a new principle for rapid prototyping, *Rapid Prototyping Journal*, 2003.
- [14] B. Lu, D. Li and X. Tian, *Development Trends in Additive Manufacturing and, 3D Printing—Perspective Research*, 2015.
- [15] Autodesk, "<https://www.autodesk.com/redshift/history-of-3d-printing/>".
- [16] M. Szilvsi-Nagy and G. Mátyási, *Analysis of STL files, Mathematical and Computer Modelling*, 2003.
- [17] K. Muita, M. Westerlund and R. Rajala, *The Evolution of Rapid Production: How to Adopt Novel Manufacturing Technology*, IFAC-PaperOnLine, 2015.
- [18] J. O. Milewski, "Additive Manufacturing of Metals," Springer, 2017.
- [19] E. Uhlmann, R. Kersting, T. B. Kleina, M. F. Cruz and A. V. Borille, Additive manufacturing of titanium alloy for aircraft components, *ScienceDirect*, 2005.
- [20] J.-P. Järvinen, V. Matilainen, X. Li, H. Piili, A. Salminen, I. Mäkelä and O. Nyrhilä, Characterization of effect of support structures in laser additive, *ScienceDirect*, 2014.
- [21] M. G. Martínez, *PFC: AlSi10Mg parts produced by Selective Laser Melting (SLM)*, Universidad Carlos III de Madrid.
- [22] X. Z. Bo SONG, S. Li, C. Han, Q. Wei, S. Wen, J. Liu and Y. Shi, Differences in microstructure and properties between selective laser melting and

traditional manufacturing for fabrication of metal parts: A review, Higher Education Press and Springer-Verlag, 2015.

- [23] T. Douglas and G. Stanley, Costs and Cost Effectiveness of Additive Manufacturing, National Institute of Standards and Technology , 2014.
- [24] C. Klahn, B. Leutenecker and M. Meboldt, Design for Additive Manufacturing – Supporting the Substitution of Components in Series Products, ScienceDirect, 2014.
- [25] A. Sehlstroem, “Multi-objective topology optimization,” Gothenburg, 2013.
- [26] D. W. Rosen, Design for Additive Manufacturing: a method to explore unexplored regions of the design space, Georgia Institute of Technology, 2007.
- [27] D. Systèmes, “Metodo SIMP per l’ottimizzazione topologica,” 1995-2019.
- [28] Y. Jijun, Z. Tao, R. Jianhua and L. Yanmei, “A topology optimization method based on element independent nodal density,” Springer, 2014.
- [29] M. Bendsoe and O. Sigmund, Topology optimization Theory, Methods and Applications, Springer, 2003.
- [30] M. Heskitt, Five Common Mistakes Made Running Topology Optimization, Enlighten, 2016.
- [31] ISO/TC261/SC and ISO/DIS52911-1:2017(E), “Additive manufacturing — Technical Design Guideline for Powder Bed Fusion — Part 1: Laser-based Powder Bed Fusion of Metals,” ISO 2017, 2017.
- [32] Crucible, “<http://www.crucibledesign.co.uk/guides/>”.
- [33] C. I. Design, “Design guidelines for Direct Metal Laser Sintering (DMLS),” 2014.

- [34] M. Król, M. Kujawa, L. Dobrzański and T. Tański, Influence of technological parameters on additive manufacturing steel parts in Selective Laser Sintering, International Scientific Journal, 2014.
- [35] J. Lewandowski and M. Seifi, Metal Additive Manufacturing: A Review of Mechanical Properties, Annual Review of Materials Research, 2016.
- [36] M. Magics, <https://www.materialise.com/it/software/magics>.
- [37] Trumpf, https://www.trumpf.com/de_INT/.
- [38] Hirtenberger, <https://hes.hirtenberger.com/en/hirtisation/>.
- [39] R. D. Cook, D. S. Malkus, M. E. Plesha and R. J. Witt, “Concepts and Applications of Finite Element Analysis,” Wiley, 2002.
- [40] E. E. Covarrubias and M. Eshraghi, Effect of Build Angle on Surface Properties of Nickel Superalloys Processed by Selective Laser Melting, JOM, 2018.
- [41] EOS, <https://www.eos.info/en>.

F. Acknowledgments

The research presented was mainly conducted in Oerlikon AM Munich Research Institute. First, I would like to express my special thanks of gratitude to Martin Pagel and Christian Haecker to have given me the possibility to be a part of this company.

I am particularly grateful for the assistance given by Dushan Pamunuwa for the help received in the writing of this work. Advice given by all the Applications Engineering team has been a great help in this project.

I would like to express my very great appreciation to Iva Zarev from Oerlikon Graziano (now Dana Incorporated) and Giorgio Scalici for supporting this collaboration.

I would like to express my gratitude to Prof. Luca Iuliano and Ing. Manuela Galati, my research supervisors, for their guidance and useful critiques of this research work.